A METHOD OF COMPENSATING FOR DIELECTRIC ABSORPTION IN CAPACITORS

by

JOHN NELSON WRIGHT

B.S., Massachusetts Institute of Technology
(1976)

SUBMITTED IN PARTIAL FULFILLMENT
OF THE REQUIREMENTS FOR THE
DEGREE OF

MASTER OF SCIENCE

at the

MASSACHUSETTS INSTITUTE OF TECHNOLOGY

(MAY, 1978)

Signature of Author .....

Department of Electrical Engineering
and Computer Science, May 19, 1978

Certified by .....

Thesis Supervisor

Accepted by .....

Chairman, Department Committee

A METHOD OF COMPENSATING FOR DIELECTRIC ABSORPTION IN CAPACITORS

by

JOHN NELSON WRIGHT

Submitted to the Department of Electrical Engineering and Computer Science on May 19, 1978 in partial fulfillment of the requirements for the Degree of Master of Science.

ABSTRACT

A novel means of compensating for the effects of dielectric absorption in capacitors is presented. It is demonstrated that, over an interval of 102 ms, more than an order of magnitude reduction in recovery voltage can be achieved. The technique should be equally effective over much longer or shorter intervals.

A procedure is described to determine accurate parameters for a linear model of the dielectric absorption characteristics of a capacitor. Model parameters for four sample capacitors are presented. Experimental results indicate that a universal model for teflon or polystyrene capacitors is not possible, although there is evidence that a generalized model may be possible for each or both dielectrics that would be reasonably accurate to within a scale factor. Such a model would be particularly well suited for use with the new compensation techniques.

James K. Roberge
Professor of Electrical Engineering
Thesis Supervisor

ACKNOWLEDGEMENT

First and foremost of those to whom I owe a measure of thanks is my Thesis Advisor, Jim Roberge. I think he represents what an educator and engineer should be, and but for him my education would have been the poorer. A debt of gratitude is also due Frank Floyd, my Group Leader at Lincoln Laboratory, for his much appreciated support and encouragement during my Master's program. Finally, no acknowledgement would be complete without mentioning my wife Linda, without whose support this endeavor would have been trying indeed.

TABLE OF CONTENTS

LIST OF ILLUSTRATIONS

LIST OF TABLES

I. DIELECTRIC ABSORPTION IN CAPACITORS

1. Introduction

The phenomenon of dielectric absorption has been well known for many years, although it is periodically rediscovered by engineers when nature reminds them that the perfect capacitor does not exist. One of the more familiar manifestations of dielectric absorption is the fact that the charging current associated with a step in potential across a dielectric has two distinct components. The first is the almost instantaneous charge transfer that approximates an ideal capacitor's response. The second is a component with a non-negligible settling time that can extend from minutes to days, depending on the dielectric.

The most straightforward method of dealing analytically with this phenomenon is to consider the dielectric constant, and thus the capacitance, as complex functions of frequency defined by

$$\begin{aligned} \varepsilon^*(\omega) &= \varepsilon'(\omega) - j\varepsilon''(\omega) \\ C^*(\omega) &= C'(\omega) - jC''(\omega) \quad . \end{aligned} \tag{1}$$

This leads to the familiar frequency domain concept of the dissipation factor of a capacitor, defined by

$$D(\omega) = \frac{\text{energy loss/radian}}{\text{peak energy stored}} = \frac{C''(\omega)}{C'(\omega)} = \frac{\varepsilon''(\omega)}{\varepsilon'(\omega)} \quad . \tag{2}$$

Whether the effort is viewed from the time or frequency domain, as an absorptive or dissipative effect, the physical cause is the same: the dielectric is capable of storing charge that is not immediately accessible to the outside world.

2. Possible Causes and Empirical Descriptions

The physics of this phenomenon are only moderately well understood. There are two mechanisms generally believed to account for it--interfacial polarization caused by inhomogeneities in the dielectric material and dipole polarization due to polar molecules.

The possibility of absorption in a two-layer dielectric, if the ratios of conductivities and dielectric constants of the two layers are not equal, was first noted by Maxwell.[1] Wagner[2] later analyzed the case of spheres suspended in a dielectric medium. The resulting dielectric constant in these and similar investigations is of the form

$$\varepsilon^*(\omega) = \varepsilon_\infty + \frac{(\varepsilon_o - \varepsilon_\infty)}{1 + j\omega\tau_o} \tag{3}$$

where ε_o is the zero frequency dielectric constant, ε_∞ is the infinite frequency dielectric constant, and τ_o is a measure of the dielectric relaxation time. A model of the resulting capacitor is drawn in Fig. 1. The resulting charging current due to absorptive effects, following a unit step change of potential across a capacitor is

$$i(t) = \frac{(C_o - C_\infty)\ e^{-t/\tau_o}}{\tau_o} \quad . \tag{4}$$

The theory of dipole polarization, as presented by Debye[3], hypothesizes a viscous damping effect on polar molecules due to molecular interactions. This damping affects the time in which polar molecules can re-orient themselves in response to a changing electric field.

[1] Superscripts refer to footnotes, p. 77.

The analysis by Debye results in a complex dielectric constant of the same form as Eq. (3).

Unfortunately, it has been found that real dielectrics differ significantly from the model of Eq. (3). Cole and Cole[4,5] have proposed an expression for the dielectric constant of the form

$$\varepsilon^*(\omega) = \varepsilon_\infty + \frac{\varepsilon_o - \varepsilon_\infty}{1 + (j\omega\tau_o)^{1-\alpha}} \tag{5}$$

where α is an empirically derived constant between 0 and 1. This expression was derived by plotting the locus of points, with frequency, of the real versus the imaginary parts of several dielectric constants and noting that they could, in general, be fitted with a circular arc. The resulting time domain representation of the transient current following a step change of potential is a series in powers of time. While this expression does seem to accurately characterize many dielectrics, there still exists no good explanation as to why it should. A more immediate drawback, from an engineering standpoint, is that Eq. (5) results in a complex capacitance that cannot be modeled with a finite number of lumped elements.

Dow[6] has proposed a capacitor model of the form shown in Fig. 2. The resulting expression for the complex capacitances is

$$C^*(\omega) = C_\infty + \sum_{k=1}^{P} \frac{C_k}{1 + j\omega R_k C_k} . \tag{6}$$

The values of the R_k's and the C_k's are chosen to match the characteristics of the capacitor in question over some appropriate time or frequency interval. The resulting charging current, due to absorptive effects, following a unit step change of potential across a capacitor is

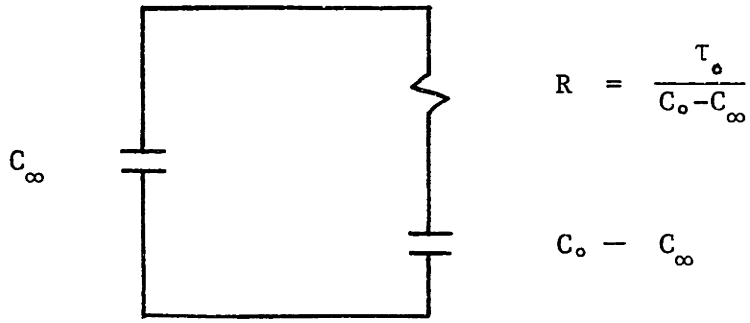

Figure 1 Theoretical capacitor model

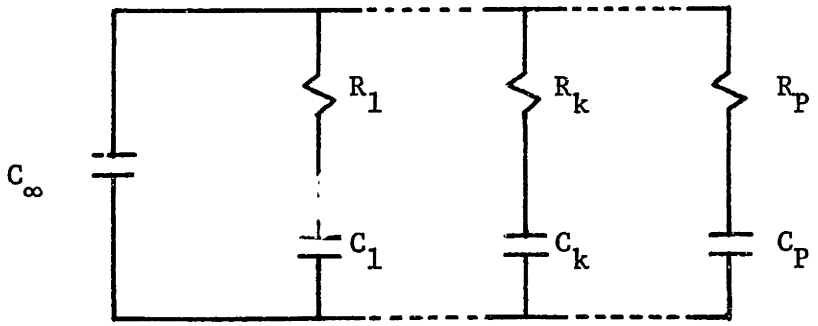

Figure 2 Empirical capacitor model, after Dow

$$i(t) = \sum_{k=1}^{P} \frac{1}{R_k} e^{-t/R_k C_k} \quad . \tag{7}$$

Dow determined the model parameters to match the discharge current associated with a 1 μF polystyrene capacitor over a range from 100 ms to 500 s.

Dow's model has a great deal of intuitive appeal, whether viewed from the time or frequency domain; the absorptive and dissipative components are clearly distinguishable. Equally important, and at the root of the intuitive appeal, is the fact that the model is linear and time invariant. The possibility is thus raised that the effects of dielectric absorption may, in some cases, be compensated for.

II. ENGINEERING IMPLICATIONS

1. Errors Due to Dielectric Absorption

The most effective method of dealing with the problem of dielectric absorption, of course, is to choose a capacitor in which the effects are small enough to be negligible. The best dielectrics in this regard are polystyrene and polytetrafluoroethylene (teflon). Specifications supplied by manufacturers are rarely, if ever, sufficient for making this judgment. Dissipation factor is generally not specified at low enough frequencies to make useful time domain models. Dielectric absorption is very rarely specified at all; when it is, the specification is one of maximum voltage recovery following a short charge-discharge cycle, and this is generally adequate for only qualitative judgments.

Early successful attempts at dealing quantitatively with this error source were in the field of analog computation.[6][7][8] Accurate integrators are essential to analog computers, and they are formed by using high quality capacitors as feedback elements around high gain amplifiers. Dielectric absorption usually manifests itself as an increase in damping in solutions to differential equations. The reason can easily be seen by considering the effect of shunting an integrating capacitor with a real impedance. Workers in this area succeeded in identifying the problem, analyzing it accurately, and, in some cases, providing partial remedies.

More recently, dielectric absorption has been widely recognized as a major (perhaps the major) source of error in sample/hold circuits. The charge stored in the absorptive component of the dielectric, after a step change of voltage, is released over a period of time and causes

the voltage across the open-circuited hold capacitor to creep back towards its value prior to the step. For high speed sample/holds in particular the time frame of dielectric relaxation becomes a significant issue in capacitor selection, but I know of no published work dealing with this issue.

In the field of analog/digital conversion, integrating converters are generally recognized as the most accurate because of their inherent linearity. There is reason to believe that dielectric absorption is the primary cause for the residual non-linearity, and thus inaccuracy, in these converters. This may be seen qualitatively by considering the output of an integrator with a dc input. It should, of course, be a ramp. Dielectric absorption in the integrating capacitor will cause the output to contain approximate exponential terms as well, which are functions of the input voltage, the initial charge stored in the absorptive component of the dielectric, and the dielectric characteristics. The error in the converter's output will contain terms that can be decomposed into offset errors, scale factor errors, quadratic errors, and higher order terms that are generally negligible. An important consideration is the fact that all these terms are functions of the capacitor's initial condition as well as of the input voltage. The result is that errors are partially dependent on the past history of the capacitor (a difficult type of error to compensate for) unless the integrator reset time is at least comparable to the conversion time.

Dow's model is an excellent tool for error analysis in general. We will be concerned primarily with the effects of dielectric absorption in the time domain, and the model can be decomposed to suit the

analysis over any time interval of interest. Sections of the model with time constants that are short compared to the interval of interest can usually be ignored. The voltage across the capacitors in RC sections with very long time constants will approach, in operation, some value that is the long term average of the voltage across the section, and these capacitors can be replaced with voltage sources; all such sections can be combined in a Norton equivalent circuit. For most problems, the model thus reduces to an ideal capacitor shunted by a resistance, a current source, and a small number of RC sections with time constants comparable to the time interval of interest.

2. Error Compensation

The possibility of compensating for dielectric absorption was raised by Dow's work, and several successful attempts at doing so were made in the field of analog computation.[7][8][9][10] Most of the techniques take form similar to Fig. 3. In this topology, the RC sections in the input circuit of the integrator supply current, as a function of the input voltage, to compensate for the current absorbed by the dielectric. Sheehan[7] has described an alternate scheme using several active components to subtract the error, calculated as a function of the input voltage, from the integrator output.

The limitations of these schemes, arising as they do from the area of analog computation, is that they are tailored for strictly linear operation. More recent areas of interest, such as sample/holds and integrating analog/digital converters, generally involve non-linear circuit operation and such compensation techniques are not well suited for this. For instance, the simple procedure of closing a switch to

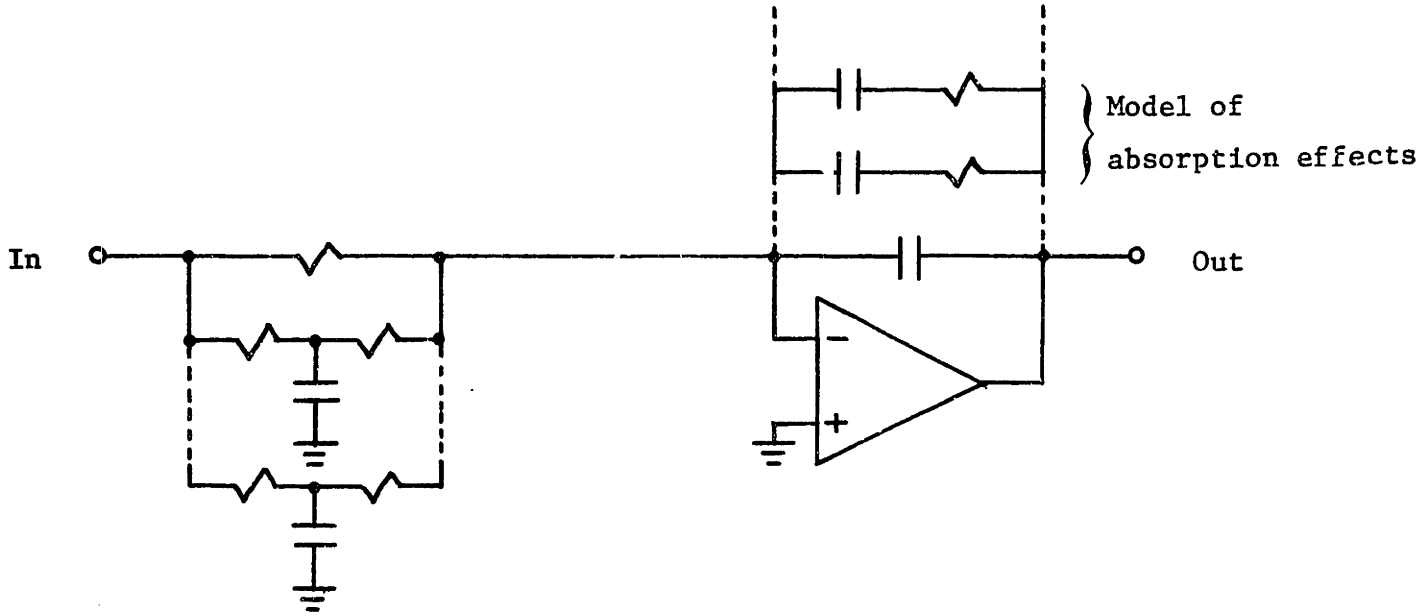

Figure 3 A method of compensating for capacitor dielectric absorption

reset the integrating capacitor would necessitate changing the state of all the compensating capacitors as well.

It is appropriate to question the assumptions of linearity and time invariance of dielectric absorption in the context of compensation. Dow, in measuring the discharge current of polystyrene capacitors, claims consistent results over a range of 23 to 110 volts of charging potential. Other investigators have reported similar findings, but true superposition has not yet been demonstrated to hold for dielectric absorption effects. (On a related subject, Single and Brussolo[11] have pointed out that voltage coefficient effects, which are definitely not linear, may be qualitatively similar to dielectric absorption effects. In a properly manufactured capacitor, where the dielectric is rigidly held in place relative to the plates, the former effects should be small compared to the latter.) Dow also reported consistent results over a temperature range of 66°F to 102°F.

To keep the subject in an engineering perspective, however, techniques to compensate for effects of this nature are usually limited to yielding perhaps an order of magnitude improvement; first, because the problem of small differences arises and second, because no finite order parametric model can emulate the effect with unlimited precision. The advantages available with compensation schemes are significant, but such inherent limitations render the question of residual dielectric non-linearity somewhat academic. Likewise, if a circuit is of sufficient accuracy to warrant compensation for dielectric absorption, the stability with time and temperature of the compensation will be of secondary importance compared to that of other major circuit components.

III. A NEW COMPENSATION TECHNIQUE

A new technique for dielectric absorption compensation is proposed. It takes the form of Fig. 4a. If the effects of dielectric absorption are described by an ideal capacitor shunted by a dependent current source, which is some linear time-invariant function i_d of the capacitor voltage v_c, then a compensating current $i_c(v_c)$ can be developed to cancel the error current. The ideal capacitor, error source, and compensation network may then be regarded as a single entity that more closely approximates an ideal capacitor.

An implementation of this scheme using Dow's model is shown schematically in Fig. 4b. It is easily seen that the transfer function of the uncompensated integrator is given by

$$\frac{V_o(s)}{V_i(s)} = -\left[\frac{1}{R_s\left(C_\infty + \sum_{k=1}^{P} \frac{C_k}{1 + R_k C_k s}\right) s}\right] \tag{8}$$

The transfer function for the compensated case can be determined by

$$V_o(s) = -V_i(s)\left[\frac{1}{R_s\left(C_\infty + \sum_{k=1}^{P} \frac{C_k}{1 + R_k C_k s}\right) s}\right]$$

$$-V_2(s)\left[\frac{1}{\alpha R_F\left(C_\infty + \sum_{k=1}^{P} \frac{C_k}{1 + R_k C_k s}\right) s}\right]$$

where

$$V_2(s) = -V_o(s) \sum_{k=1}^{P} \frac{\alpha R_F C_k s}{1 + R_k C_k s}$$

yielding

$$V_o(s) \left[\frac{C_\infty}{C_\infty + \sum_{k=1}^{P} \frac{C_k}{1 + R_k C_k s}} \right] =$$

$$- V_i(s) \left[\frac{1}{R_s \left(C_\infty + \sum_{k=1}^{P} \frac{C_k}{1 + R_k C_k s} \right) s} \right] .$$

Thus

$$\frac{V_o(s)}{V_i(s)} = -\frac{1}{R_s C_\infty s} \quad . \tag{9}$$

This is the ideal response desired.

Note that there are minimal constraints on how the capacitor is used in such a circuit; it may be shorted or left floating, or switched to different sources, and the compensation network will continue to supply the appropriate compensation current. While the frequency response of the compensation is limited by the bandwidth of amplifier A2 in Fig. 4b, this should not be a severe restriction as this can easily be comparable to that of amplifier A1. There are other potential benefits, such as minimization of noise, offsets, etc., by removing the compensation network from the signal path.

There is conceptual simplicity in that, if the scale factor α is chosen to be unity, the $R_k C_k$ sections in the compensation network are the same as those in Dow's model and the value of resistor R_F is (ideally) arbitrary. In practice, α is chosen to be some large number

in order to scale the C_k's up to reasonable values, to scale the R_k's down to reasonable values, and to insure that any offset current through αR_F is small. The value of R_F should be chosen, along with α, to insure that the compensation amplifier operates over a reasonable dynamic range. It is clear that dielectric absorption in the compensation capacitors is of minimal importance. The resultant errors will appear in the signal path only as a small function of a small function.

It is interesting to note that the scheme works through a positive feedback loop. It is simple to show that either amplifier is stable if the loop is open. The loop transmission of the complete circuit is approximately

$$L(s) \simeq \left(-\frac{1}{\alpha R_F C_\infty s}\right)\left(-\sum_{k=1}^{P}\frac{\alpha R_F C_k s}{1 + R_k C_k s}\right)$$

$$\simeq \sum_{k=1}^{P}\frac{C_k}{C_\infty}\,\frac{1}{1 + R_k C_k s} \quad . \tag{10}$$

The configuration is thus stable for

$$\sum_{k=1}^{P}\frac{C_k}{C_\infty} < 1 \tag{11}$$

which will always be the case for any useful capacitor.

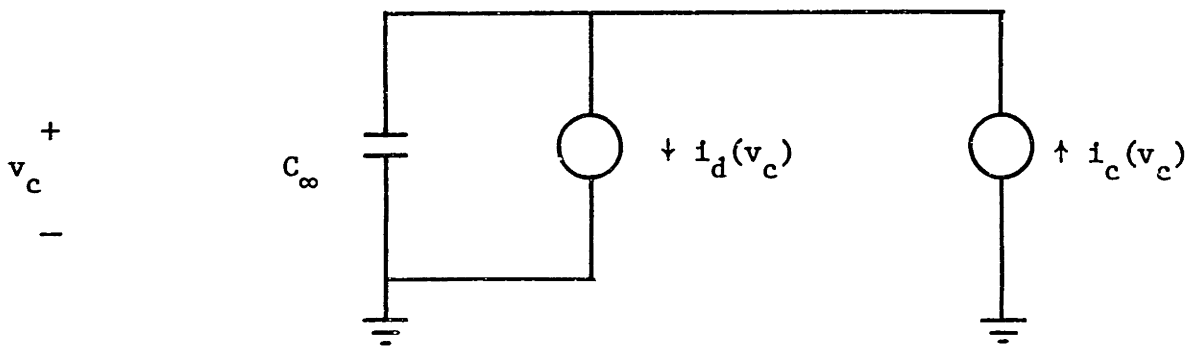

Figure 4a Proposed compensation technique

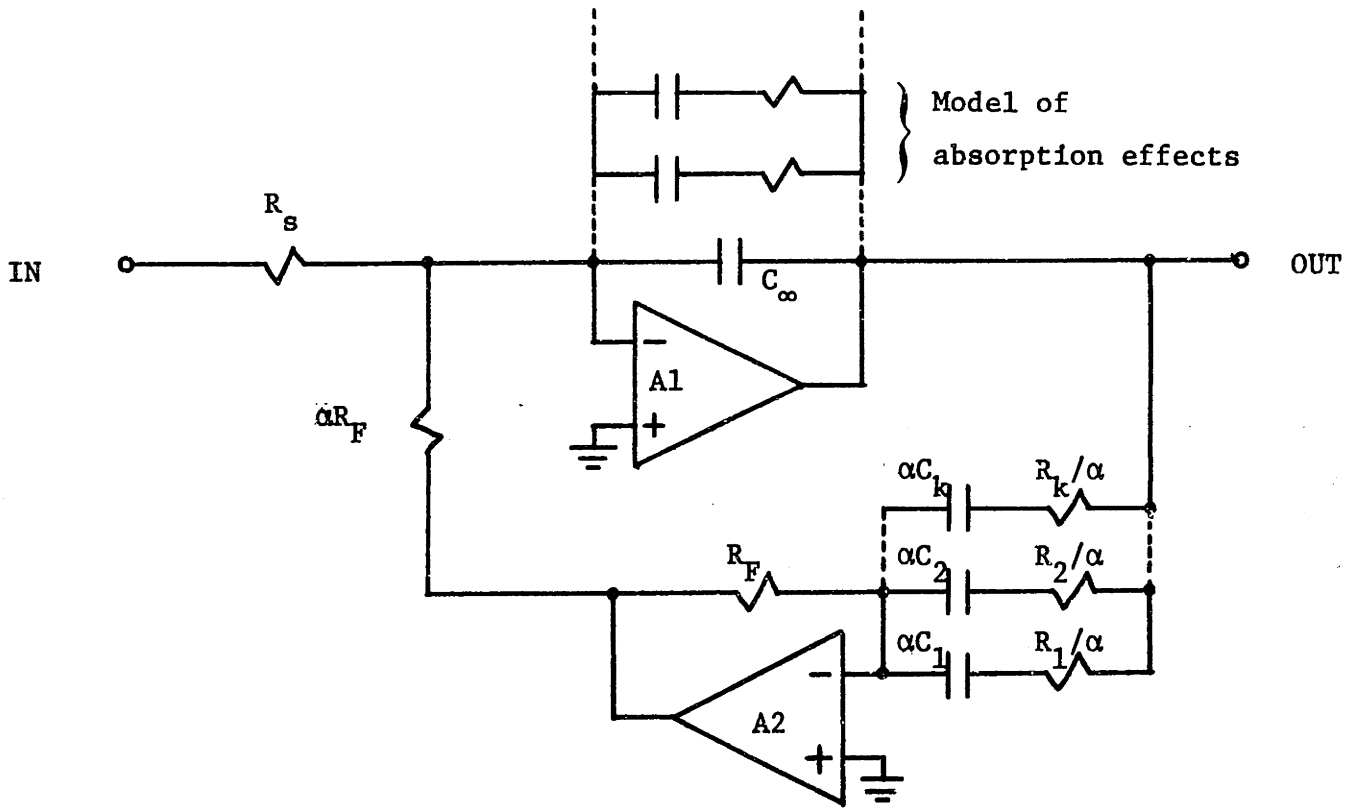

Figure 4b Implementation of the new technique

IV. PARAMETRIC MODELING OF THE RECOVERY VOLTAGE

1. Obtaining a Model

A prerequisite for constructing a compensator is knowledge of the parameters for the capacitor model to be used. Such knowledge is not generally available. In fact, it appears that Dow's paper, which includes a model for a 1 μF polystyrene capacitor, is still the only published work with this information. Unfortunately, the model is not accurate down to short enough time intervals to be of general interest today. The engineer desiring to implement compensation for dielectric absorption is thus usually required to determine the appropriate parameters on his own.

Consequently, a major part of this investigation was concerned with achieving the following four goals:

1. Development of a simple, automated procedure to gather accurate data on the effects of dielectric absorption over a time interval of interest.

2. Demonstration of a technique to perform a least mean square error fit to the acquired data in order to model these effects.

3. Characterization of a small sample of polystyrene and teflon capacitors with appropriate models.

4. Demonstration of the effectiveness of the new compensation technique using the models thus obtained.

There is a question of the most appropriate measurements to make for model determination. If we limit ourselves to the time domain, we can measure charge (or discharge) current following a voltage step, or we can measure the voltage recovery following a current impulse. From Dow's model it is easily shown that, if the capacitor is in a quiescent state, the absorption current following a step in voltage

of V_B is

$$i_d(t) = V_B \sum_{k=1}^{P} \frac{1}{R_k} e^{-t/R_k C_k} \tag{12}$$

In practice this measurement is made by shorting a fully charged capacitor. This simplifies the measurement and eliminates errors due to stray conductance across the capacitor.

If the capacitor under test is subjected to an appropriate current impulse, the voltage across it will undergo an instantaneous step change, V_B. The subsequent absorption current will cause a voltage recovery that can be approximated

$$v_r(t) \simeq \frac{1}{C_\infty} \int_o^t i_d(\tau)\, d\tau$$

$$\simeq V_B \sum_{k=1}^{P} \frac{C_k}{C_\infty} (1-e^{-t/R_k C_k}) \quad . \tag{13}$$

This approximation is valid as long as the recovery voltage v_r is small compared to the step V_B. In practice the voltage step is implemented by shorting a fully charged capacitor for a time that is short compared to any time constants of interest.

The latter technique has several advantages over the former. The absorption current can have a high dynamic range over a resonable time interval, and chances of accurately resolving small components is increased through integration. More importantly, in many circuits that we may wish to compensate (e.g., high accuracy sample/hold circuits) it is important to recognize that it is not the absorption current per se that results in errors, but the recovery voltage. If we choose to compensate with a model derived from the absorption current,

then the recovery voltage will be a weighted integral of the error between the absorption and compensation currents; this, in general, will not guarantee optimum voltage recovery characteristics. Alternatively, basing our model parameters on the recovery voltage provides us with the best chance of minimizing some measure of that error.

2. Data Acquisition

A breadboard for testing capacitor dielectric absorption characteristics was designed and built. The circuit is shown schematically in Fig. 5. It has several features to avoid introducing any irreducible system errors into the measurements, and warrants some description.

The capacitor under test is connected as the feedback element of operational amplifier A1, in a standard integrator configuration. During the charging interval switches SW1A and SW1B are closed to ground, and switches SW2A and SW2B are closed to connect a 10 kΩ resistor between the output of instrumentation amplifier A2 and the input of A1. In this configuration, the output of A1, and thus the voltage across the capacitor, is forced to the value of the reference voltage at the inverting input of A2. This voltage is supplied by ± 10 volt reference R1, and the polarity is selected via switch SW3A. Switch SW3B is for test purposes only. During the charging interval, switch SW4 is closed to prevent the X100 amplifier A3 from saturating.

During the discharge interval switches SW1A and SW1B are closed to short out the capacitor, and switches SW2A and SW2B are closed to ground.

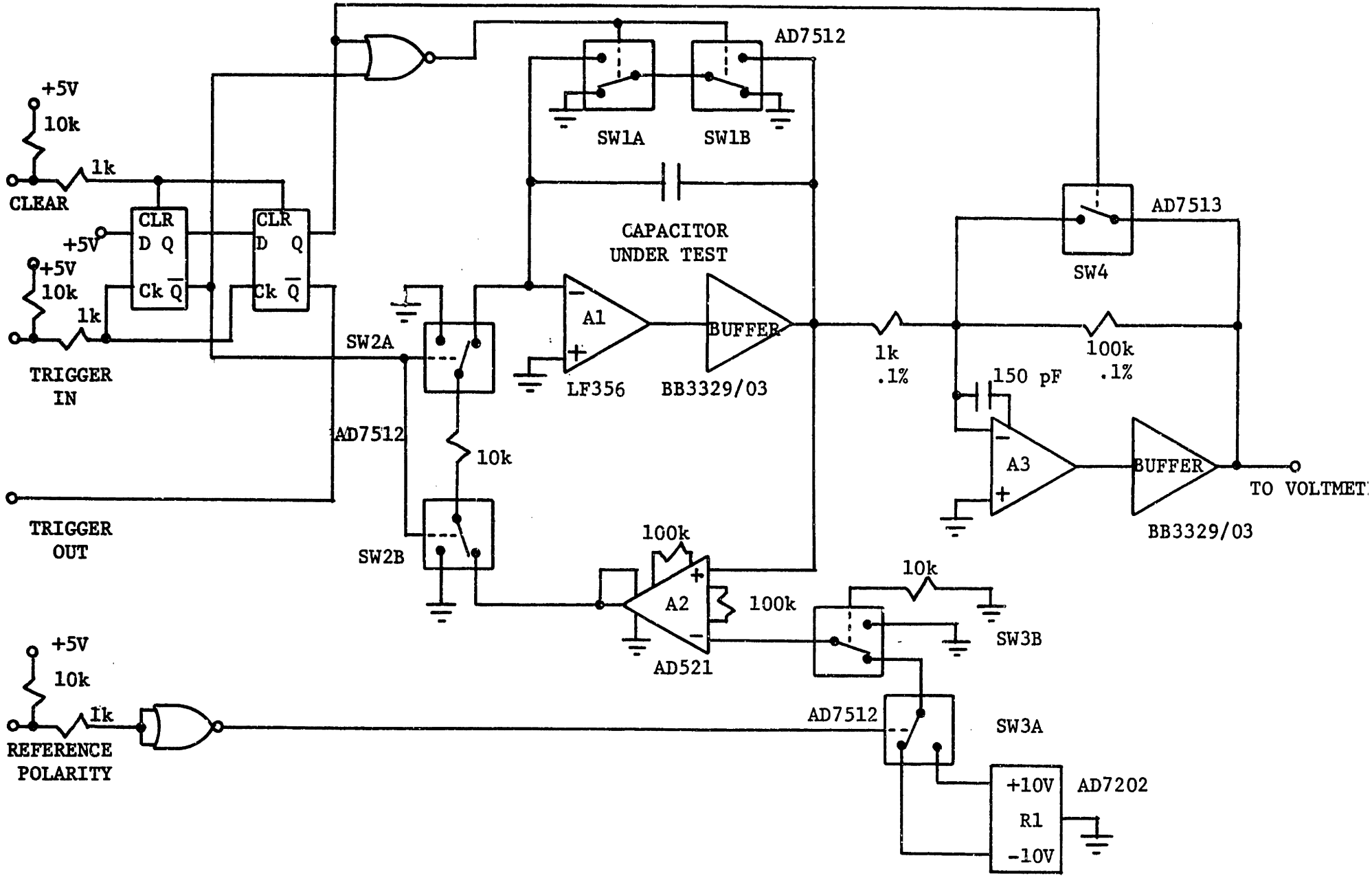

Figure 5 Circuit for measuring capacitor dielectric absorption characteristics

At the beginning of the measurement interval, switches SW1A and SW1B are again closed to ground to leave the capacitor floating, and switch SW4 is opened to amplify the subsequent recovery voltage. At this time, the logic also supplies a trigger to initiate measurements by a digital voltmeter.

The unusual configuration of the dual single-pole double-throw CMOS switches SW1 and SW2 was selected to prevent any voltage drop across them during the measurement interval. It was found that such a situation could modify the channel leakage and significantly affect the results. The selection of switch and amplifier configurations was chosen to minimize currents in the ground circuit as well.

Thermal effects in the critical amplifiers A1 and A3 are minimized by the inclusion of current buffers, in their feedback loops, at their outputs.

Logic to drive the switches is all CMOS to minimize any supply or ground transients. The logic also uses a ground return separate from the analog circuitry. An on-board 5 volt regulator is included to simplify external power connections and to protect the CMOS switches from being driven while powered down. Overall control is supplied through external computer-generated logic signals.

There are several apparent sources of measurement error (particularly amplifier offsets, amplifier and switch bias currents, and charge pumping from the switches to the capacitor under test) that were eliminated from the final results by a simple technique. The charging voltage was alternated in polarity for successive measurement runs, and the resulting measurements alternately added to or subtracted from a running

total. A total of ten runs for each capacitor was made. Any error independent of the initial capacitor charge was thus subtracted out. This averaging technique had the added benefit of reducing measurement uncertainty; because the signal always had a noise component with a peak value comparable to two levels of voltmeter quantization, the mean of several measurements was statistically driven to a point close to the true signal value.

All measurements were made at room temperature, with the breadboard protected from stray air currents to prevent thermal anomalies.

The measurements were made with a Hewlett-Packard Model 3437A system voltmeter, connected through the IEEE instrument bus to a PDP-11/03 DECLAB minicomputer. The programs are included in the Appendix. A capacitor charge time of 10 minutes was used (which was later found to be excessively conservative) along with a discharge time of 50 μs. A total of 9999 samples were taken during each run, using a sampling rate of 5000 Hz.

Measurements were taken on four capacitors, two each of polystyrene and teflon. The value of each was .01 μF, ± 1%. The units were manufactured by Component Research Co., and are typical of capacitors that might be used in high accuracy applications.

Results of the measurements are shown graphically in Figs. 6-9. Although the effects of dielectric absorption are small compared to those of offsets, bias currents, and charge pumping in the measurement setup, these results were found to be stable and highly repeatable.

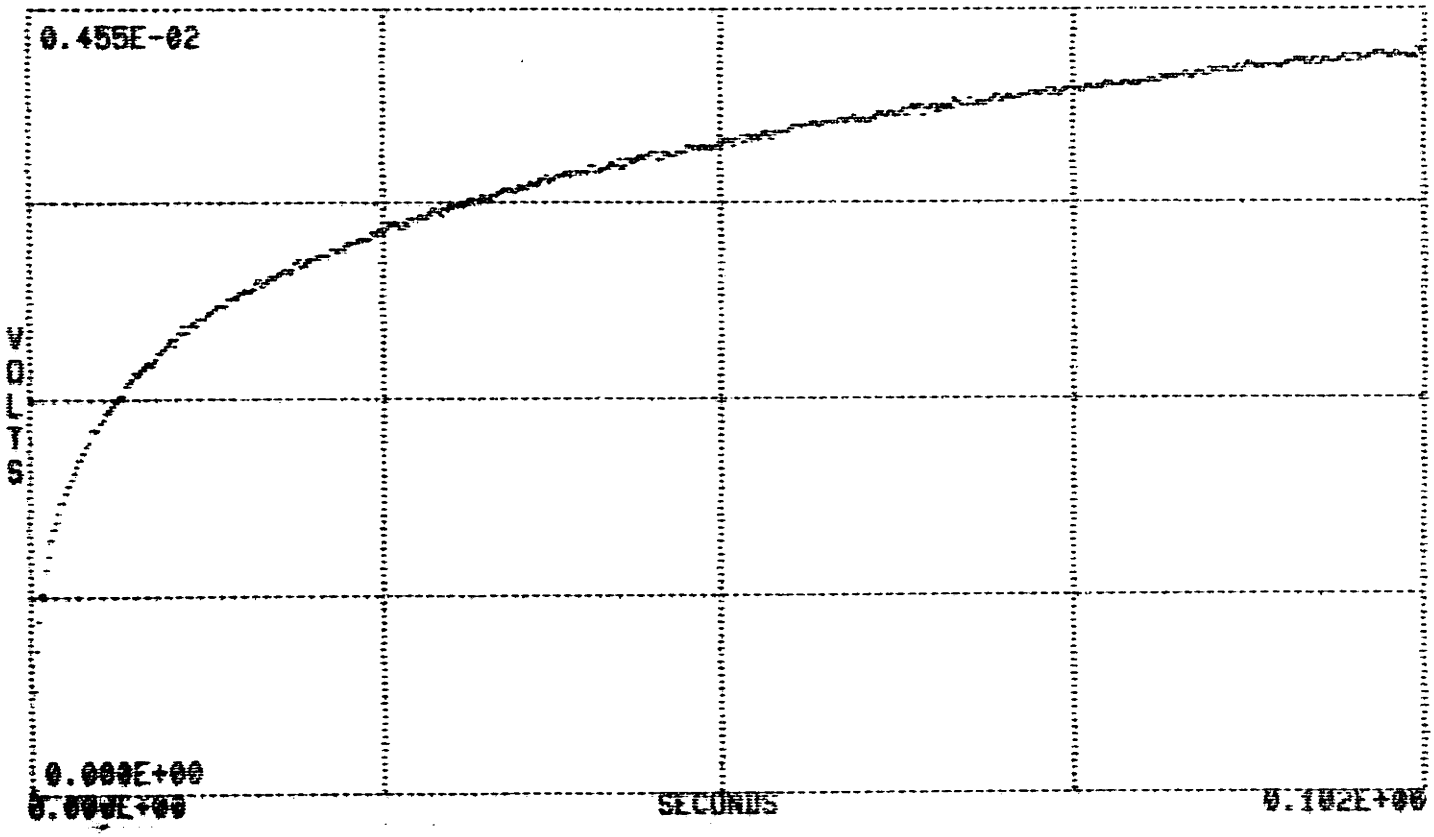

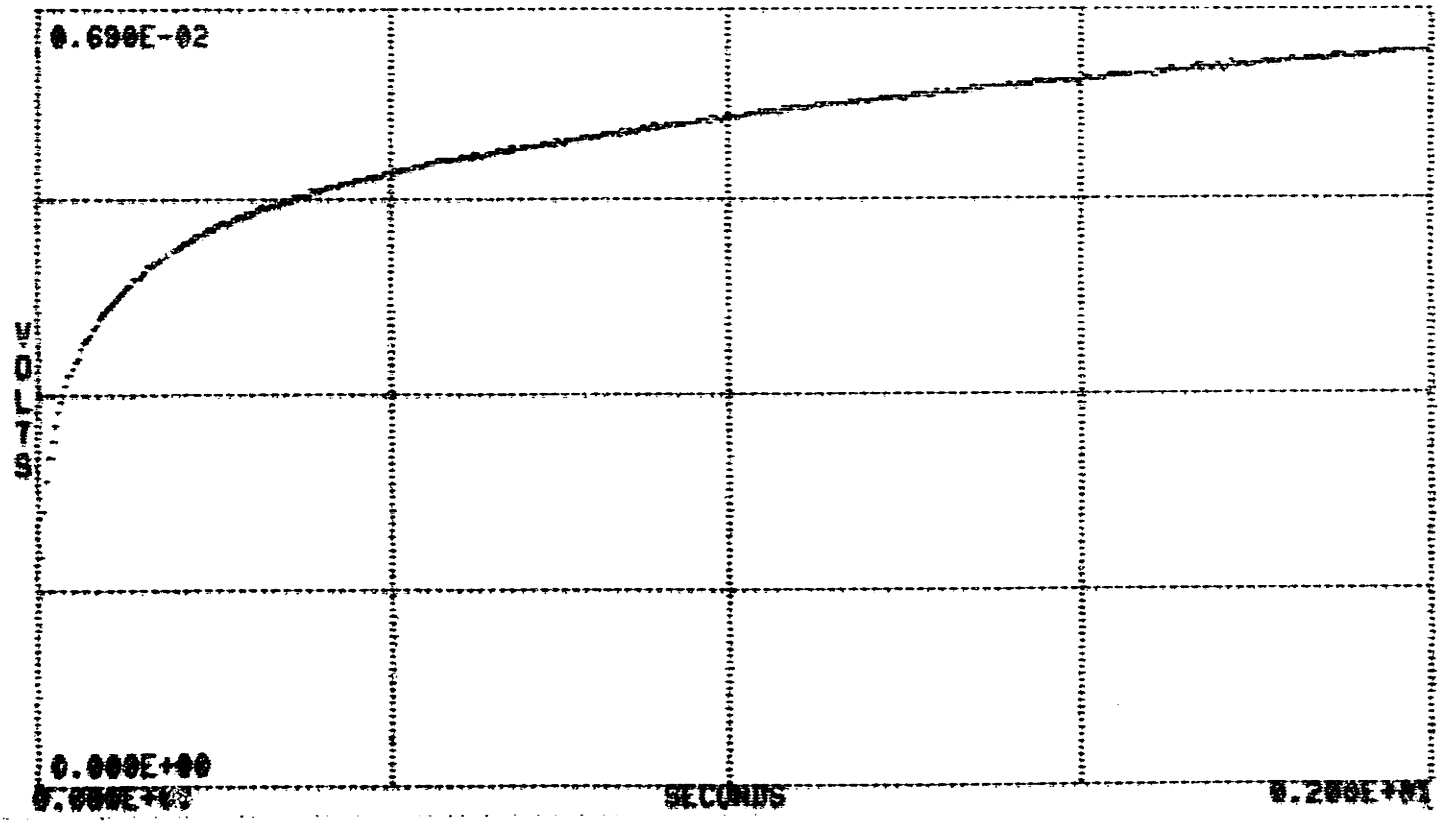

Figure 6 Recovery voltage of .01 μF teflon capacitor, sample 1.

102 ms interval (top) and
2 s interval (bottom)

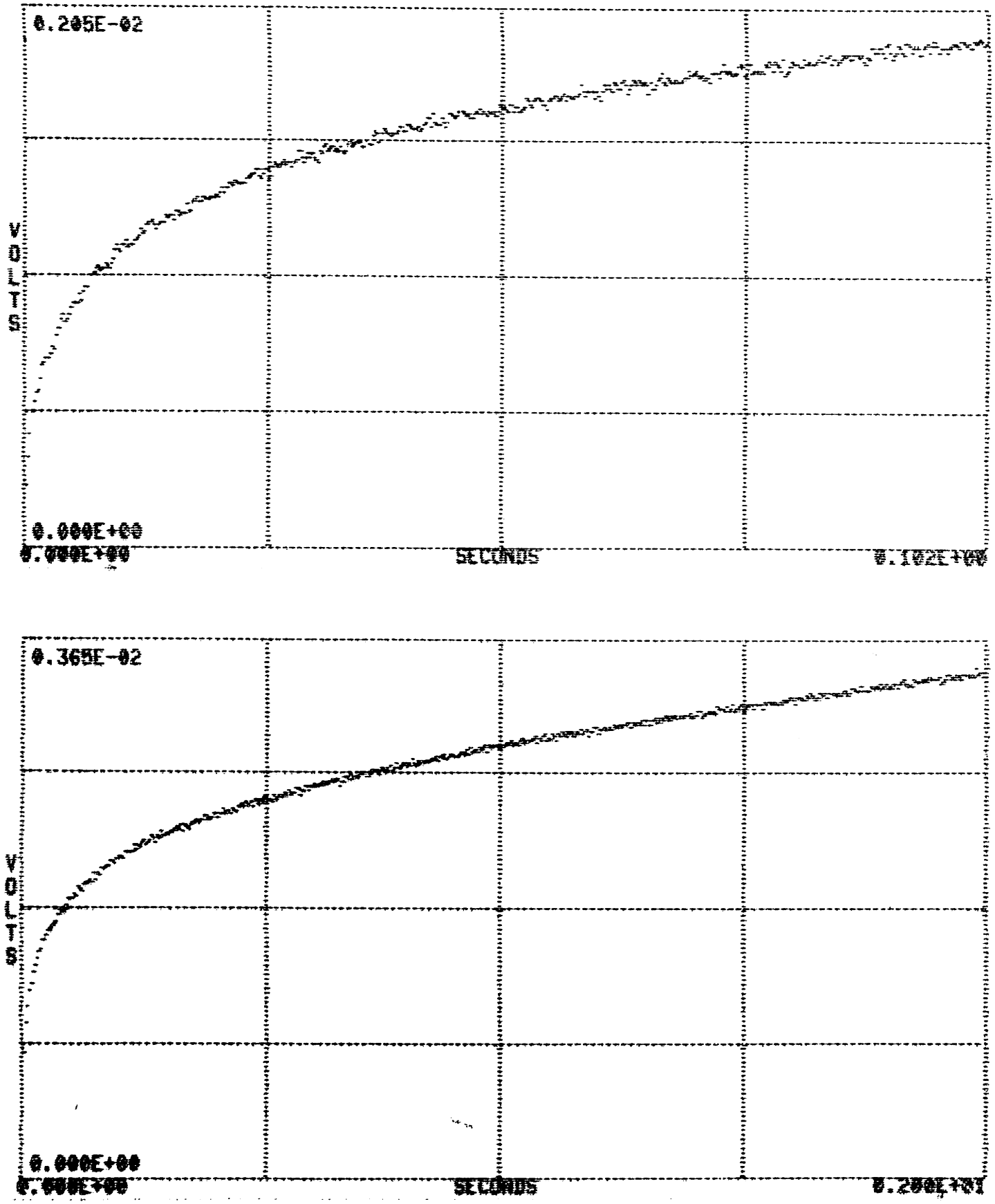

Figure 7 Recovery voltage of .01 μF teflon capacitor, sample 2.

102 ms interval (top) and
2 s interval (bottom)

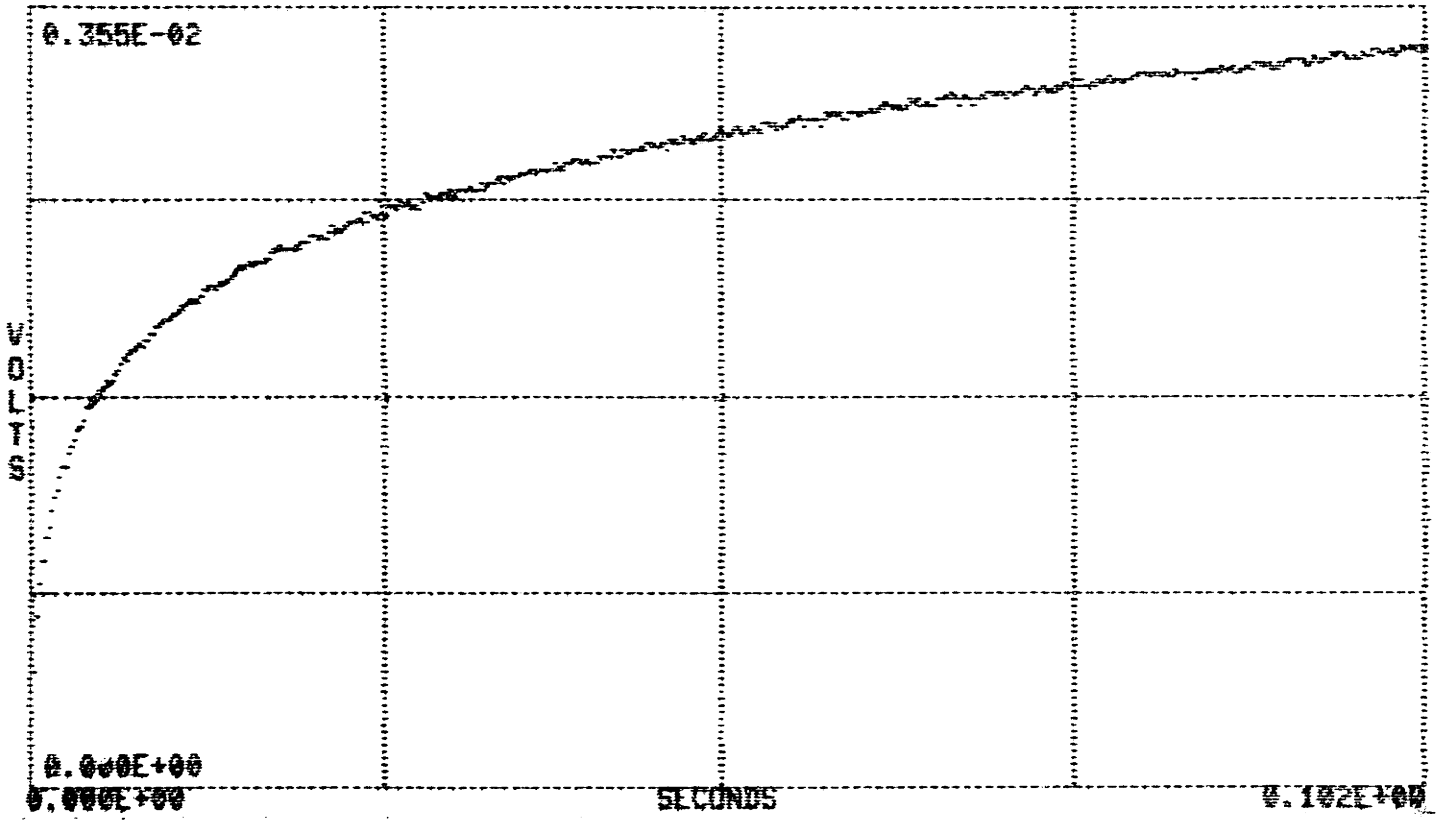

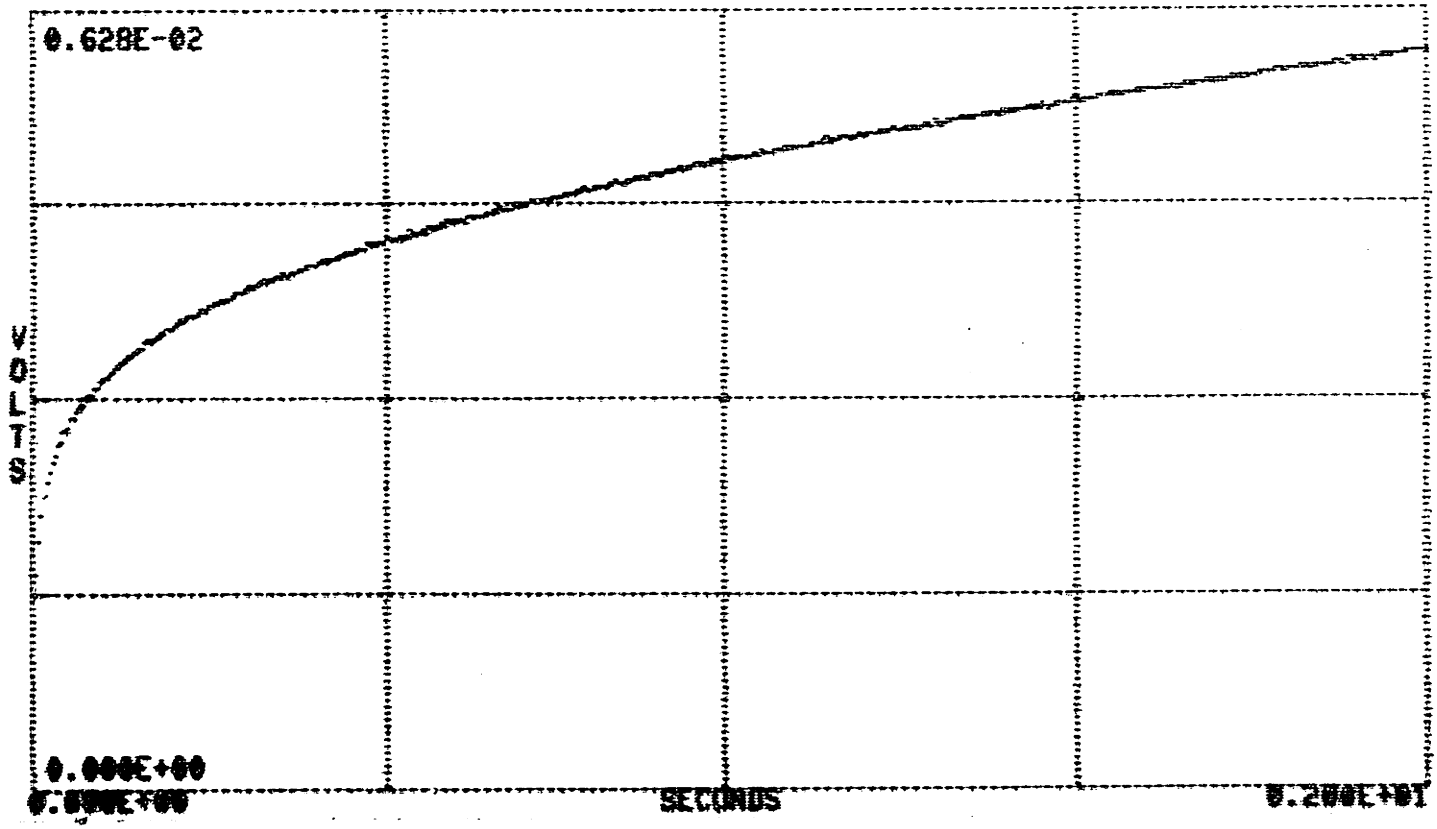

Figure 8 Recovery voltage of .01 μF polystyrene capacitor, sample 1.

102 ms interval (top) and
2 s interval (bottom)

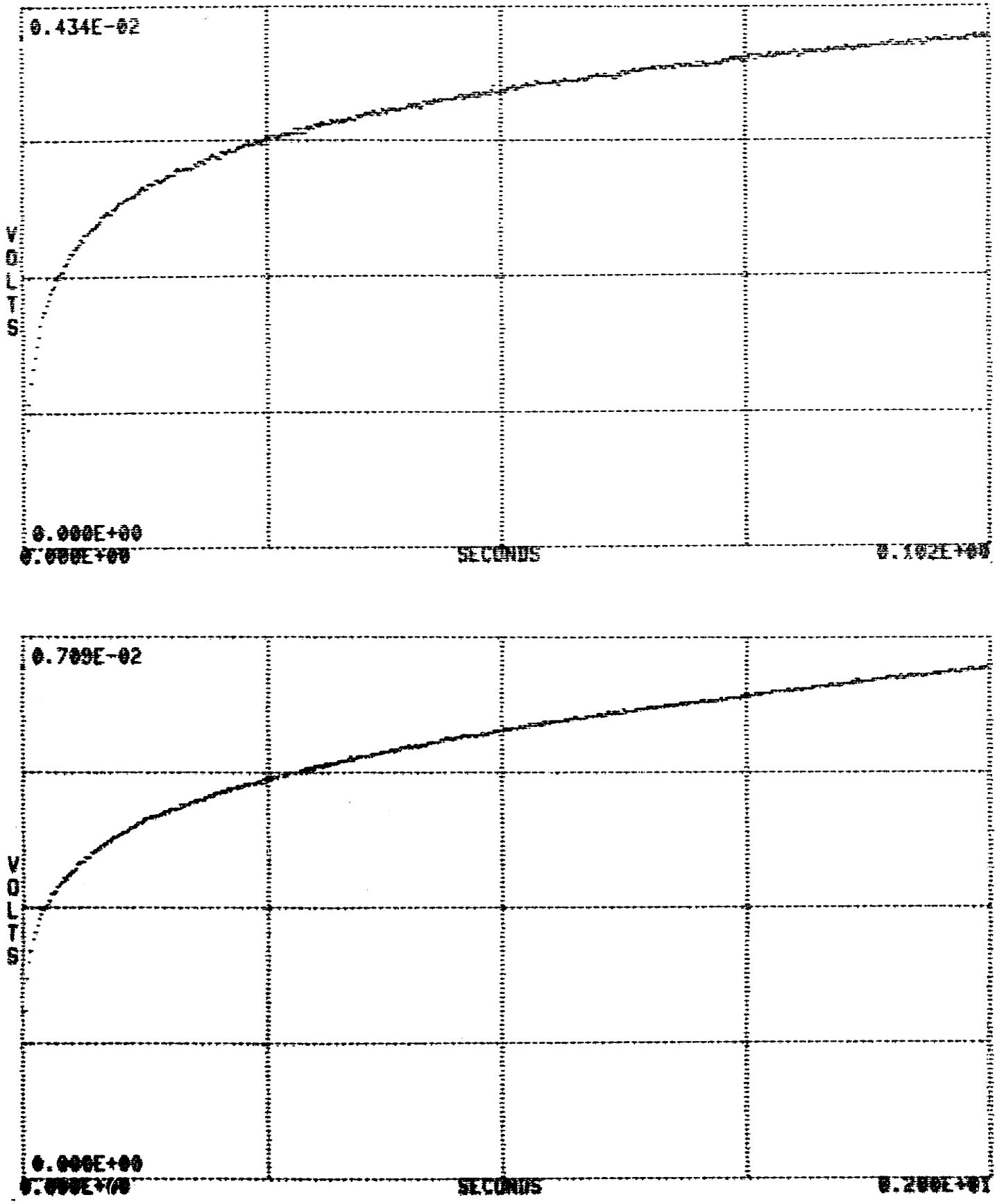

Figure 9 Recovery voltage of .01 μF polystyrene capacitor, sample 2.

102 ms interval (top) and
2 s interval (bottom)

3. Data Reduction

Knowing the recovery voltage of a capacitor, we may apply a procedure generally known as parametric modeling to obtain an appropriate linear model. The procedure assumes knowledge of the input to a system and its subsequent output, and determines the parameters of a model of specified form to minimize some measure of the error between the system's response and the model's response. The problem becomes, then, one of optimization, with the model parameters as the variables.

A mean square error norm was selected for the modeling procedure, because of its analytic tractability. In the general case, we may write

$$e[n] = v_r[n] - h[n] \tag{14}$$

$$E = \sum_{n=o}^{M-1} w^2[n]\, e^2[n] \tag{15}$$

where $v_r[n]$ is our data and $h[n]$ is the sampled response of our model to a current impulse over an interval $n = 0, 1, \ldots, M-1$. The weighting function $w[n]$ allows us the option of placing a greater penalty on errors over some portion of the interval. We wish to minimize the error measure E with respect to N model parameters a_i. A necessary condition that the optimum parameters a_i^* must satisfy is

$$\frac{\partial E}{\partial a_i^*} = 0$$

Thus

$$-2 \sum_{n=o}^{M-1} w^2[n]\, e[n]\, \frac{\partial h[n]}{\partial a_i^*} = 0 \quad ; \quad i = 1, 2, \ldots, N \tag{16}$$

If the N equations given by (16) are linear, then the answer can be obtained analytically in closed form, and the minimum is guaranteed to be a global one.

This is not the case when Dow's model is used. The equations are linear with respect to the coefficients, but not with respect to the time constants. There are added constraints (which are obvious from the physical model but, in general, must be incorporated in the optimization) that each R_k and C_k must be real and non-negative. It is also the case for higher order models (as will be demonstrated) that local minima exist on the error surface that are substantially removed from the true optimum; there is no well defined technique for preventing an algorithm from converging on these points. All these considerations define a fairly difficult optimization problem.

This is not, of course, a failing of Dow's model. It can be shown that any linear, time invariant, lumped parameter model (i.e., one whose impulse response is a sum of expcnentials) will bring us to the same difficulty.

Several techniques to perform this curve fit were investigated, including Prony's method[12][13], Shank's method[14], the Newton-Raphson method[15], fitting with orthogonal exponential functions[12], and fitting to some intermediate approximation[12]. None were satisfactory. Most of these approaches suffer from one or both of the facts that we do not know the time constants and that there are constraints on the parameters.

As a result, the gradient descent method of Fletcher and Powell was employed. Gradient descent methods in general place no demands on the

linearity of the function to be minimized, only on its continuity and differentiability. They are also potentially more accurate than other methods, but the computational burden is high. In order to meet the constraints on the parameters, a simple trick was used. Rather than minimize with respect to the parameters we want, the algorithm was configured to minimize with respect to parameters that are defined as the square roots of those we want. The minimization thus becomes unconstrained.

From Eqs. (13) and (15) the problem may be stated formally.

$$\text{minimize} \quad E = \sum_{n=o}^{M-1} w^2[n] \left(v_r[n] - \sum_{k=1}^{P} b_k^2 (1-\exp(-nT/a_k^2))\right)^2 \tag{17}$$

with respect to b_k, a_k; k = 1, 2, ..., P,

where

$$a_k^2 = R_k C_k$$

$$b_k^2 = V_B \frac{C_k}{C_\infty} \tag{18}$$

$$T = 200 \times 10^{-6} \text{ (sampling period)}$$

The minimization thus takes place in 2P-dimensional space, and the algorithm operates by trying to drive the gradient to zero. This, of course is equivalent to trying to satisfy Eq. (16). The entries in the gradient vector are given by

$$\frac{\partial E}{\partial a_i} = 4 \sum_{n=0}^{M-1} w^2[n]\, e[n]\, \left(b_i^2 \frac{nT}{a_i^3} \exp\left(-nT/a_i^3\right)\right)$$

$$\frac{\partial E}{\partial b_i} = -4 \sum_{n=0}^{M-1} w^2[n]\, e[n]\, \left(b_i \left(1-\exp\left(-nT/a_i^2\right)\right)\right) \qquad (19)$$

$$i = 1,2, \ldots P$$

where

$$e[n] = v_r[n] - \sum_{k=0}^{P} b_k^2 \left(1-\exp\left(-nT/a_k^2\right)\right) \quad .$$

Note that $\frac{\partial E}{\partial a_i}$ does not exist for $a_i=0$, and this could be troublesome. In practice, it was not an issue.

One of the simpler gradient search techniques is the method of steepest descent, or the method of optimum gradients. If we denote the parameter vector by X, and the gradient by $\nabla E(X)$, the algorithm iterates according to

$$X_{i+1} = X_i - \alpha_i \nabla E(X_i)$$

where α_i is a scaler chosen to minimize the function

$$E(X_i - \alpha \nabla E(X_i))$$

At each iteration, then, the algorithm steps down the gradient until it finds a minimum along that direction, then finds the gradient at that point and reiterates until some stopping condition is reached.

In this way, the direction at each iteration is orthogonal to the direction at the prior iteration.

This orthogonality of successive directions leads to slow convergence for most functions of interest. More efficient algorithms have been developed, based on the concept of conjugate directions, and the method of Fletcher and Powell is generally accepted as being the most powerful of these. Central to the method is a positive definite matrix H which is updated at each step and which modifies the direction of search.

The algorithm is defined by

$$X_{i+1} = X_i - \alpha_i \, H \, \nabla E(X_i)$$

$$H_{i+1} = H_i + A_i + B_i \tag{20}$$

where α_i is a scalar chosen to minimize the function

$$E(X_i - \alpha \, H \, \nabla E(X_i))$$

and matrices A_i and B_i are defined by

$$A_i = \frac{\sigma_i \, \sigma_i^T}{\sigma_i^T \, y_i}$$

$$B_i = - \frac{H_i \, y_i \, y_i^T \, H_i}{y_i^T \, H_i \, y_i}$$

$$\sigma_i = - \alpha_i \, H_i \, \nabla E(X_i)$$

$$y_i = \nabla E(X_{i+1}) - \nabla E(X_i) \tag{21}$$

The initial steering matrix H_o can be chosen to be any positive definite matrix, and in practice is usually the identity matrix.

Fletcher and Powell prove a number of important properties of this rather formidable looking algorithm in Ref. [16]. Suffice to say it is relatively simple to implement and, in our application, proved itself significantly more efficient than the method of steepest descent.

Computationally, the most time consuming portion of each iteration is determining the optimum step size α. At the start of this procedure a minimum step size is computed, which is scaled to cause no more than a one percent change in any of the parameters when taken down the direction of search. The procedure then starts with a step in the direction of search that is sixteen times this length, determines the error at the new point, and decides to continue stepping forward or to reverse. Subsequent step sizes are scaled up or down by factors of two as the procedure steps back and forth to converge on α_i. When the interval of uncertainty has been reduced to the minimum step size, the interval is bisected and the error determined at the center point. Finally, another point is determined by fitting a quadratic to the error values at these three points and determining the error at the point corresponding to the minimum of the quadratic. The final point is the one of these four with the lowest corresponding error value. In this way, the update of the parameters at each iteration is guaranteed to be optimum within one-half percent. Convergence is defined when no step size larger than the minimum can be taken to decrease the error. It was found to be advantageous to reset the H matrix to H_o at this point and do another iteration as a final check on convergence. In some cases, this resulted in a

new series of iterations, indicating that the algorithm had not, in fact, converged. It is assumed that this was due to accumulated round-off errors in the matrix H.

An essential part of getting a gradient search started is making a reasonable initial guess for the parameters. This was done in two steps. First, the time constants were chosen to be geometrically spaced along the interval of interest. All the coefficients were then set equal to a single value, which was determined through a simple least mean square fit over the interval. The resulting initial parameters are given by

$$a_k 2 = R_k C_k = TM^{-k/P+1}$$

$$b_k^2 = V_B \frac{C_k}{C_\infty} = \frac{\sum_{n=0}^{M-1} w^2[n]\, v_r[n] \sum_{k=1}^{P} (1-\exp(-nT/R_k C_k))}{\sum_{n=0}^{M-1} w2[n] \sum_{k=1}^{P} (1-\exp(-nT/R_k C_k))}$$

$$k = 1,2,\ldots P \qquad (22)$$

This simple initialization defines a model in which the C_k's are equal and the R_k's form a geometric series.

Finally, the weighting function was chosen to be of the form

$$w[n] = w_c^{\,n}$$

where w_c is a constant chosen by the user. Least mean square error optimization procedures often result in an error with a high peak to average ratio, and the weighting function was incorporated to lessen the effect, should it arise. In practice, this was not a major issue.

The programs to perform the curve fit are included in the Appendix. As the main program begins, the user interactively specifies the data block length M (i.e. the interval of interest), the number of poles P in the model (i.e. the number of sections), the weighting parameter w_c, and the maximum number of iterations the descent algorithm is to perform. Upon termination, the program returns the parameters b_k^2 and a_k^2.

V. EXPERIMENTAL RESULTS

The choice of the interval length over which to model is, of course, highly application dependent. An equally important application dependent choice is that of resolution, determined by the sampling rate of the recovery voltage. Together, these choices determine the block length and have a first order effect on the amount of computation necessary to determine a model; because of the relative ease of gathering large amounts of data, and the relative difficulty of reducing it, it is important to recognize that the problem of selecting a reasonable block length for parameter estimation involves fundamental trade-offs.

As a consequence of the computational burden of the parametric modeling procedure, this investigation focused primarily on data block lengths of 512 points, corresponding to time intervals of 102 ms, rather than on the full available block lengths of 9999 points. The results of the modeling procedure over the shorter interval for one capacitor (teflon, sample 1) are shown graphically in Figs. 10-17 for model orders one through eight. The results for the other three samples are qualitatively similar and are not included here in graphical form.

There are two speculations concerning these issues which were not investigated in detail. First, it is reasonable to expect that the density of sample points in the interval of interest, beyond some minimal criteria, will not have a major effect on the final model parameters. This can be expected because of the obvious exponential character of the recovery voltage, and the fact that the fitting functions are exponentials. In practice, this could have the effect of

substantially reducing the amount of computation necessary to obtain a model. Second, it can be expected that the results obtained over the primary interval of interest in this report may be generalized to other intervals, both longer and shorter, because of the similar character of the recovery voltage over different intervals, as shown in Figs. 6-9. There is some support for these speculations in Figs. 18-20. These graphs are the results of parametric modeling, using the data from the same teflon capacitor as before, over a block length of 9999 points, corresponding to an interval of 2s. The character of the error curves, and the resulting mean square errors, are very similar to those obtained over the much shorter block length of 512 points.

The propensity of least mean square error procedures for yielding peaked error curves can be seen in these graphs. In most of the cases, the location of the peaks is confined primarily to the first few percent of the interval, and these errors may not be important in many applications.

It is also clear from the graphs, and from the tables to be presented, that model orders greater than two or three will yield diminishing returns for most compensation applications, at least over the intervals presented here.

We may also see that, for some model orders, the modeling procedure failed to find a global minimum (as evidenced by the fact that the mean square error sometimes increases with model order; a high order model can, ideally, always do at least as well as the next lower order model by setting one coefficient to zero and converging to otherwise equal parameters). Since the descent algorithm always converged to a point with

zero gradient, this is a demonstration of the fact that the error surfaces of at least some models contain local minima that do not correspond to the best solution. It is reasonable to expect error surfaces of higher order models to exhibit more points of local minima than those of lower order, and the results obtained are consistent with this expectation.

It should be emphasized that it is usually difficult or impossible, in theory and practice, to guarantee that solutions to this type of problem (i.e. minimization of a non-linear function through a gradient descent technique) are optimal. In applications where this issue is important, it is often dealt with, though never eliminated, by performing several minimizations with different initial conditions. Some of the models presented here are the result of this strategy. However, the strongest statement we can make concerning these models is that they are good, with respect to the error measure; we cannot claim that they are optimal.

The models and corresponding errors for all four capacitors are included here in Tables 1-4. In all cases, the modeling was done over a 512 point interval. (The coefficients in these tables have been corrected according to a procedure described in the next section.) One important result, with major impact on the issue of compensation, is that no single model is appropriate for either dielectric. This is clearly evident from the data plots of Figs. 6-9 as well, where the recovery voltage of the two teflon capacitors, for example, differ in magnitude by an approximate factor of two. This consistent with the generally held belief that the lower frequency characteristics of

dielectric absorption, which include the characteristics we are modeling, are primarily a function of interfacial polarizations, as discussed in Chapter I. If this is the case, then it would not be unexpected to find that the dielectric inhomogeneities causing this effect were a function of variables in processing the dielectric material and in manufacturing the capacitors. Interestingly, the manufacturer specifies dielectric absorption for the teflon capacitors at .01% (recovery voltage following a short charge-discharge cycle), but offers to select units guaranteed to .0035%. From this evidence alone, we should not be surprised to find samples that differ in magnitude of recovery voltage by a factor of three.

The data presented here raise an interesting speculation that merits further investigation. It is notable that, aside from a scale factor, all four capacitors have recovery characteristics that are quite similar. The possibility suggests itself that it may be possible to specify a general model, reasonably accurate to within some scale factor, to characterize one or more dielectrics. This existence of such a model would assume that the rate of charge release by the absorptive component of the dielectric, referenced to the total charge in this component, was well controlled from capacitor to capacitor, while the total amount of charge there was not. While it cannot be claimed that the small number of samples investigated in this report are statistically significant, Tables 1-4 contain some modest quantitative support for this speculation. The time constants for several models correspond reasonably well from sample to sample (at least in those cases where the minimization procedure appears to have converged to corresponding relative minima, as

evidenced by the rms error). In these cases, there is also correspondence in the relative magnitudes of the coefficients.

Because the recovery voltage is monotonically increasing and exponential in character, it is reasonable to assume that a wide range of model parameters would work at least moderately well; in other words, that the minima of the error surfaces lie in a region that is broad and low. (This assumption was partially verified by observing the operation of the descent algorithm. Generally, the initial guess at the beginning of the procedure succeeded in achieving over 90% of the final rms error reduction.) The implications are important to any efforts at compensation. If a general model of any order could be specified for a dielectric, reasonably accurate to within a scale factor, it would mean that the user would have to determine only a single parameter for any capacitor to successfully compensate for dielectric absorption effects. For the technique described in Chapter III, this would mean determining the scale factor α in the compensation network. This parameter could be adjusted by changing the value of a single resistor, and could be made part of a simple trimming procedure.

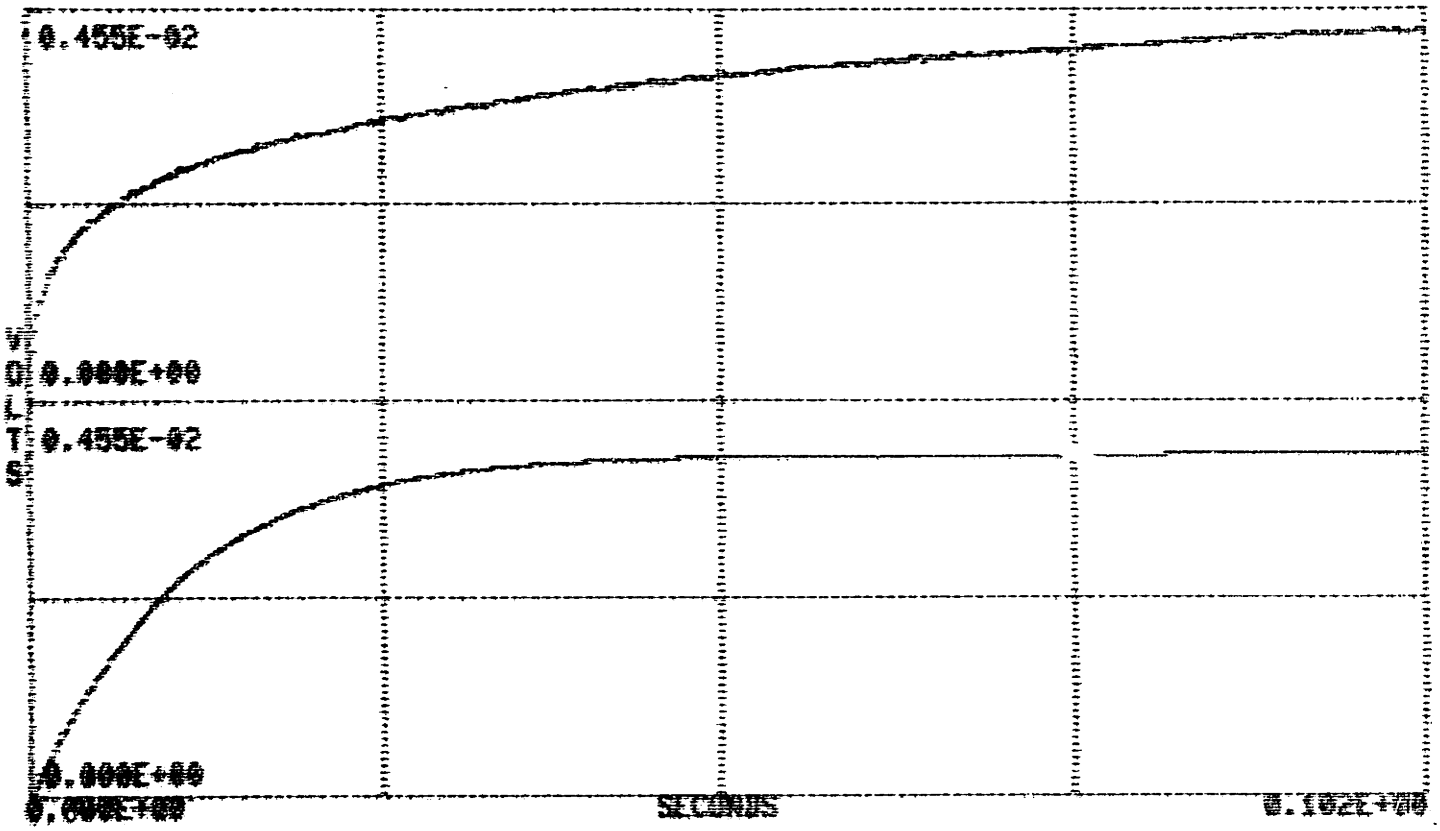

DATA (TOP GRAPH) AND APPROXIMATION (LOWER GRAPH) 30-APR-78

BLOCK LENGTH PLOTTED:	512
BLOCK LENGTH FOR PARAMETER ESTIMATION:	512
NUMBER OF POLES:	1
EXPONENTIAL ERROR WEIGHTING:	1.00000

ESTIMATED SIGNAL PARAMETERS

COEFFICIENTS	TIME CONSTANTS
0.3048E-02	0.1046E-01

Figure 10a First order approximation to recovery voltage of .01 μF teflon capacitor, sample 1.

102 ms interval

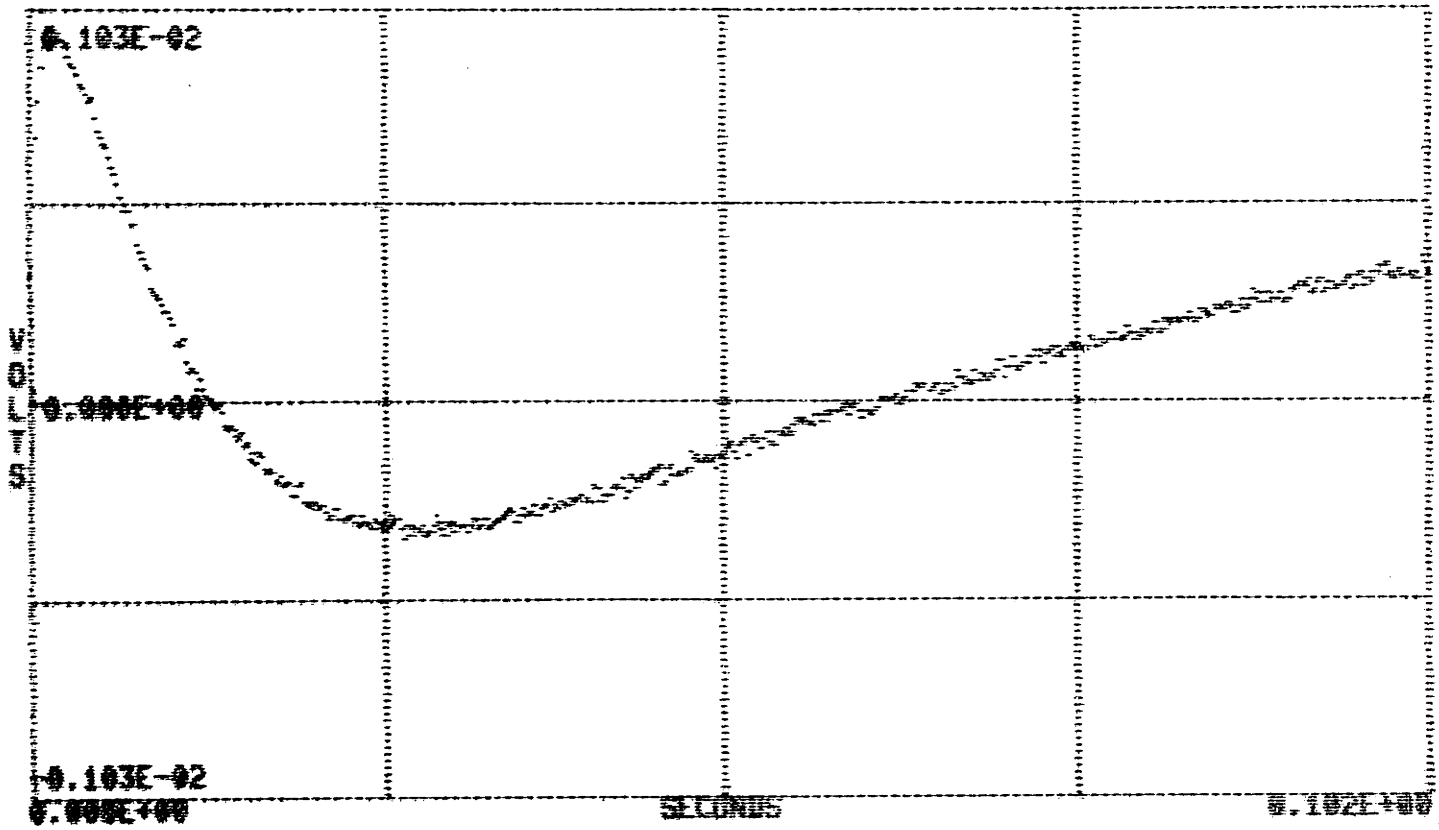

ERROR (DATA MINUS APPROXIMATION) 30-APR-76

BLOCK LENGTH PLOTTED:	512
BLOCK LENGTH FOR PARAMETER ESTIMATION:	512
NUMBER OF POLES:	1
EXPONENTIAL ERROR WEIGHTING:	1.00000
TOTAL NORMALIZED WEIGHTED MEAN SQUARE ERROR:	0.680197E-02

Figure 10b Error of first order approximation.

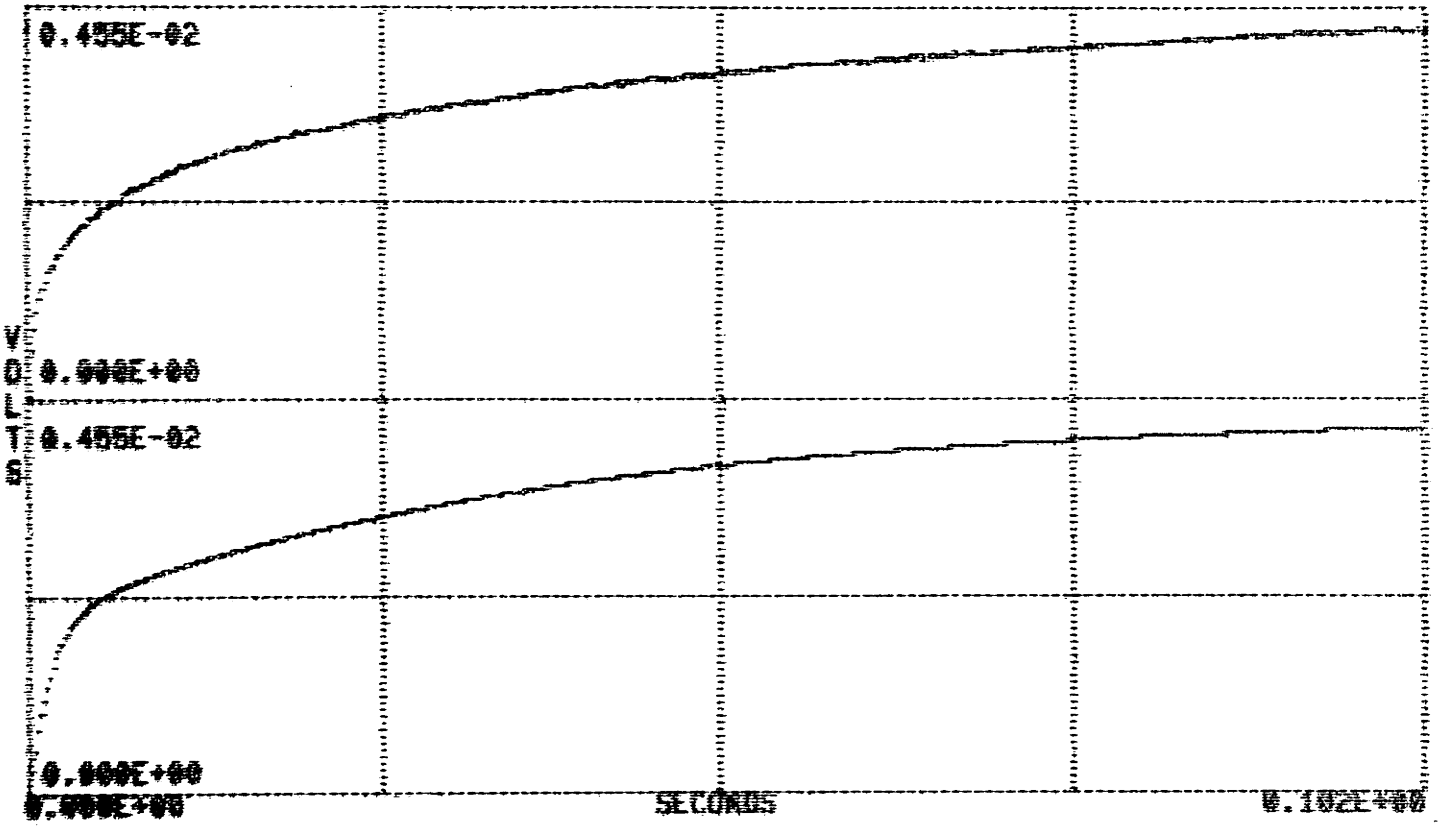

DATA (TOP GRAPH) AND APPROXIMATION (LOWER GRAPH) 30-APR-78

BLOCK LENGTH PLOTTED:	512
BLOCK LENGTH FOR PARAMETER ESTIMATION:	512
NUMBER OF POLES:	2
EXPONENTIAL ERROR WEIGHTING:	1.00000

ESTIMATED SIGNAL PARAMETERS

COEFFICIENTS	TIME CONSTANTS
0.2065E-02	0.1428E-02
0.2328E-02	0.3671E-01

Figure 11a Second order approximation to recovery voltage of .01 μF teflon capacitor, sample 1.

102 ms interval

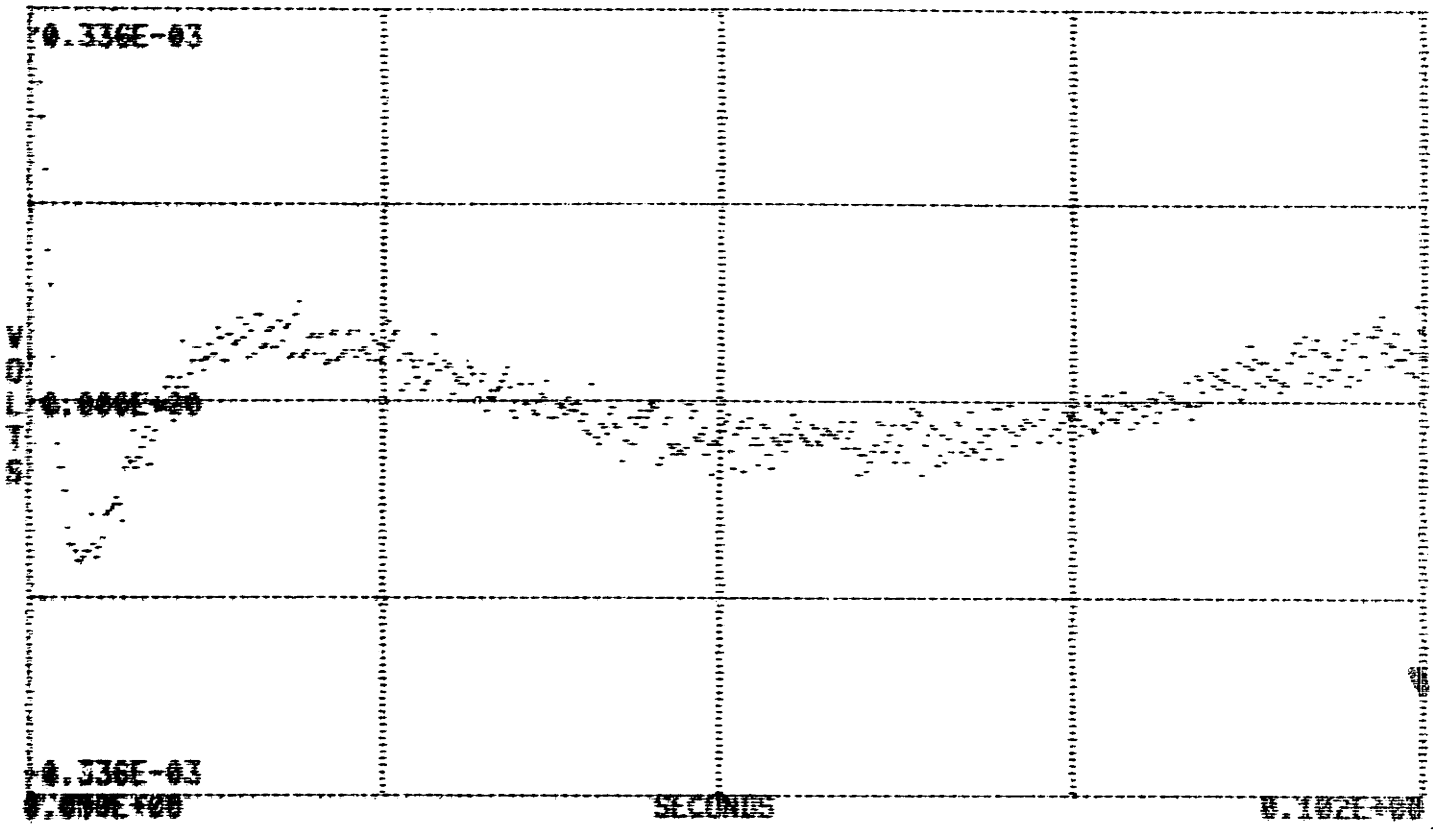

ERROR (DATA MINUS APPROXIMATION) 30-APR-78

BLOCK LENGTH PLOTTED:	512
BLOCK LENGTH FOR PARAMETER ESTIMATION:	512
NUMBER OF POLES:	2
EXPONENTIAL ERROR WEIGHTING:	1.00000
TOTAL NORMALIZED WEIGHTED MEAN SQUARE ERROR:	0.100237E-03

Figure 11b Error of second order approximation.

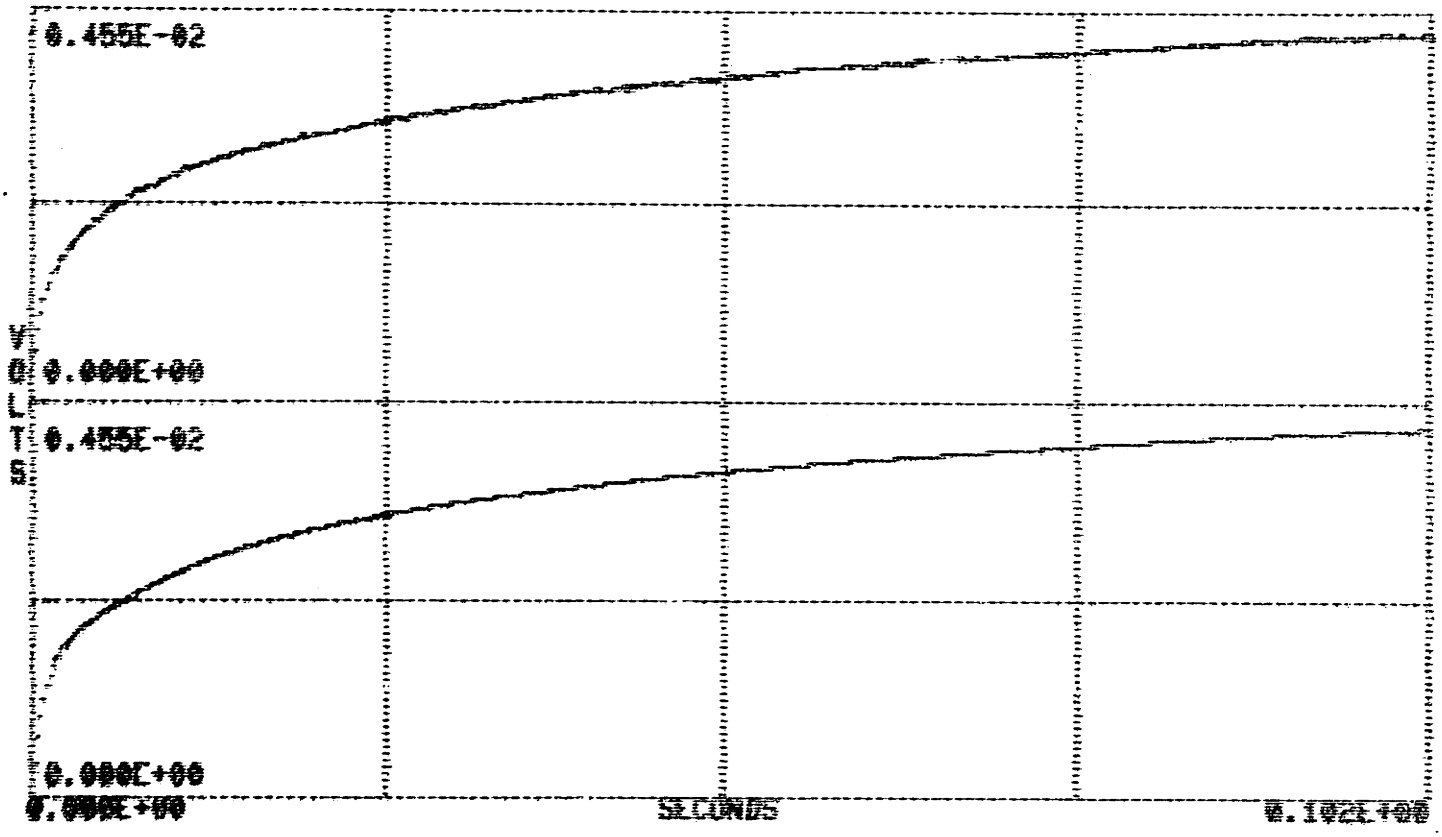

DATA (TOP GRAPH) AND APPROXIMATION (LOWER GRAPH) 01-MAY-78

BLOCK LENGTH PLOTTED:	512
BLOCK LENGTH FOR PARAMETER ESTIMATION:	512
NUMBER OF POLES:	3
EXPONENTIAL ERROR WEIGHTING:	1.00000

ESTIMATED SIGNAL PARAMETERS

COEFFICIENTS	TIME CONSTANTS
0.1534E-02	0.7431E-03
0.2057E-02	0.7357E-01
0.1224E-02	0.9333E-02

Figure 12a Third order approximation to recovery voltage of .01 μF teflon capacitor, sample 1.

102 ms interval

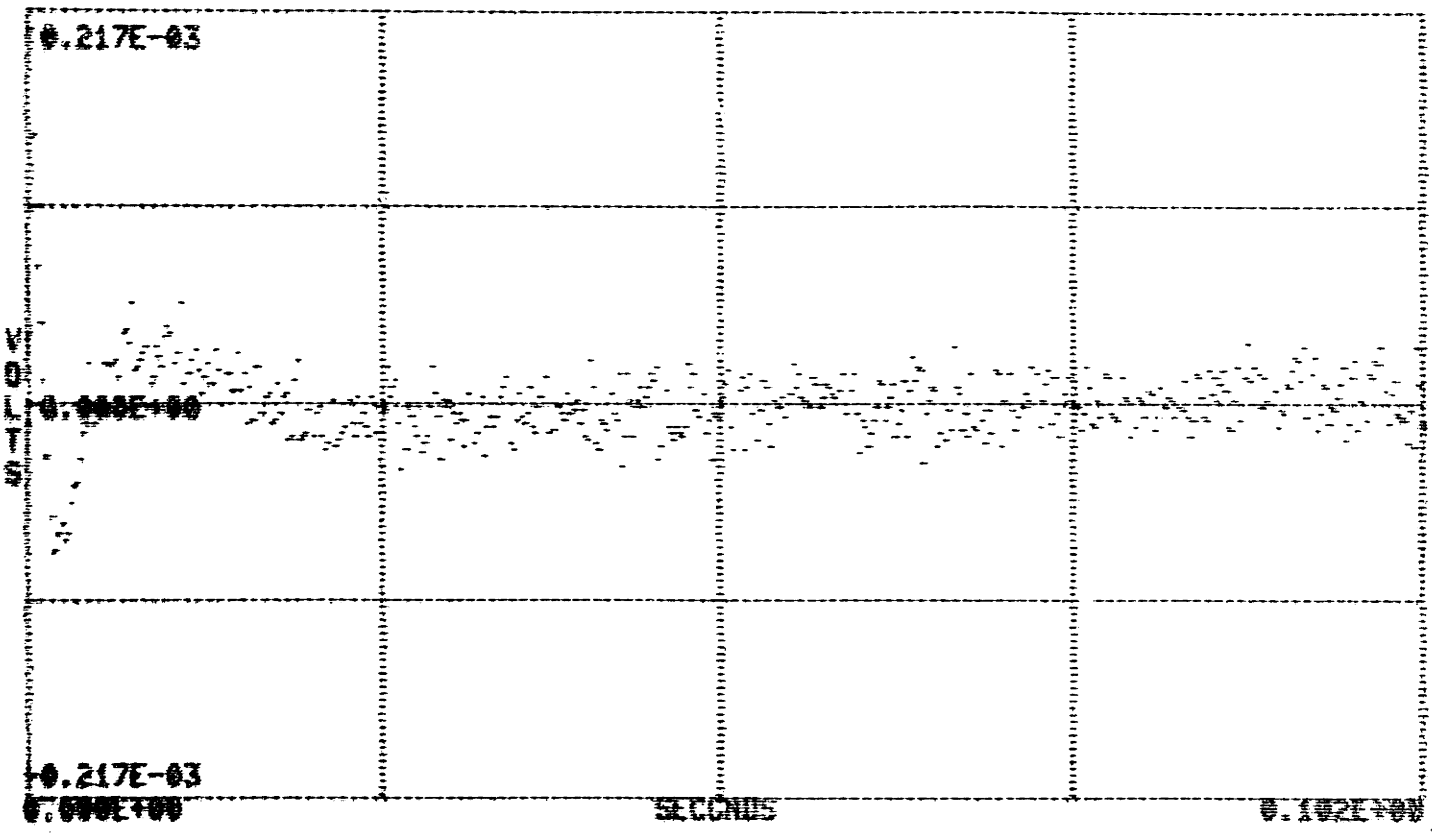

ERROR (DATA MINUS APPROXIMATION) 01-MAY-78

BLOCK LENGTH PLOTTED:	512
BLOCK LENGTH FOR PARAMETER ESTIMATION:	512
NUMBER OF POLES:	3
EXPONENTIAL ERROR WEIGHTING:	1.00000
TOTAL NORMALIZED WEIGHTED MEAN SQUARE ERROR:	0.3580673E-04

Figure 12b Error of third order approximation.

PRINT ON THE FOLLOWING PAGES IS PARTIALLY ILLEGIBLE

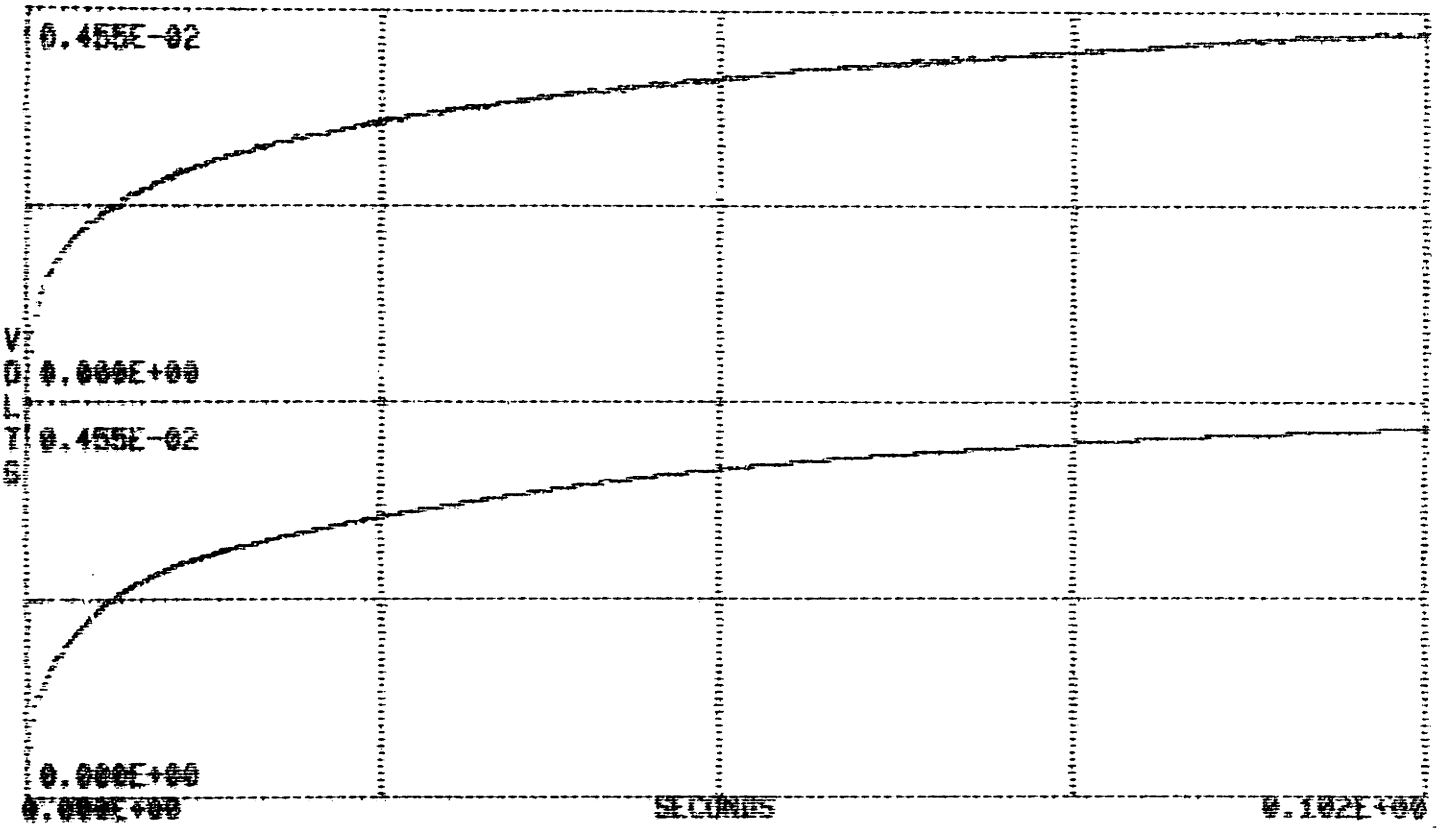

DATA (TOP GRAPH) AND APPROXIMATION (LOWER GRAPH) 30-APR-78

BLOCK LENGTH PLOTTED:	512
BLOCK LENGTH FOR PARAMETER ESTIMATION:	512
NUMBER OF POLES:	4
EXPONENTIAL ERROR WEIGHTING:	1.00000

ESTIMATED SIGNAL PARAMETERS

COEFFICIENTS	TIME CONSTANTS
0.6631E-03	0.2265E-03
0.1351E-02	0.3208E-02
0.9781E-04	0.7553E-02
0.2197E-02	0.4567E-01

Figure 13a Fourth order approximation to recovery voltage of .01 μF teflon capacitor, sample 1.

102 ms interval

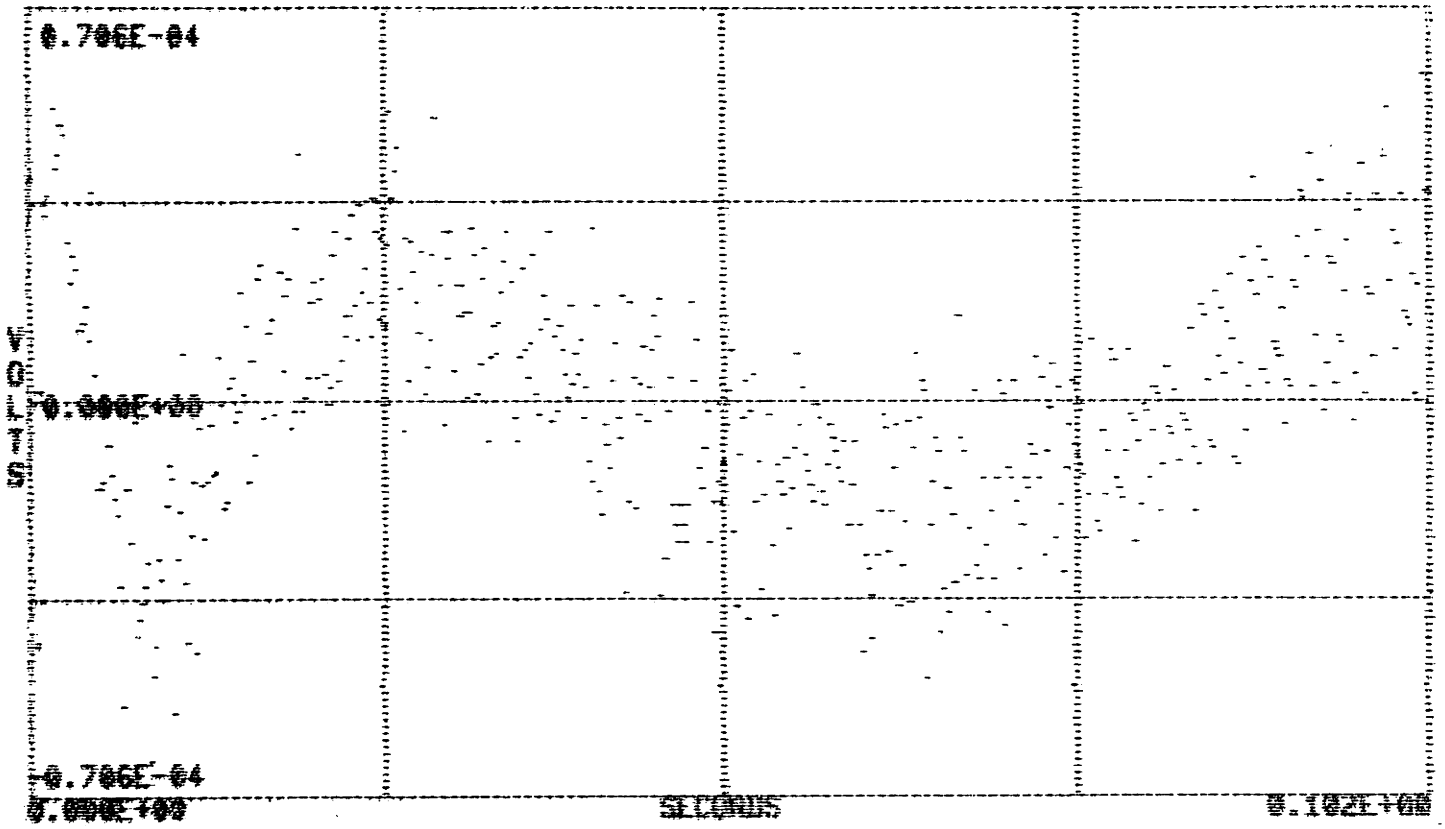

ERROR (DATA MINUS APPROXIMATION)

30-APR-78

BLOCK LENGTH PLOTTED:	512
BLOCK LENGTH FOR PARAMETER ESTIMATION:	512
NUMBER OF POLES:	4
EXPONENTIAL ERROR WEIGHTING:	1.000000
TOTAL NORMALIZED WEIGHTED MEAN SQUARE ERROR:	0.3551906E-04

Figure 13b Error of fourth order approximation.

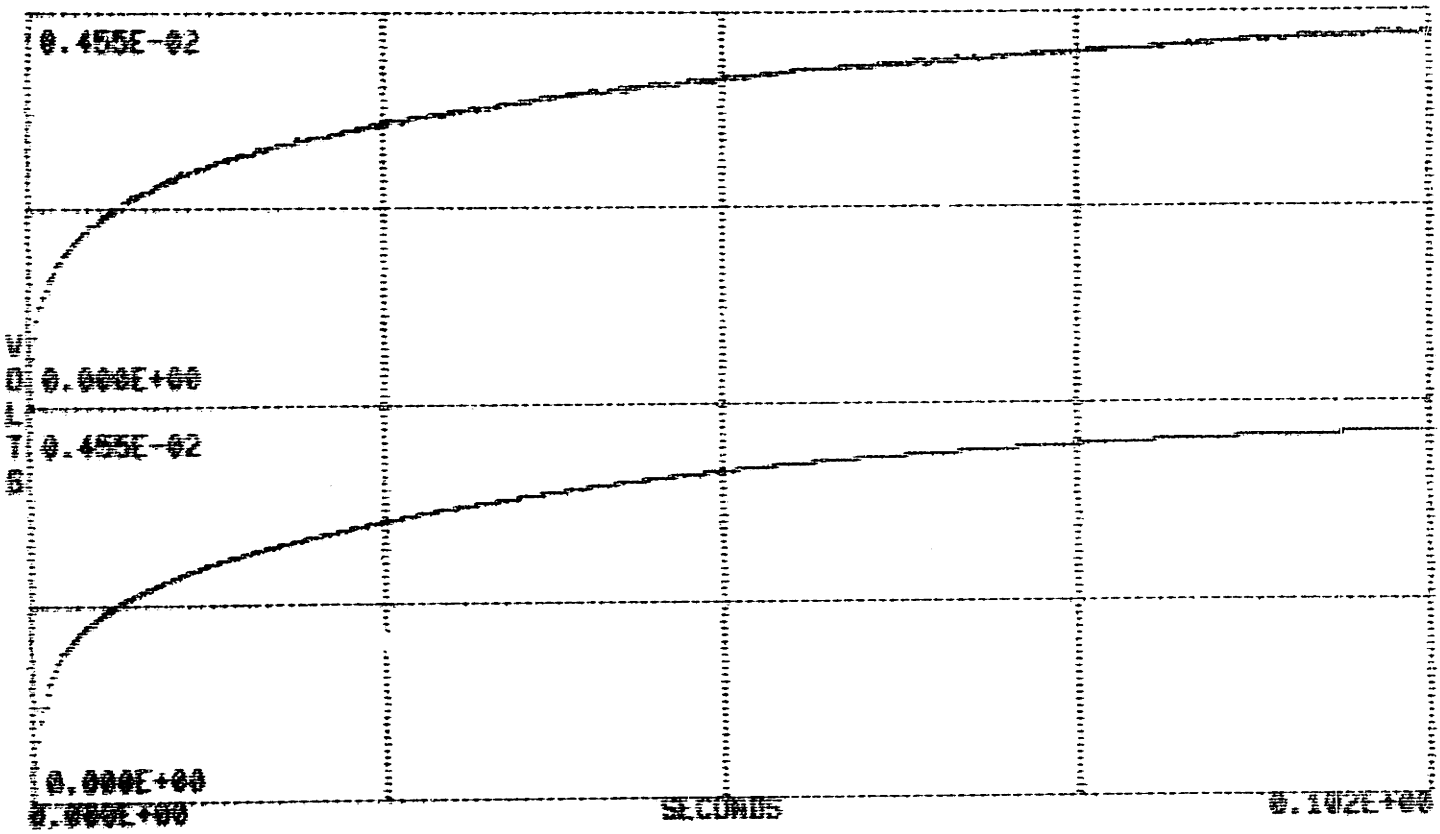

DATA (TOP GRAPH) AND APPROXIMATION (LOWER GRAPH) 30-APR-78

BLOCK LENGTH PLOTTED:	512
BLOCK LENGTH FOR PARAMETER ESTIMATION:	512
NUMBER OF POLES:	5
EXPONENTIAL ERROR WEIGHTING:	1.00000

ESTIMATED SIGNAL PARAMETERS

COEFFICIENTS	TIME CONSTANTS
0.8371E-03	0.4165E-03
0.7332E-03	0.1497E-02
0.4817E-03	0.4099E-02
0.2494E-03	0.1368E-01
0.2113E-02	0.4022E-01

Figure 14a Fifth order approximation to recovery voltage of .01 μF teflon capacitor, sample 1.

102 ms interval

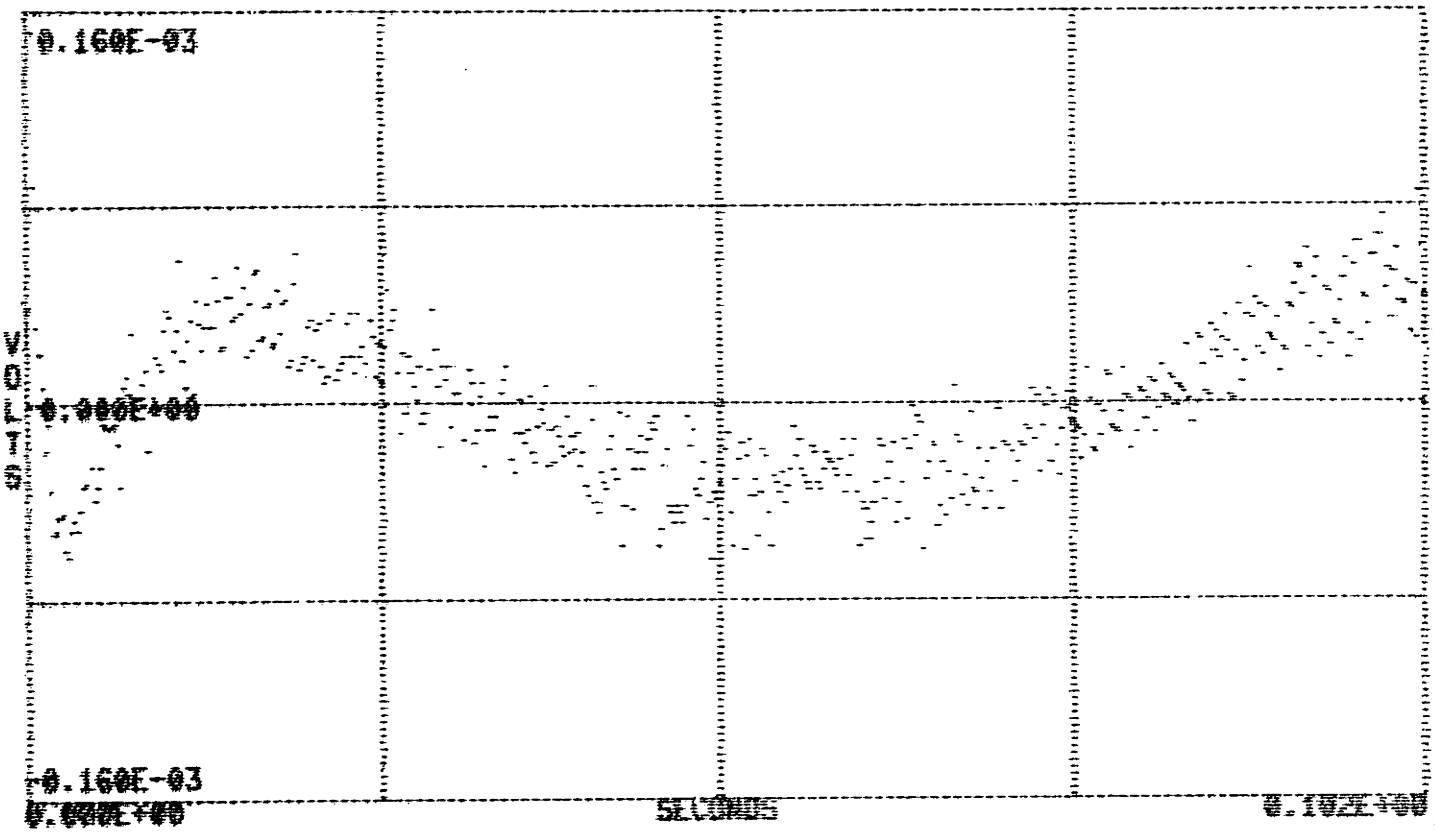

ERROR (DATA MINUS APPROXIMATION) 30-APR-78

BLOCK LENGTH PLOTTED:	512
BLOCK LENGTH FOR PARAMETER ESTIMATION:	512
NUMBER OF POLES:	5
EXPONENTIAL ERROR WEIGHTING:	1.00000
TOTAL NORMALIZED WEIGHTED MEAN SQUARE ERROR:	0.756865E-04

Figure 14b Error of fifth order approximation.

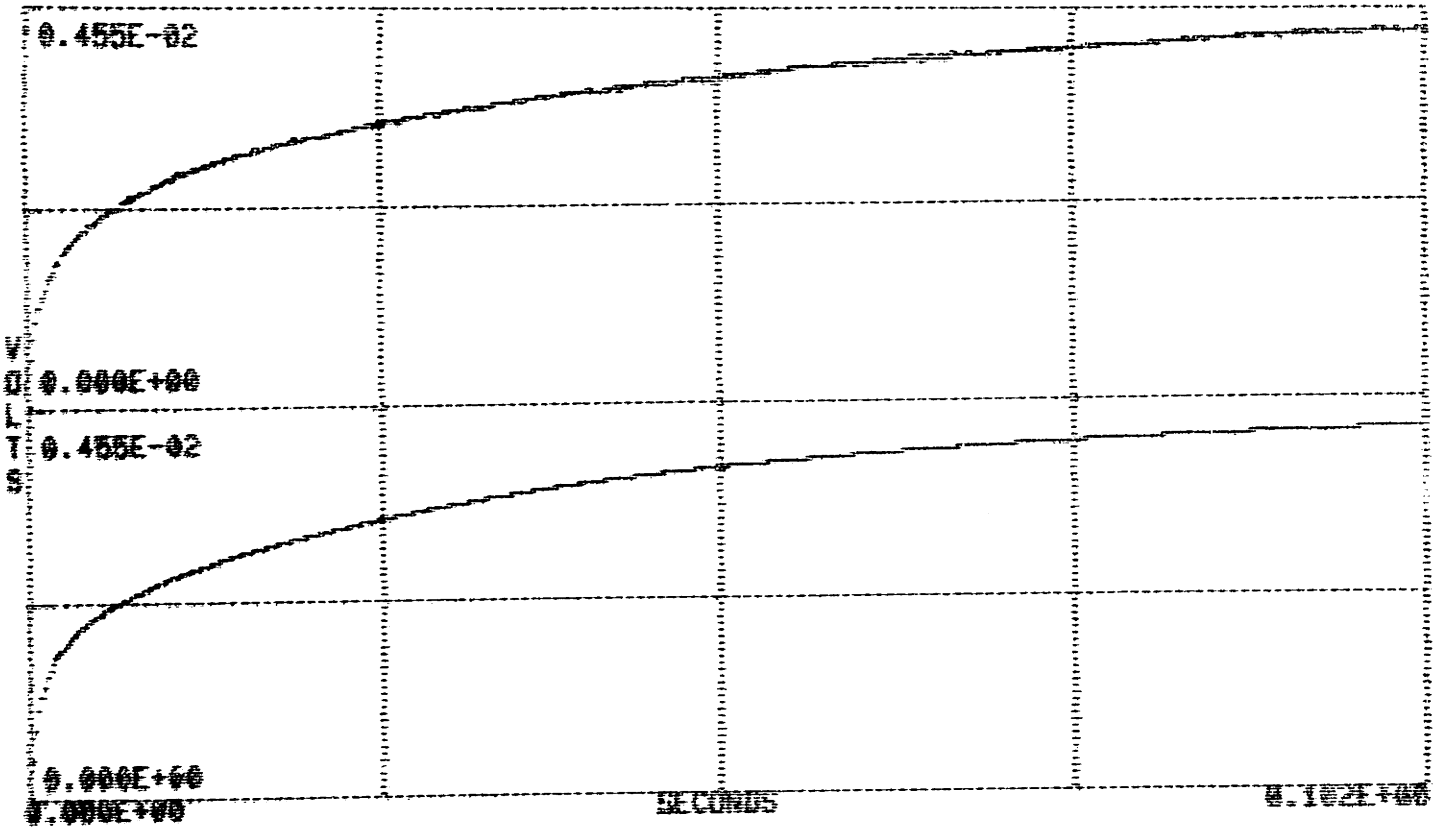

DATA (TOP GRAPH) AND APPROXIMATION (LOWER GRAPH) 30-APR-76

BLOCK LENGTH PLOTTED:	512
BLOCK LENGTH FOR PARAMETER ESTIMATION:	512
NUMBER OF POLES:	6
EXPONENTIAL ERROR WEIGHTING:	1.000000

ESTIMATED SIGNAL PARAMETERS

COEFFICIENTS	TIME CONSTANTS
0.7718E-03	0.3679E-03
0.6110E-03	0.9785E-03
0.4864E-03	0.2618E-02
0.2685E-03	0.7059E-02
0.5421E-03	0.1852E-01
0.1614E-02	0.4334E-01

Figure 15a Sixth order approximation to recovery voltage of .01 μF teflon capacitor, sample 1.

102 ms interval

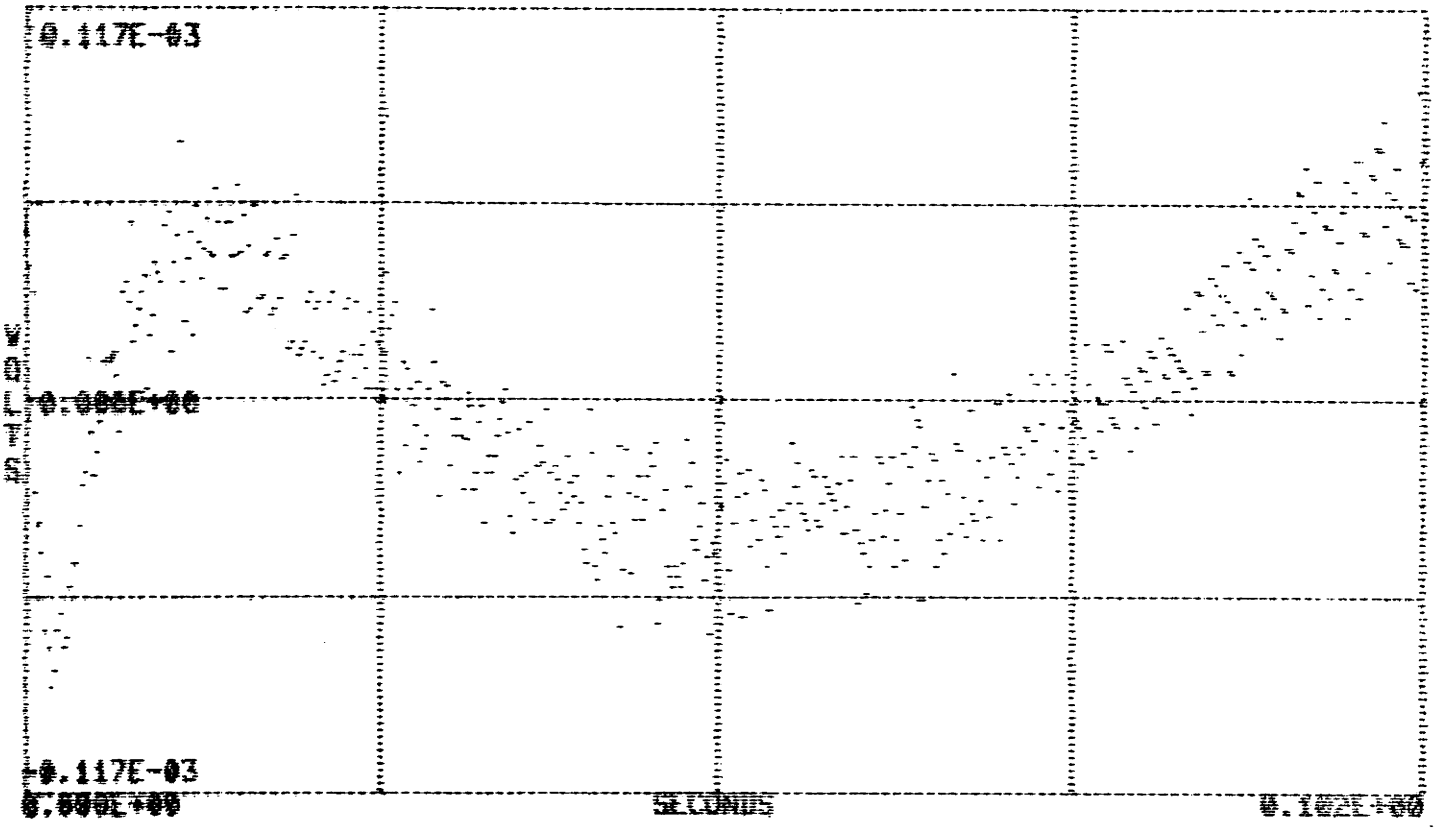

ERROR (DATA MINUS APPROXIMATION) 30-APR-78

BLOCK LENGTH PLOTTED:	512
BLOCK LENGTH FOR PARAMETER ESTIMATION:	512
NUMBER OF POLES:	6
EXPONENTIAL ERROR WEIGHTING:	1.000000
TOTAL NORMALIZED WEIGHTED MEAN SQUARE ERROR:	0.976732E-04

Figure 15b Error of sixth order approximation.

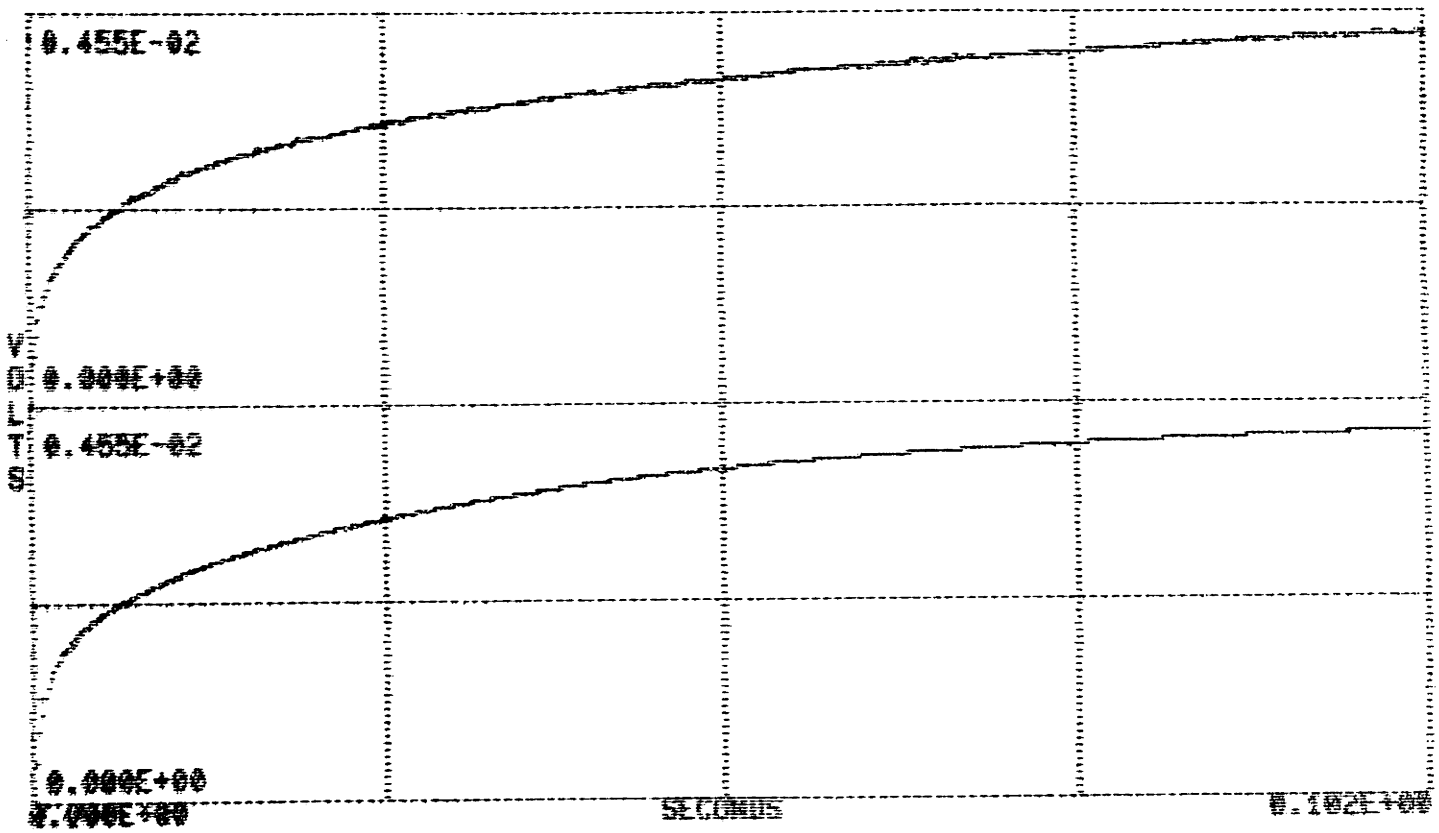

DATA (TOP GRAPH) AND APPROXIMATION (LOWER GRAPH) 30-APR-79

BLOCK LENGTH PLOTTED:	512
BLOCK LENGTH FOR PARAMETER ESTIMATION:	512
NUMBER OF POLES:	7
EXPONENTIAL ERROR WEIGHTING:	1.000000

ESTIMATED SIGNAL PARAMETERS

COEFFICIENTS	TIME CONSTANTS
0.6612E-03	0.3461E-03
0.9578E-03	0.7994E-03
0.4186E-03	0.1850E-02
0.2820E-03	0.4336E-02
0.2074E-03	0.1016E-01
0.6572E-03	0.2283E-01
0.1609E-02	0.4786E-01

Figure 16a Seventh order approximation to recovery voltage of .01 μF teflon capacitor, sample 1.

102 ms interval

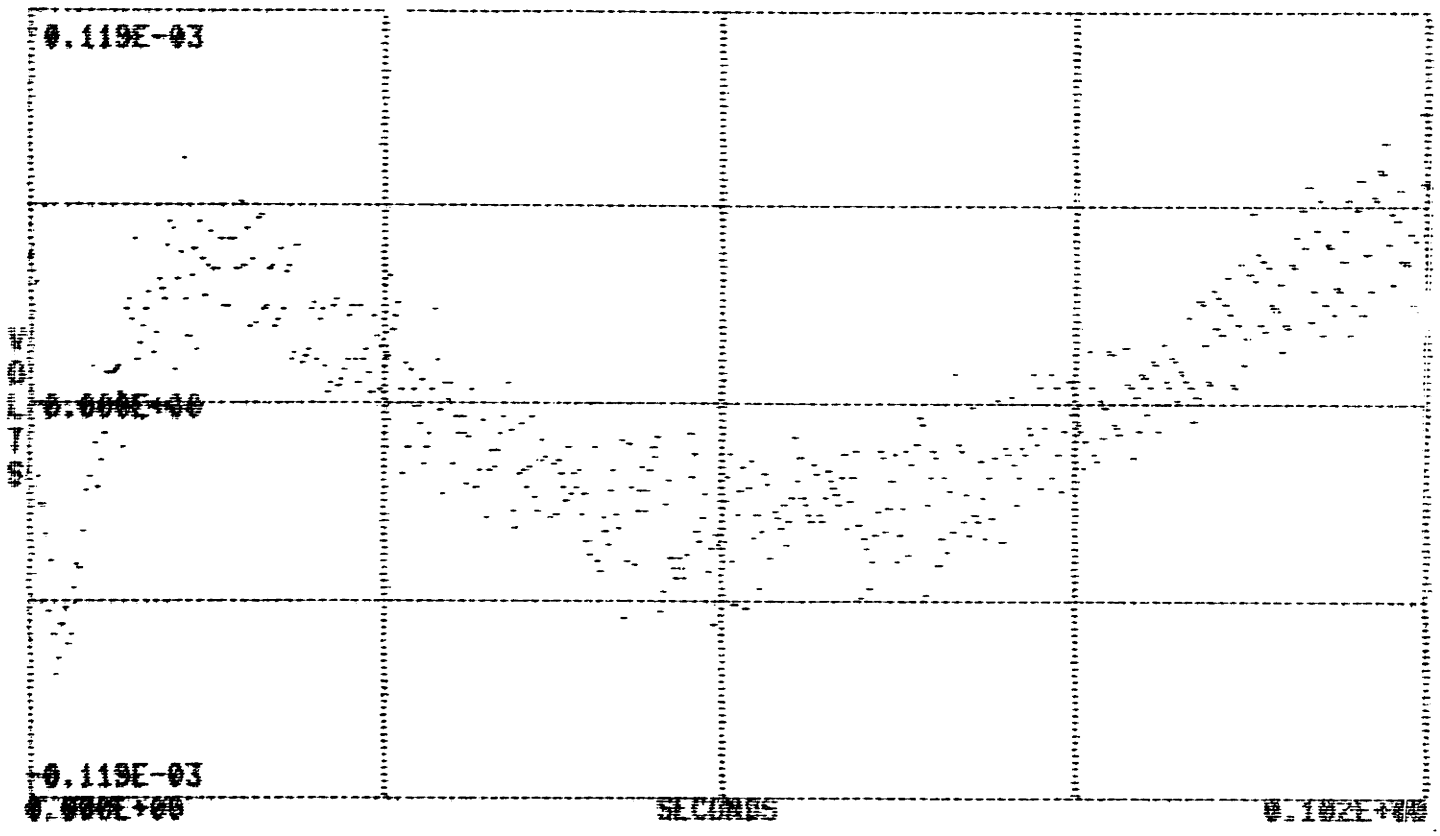

ERROR (DATA MINUS APPROXIMATION) 30-APR-78

BLOCK LENGTH PLOTTED:	512
BLOCK LENGTH FOR PARAMETER ESTIMATION:	512
NUMBER OF POLES:	7
EXPONENTIAL ERROR WEIGHTING:	1.000000
TOTAL NORMALIZED WEIGHTED MEAN SQUARE ERROR:	0.861341E-04

Figure 16b Error of seventh order approximation.

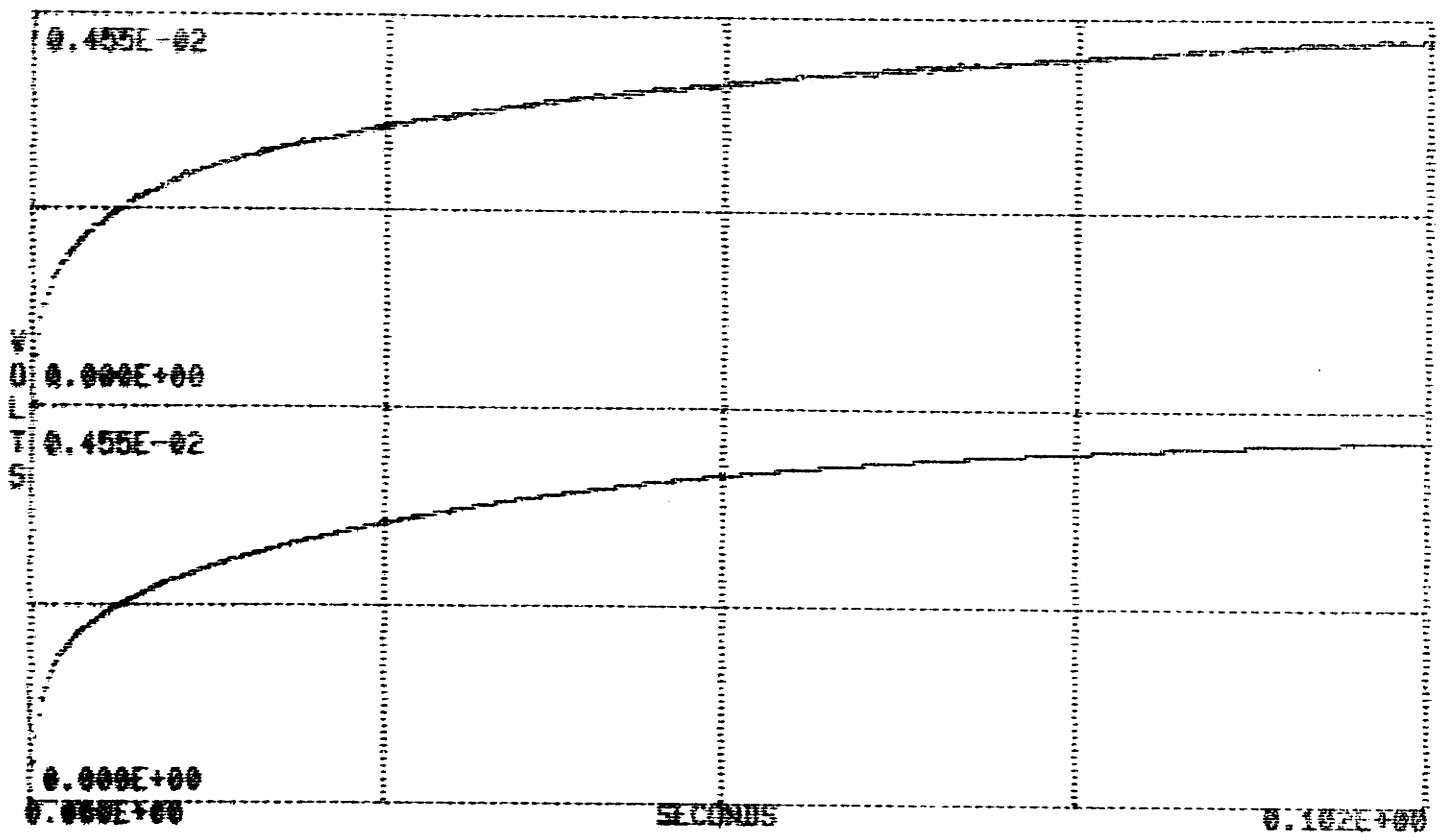

DATA (TOP GRAPH) AND APPROXIMATION (LOWER GRAPH) 30-APR-79

BLOCK LENGTH PLOTTED:	512
BLOCK LENGTH FOR PARAMETER ESTIMATION:	512
NUMBER OF POLES:	8
EXPONENTIAL ERROR WEIGHTING:	1.00000

ESTIMATED SIGNAL PARAMETERS

COEFFICIENTS	TIME CONSTANTS
0.5799E-03	0.3236E-03
0.5032E-03	0.6930E-03
0.4103E-03	0.1464E-02
0.3101E-03	0.3050E-02
0.2332E-03	0.6362E-02
0.2748E-03	0.1326E-01
0.6911E-03	0.2677E-01
0.1467E-02	0.5196E-01

Figure 17a Eighth order approximation to recovery voltage of .01 μF teflon capacitor, sample 1.

102 ms interval

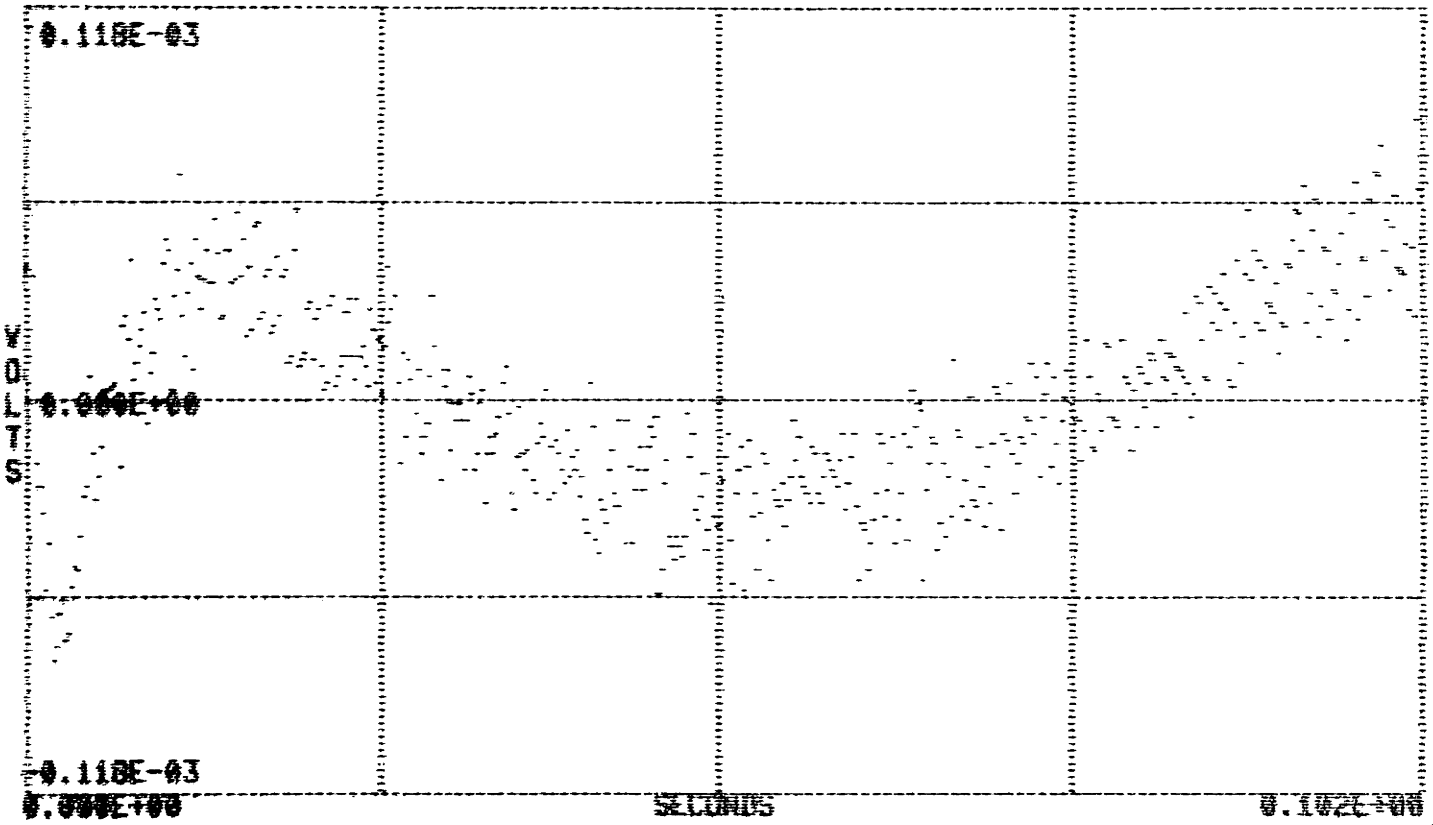

ERROR (DATA MINUS APPROXIMATION) 30-APR-78

BLOCK LENGTH PLOTTED:	512
BLOCK LENGTH FOR PARAMETER ESTIMATION:	512
NUMBER OF POLES:	8
EXPONENTIAL ERROR WEIGHTING:	1.000000
TOTAL NORMALIZED WEIGHTED MEAN SQUARE ERROR:	0.725596E-04

Figure 17b Error of eighth order approximation.

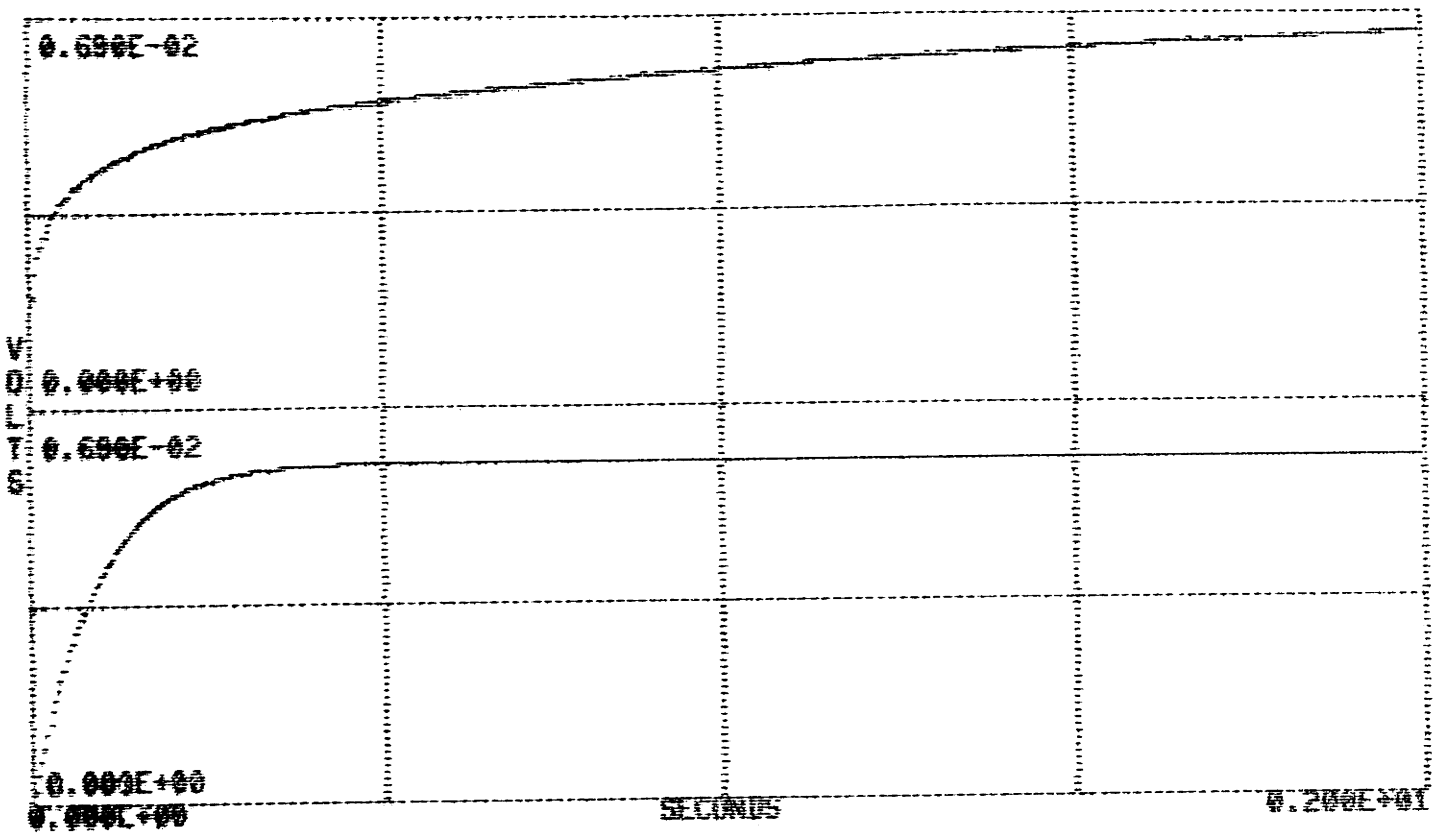

DATA (TOP GRAPH) AND APPROXIMATION (LOWER GRAPH) 30-APR-78

BLOCK LENGTH PLOTTED:	9999
BLOCK LENGTH FOR PARAMETER ESTIMATION:	9999
NUMBER OF POLES:	1
EXPONENTIAL ERROR WEIGHTING:	1.00000

ESTIMATED SIGNAL PARAMETERS

COEFFICIENTS	TIME CONSTANTS
0.5965E-02	0.8414E-01

Figure 18a First order approximation to recovery voltage of .01 μF teflon capacitor, sample 1.

2 s interval

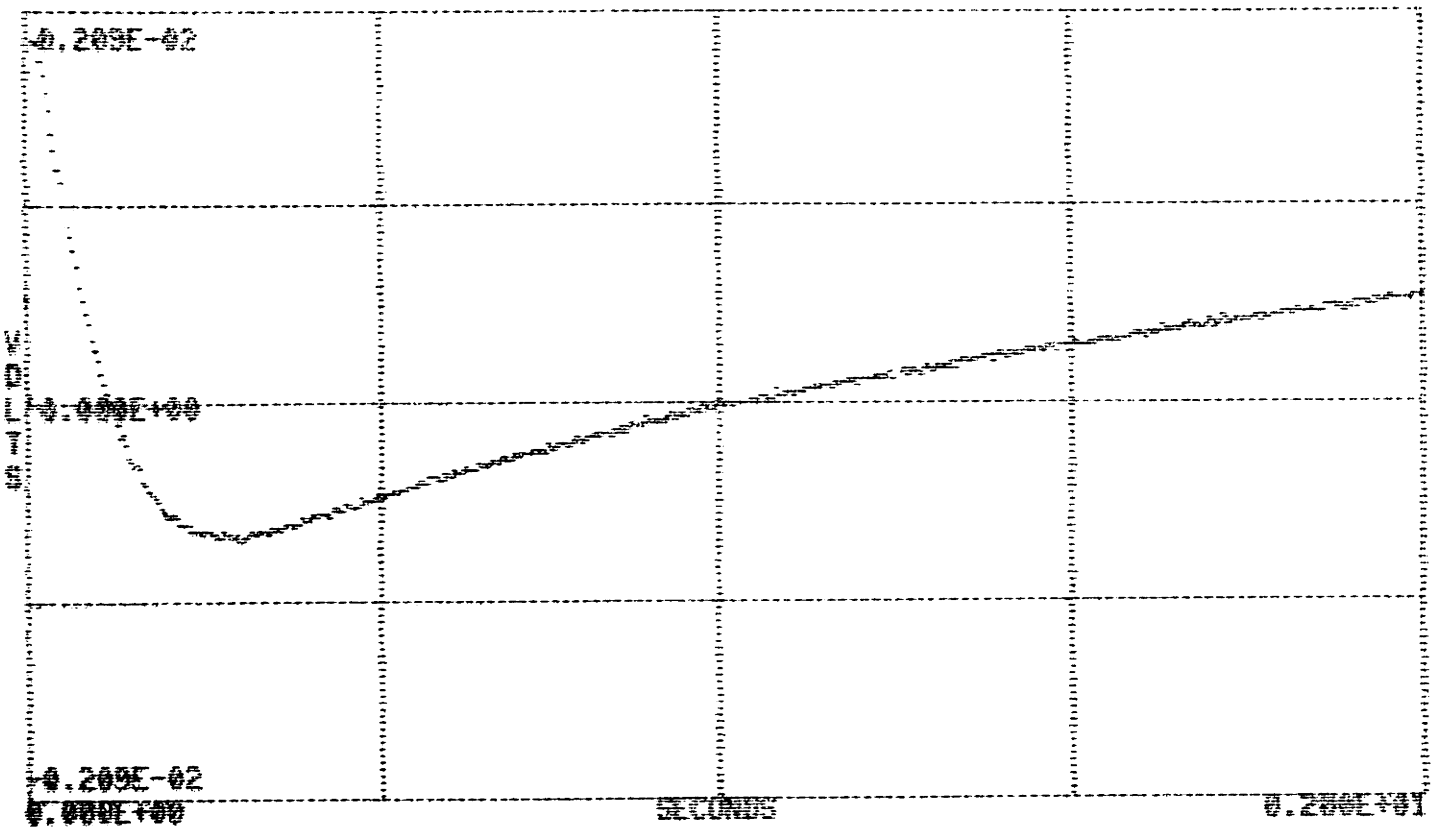

ERROR (DATA MINUS APPROXIMATION) 30-APR-78

BLOCK LENGTH PLOTTED:	9999
BLOCK LENGTH FOR PARAMETER ESTIMATION:	9999
NUMBER OF POLES:	1
EXPONENTIAL ERROR WEIGHTING:	1.00000
TOTAL NORMALIZED WEIGHTED MEAN SQUARE ERROR:	0.6737825E-02

Figure 18b Error of first order approximation.

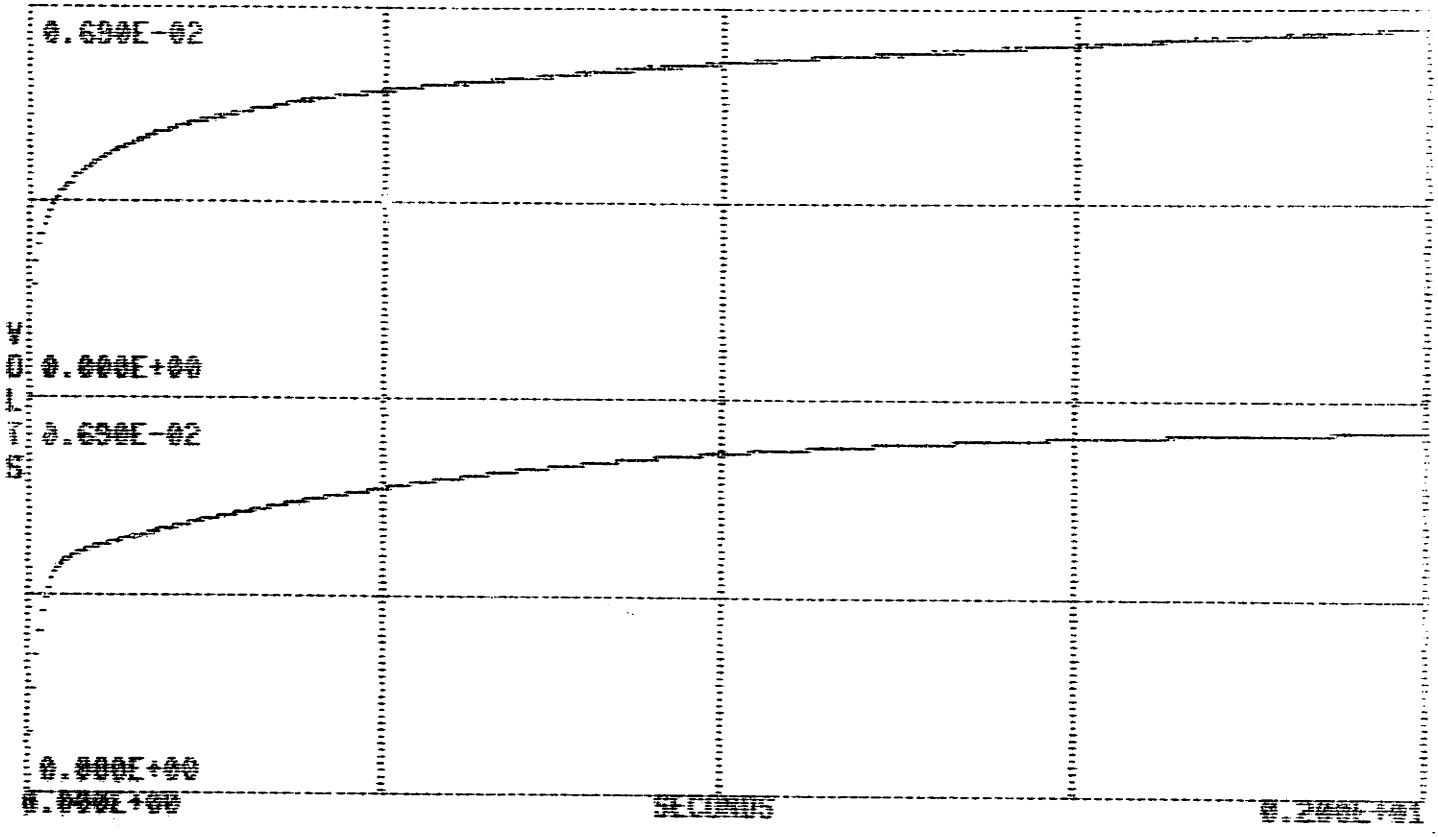

DATA (TOP GRAPH) AND APPROXIMATION (LOWER GRAPH) 15-MAY-78

BLOCK LENGTH PLOTTED:	9999
BLOCK LENGTH FOR PARAMETER ESTIMATION:	9999
NUMBER OF POLES:	2
EXPONENTIAL ERROR WEIGHTING:	1.00000

ESTIMATED SIGNAL PARAMETERS

COEFFICIENTS	TIME CONSTANTS
0.4014E-02	0.1295E-01
0.2516E-02	0.6308E+00

Figure 19a Second order approximation to recovery voltage of .01 μF teflon capacitor, sample 1.

2 s interval

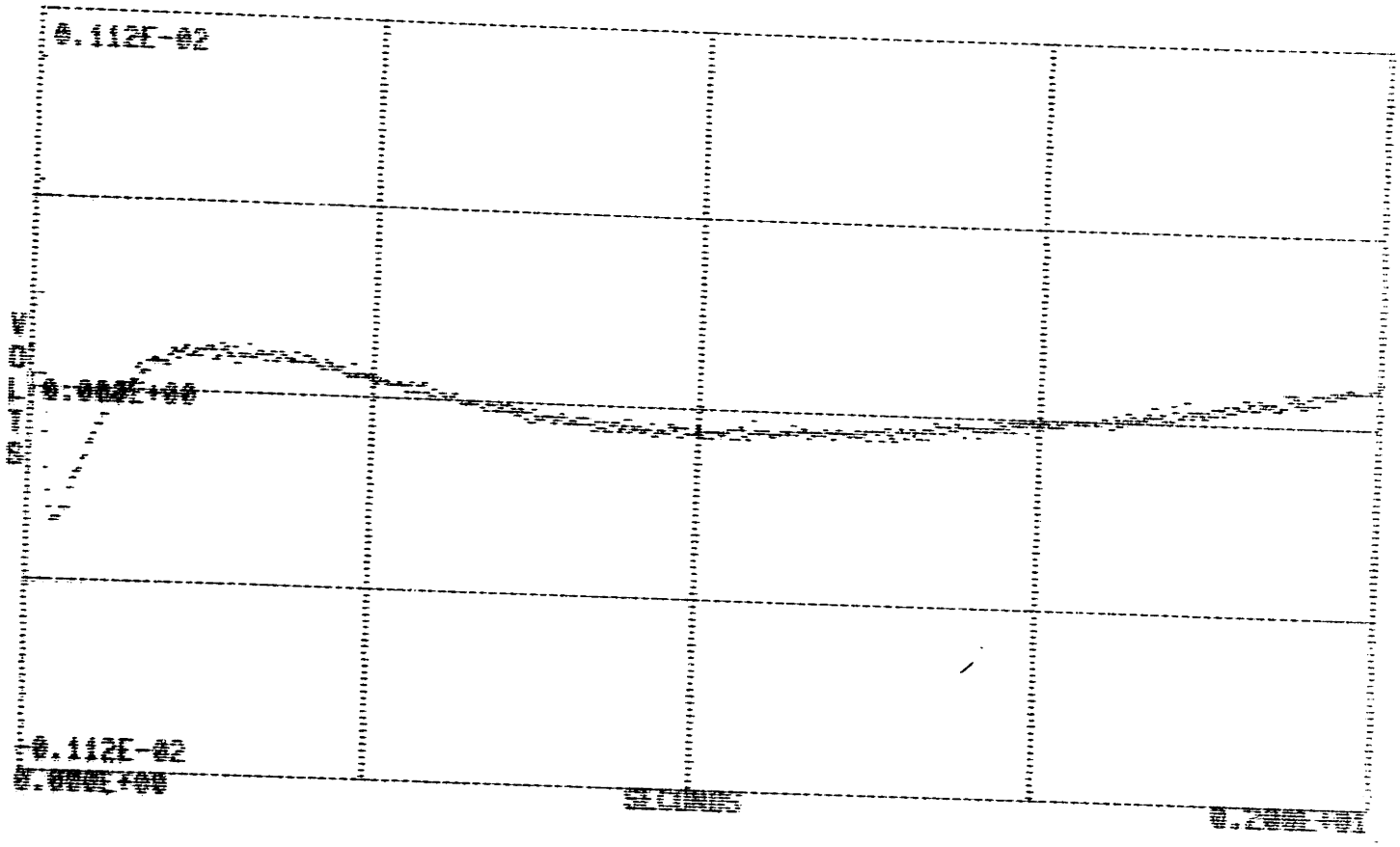

ERROR (DATA MINUS APPROXIMATION)

15-MAY-70

BLOCK LENGTH PLOTTED:	9999
BLOCK LENGTH FOR PARAMETER ESTIMATION:	9999
NUMBER OF POLES:	2
EXPONENTIAL ERROR WEIGHTING:	1.00000
TOTAL NORMALIZED WEIGHTED MEAN SQUARE ERROR:	0.332209E-03

Figure 19b Error of second order approximation.

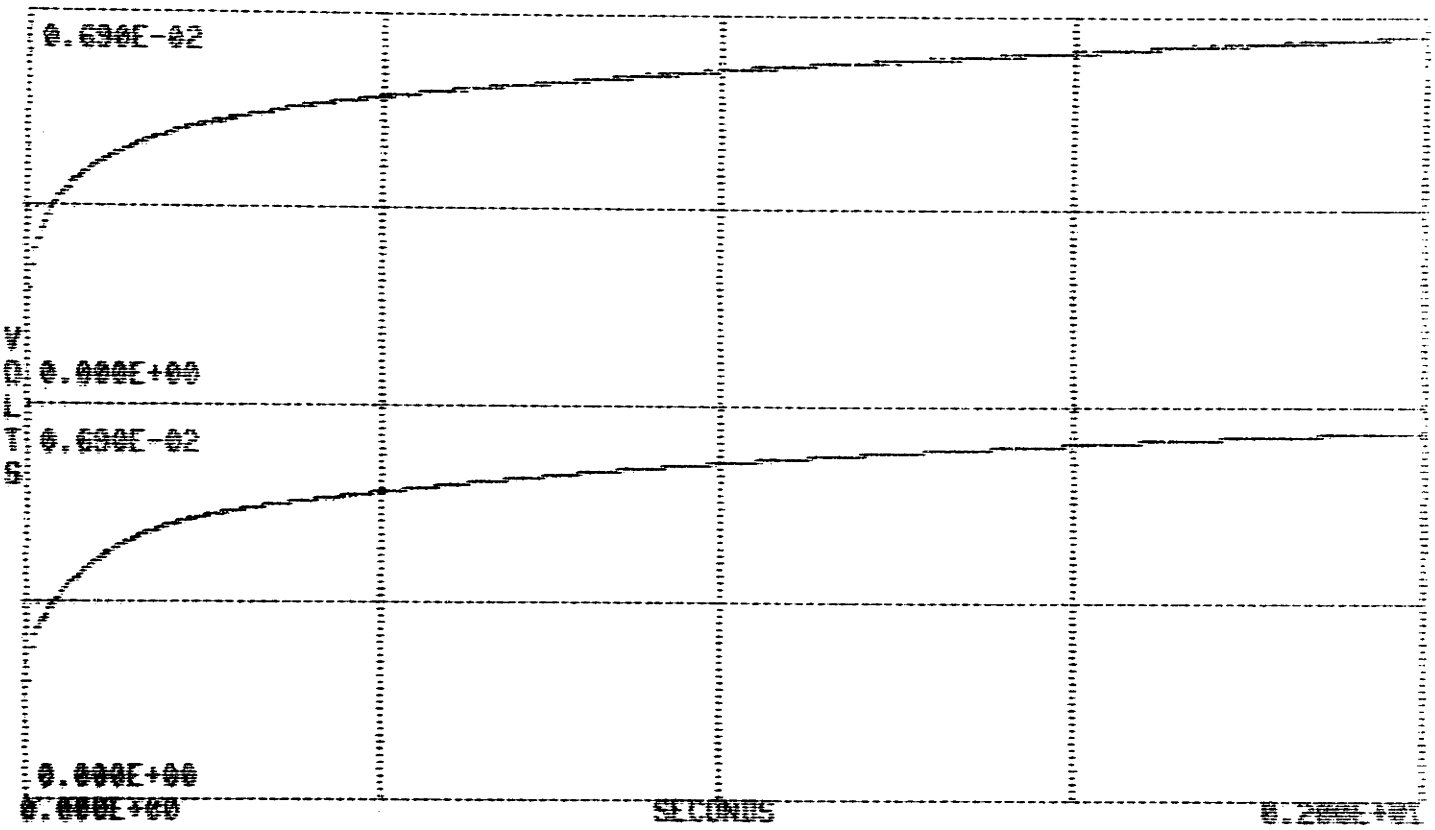

DATA (TOP GRAPH) AND APPROXIMATION (LOWER GRAPH) 15-MAY-78

BLOCK LENGTH PLOTTED:	9999
BLOCK LENGTH FOR PARAMETER ESTIMATION:	9999
NUMBER OF POLES:	3
EXPONENTIAL ERROR WEIGHTING:	1.00000

ESTIMATED SIGNAL PARAMETERS

COEFFICIENTS	TIME CONSTANTS
0.2627E-02	0.2863E-02
0.2006E-02	0.7584E-01
0.2319E-02	0.1194E+01

Figure 20a Third order approximation to recovery voltage of .01 μF teflon capacitor, sample 1.

2 s interval

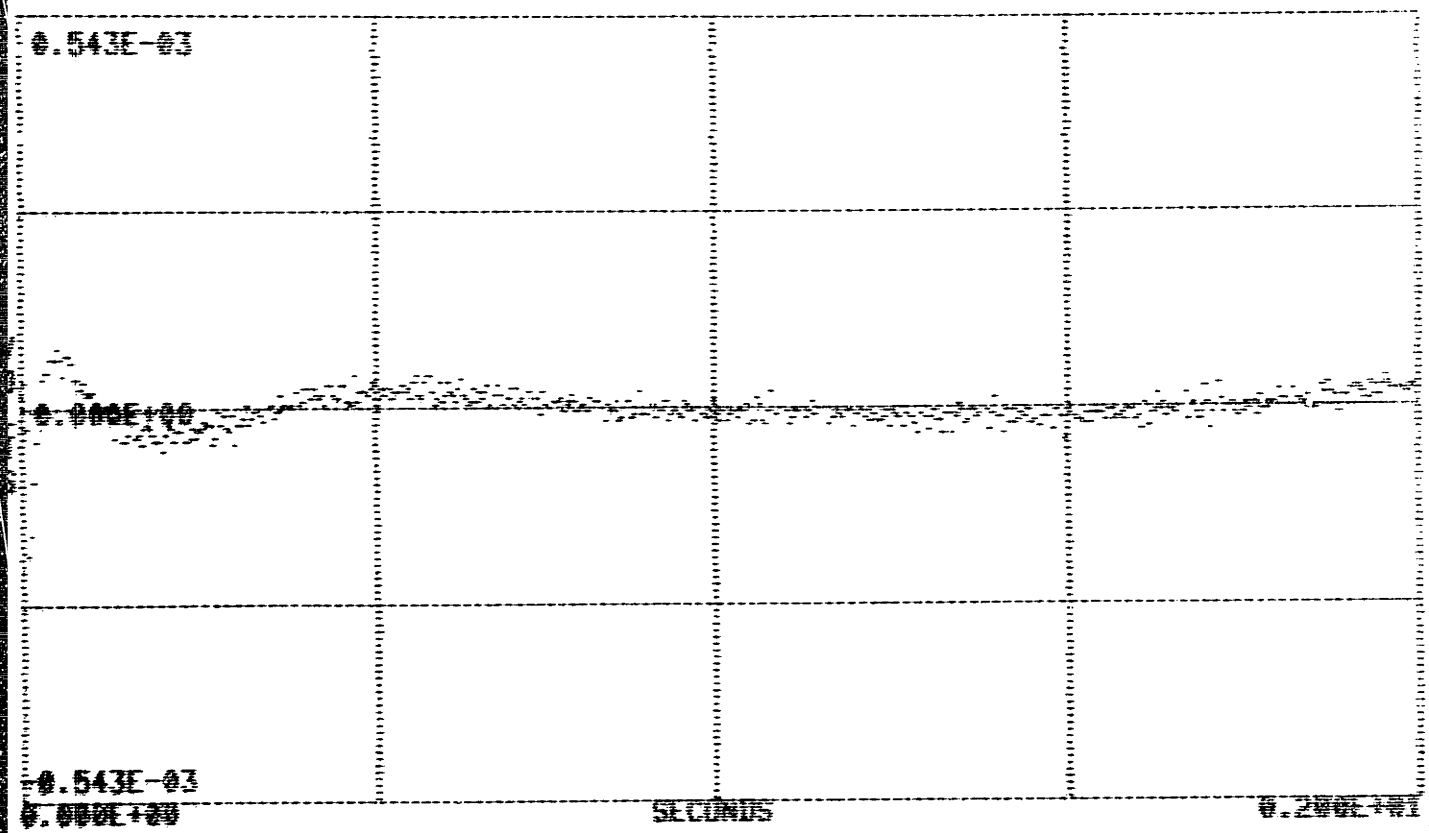

ERROR (DATA MINUS APPROXIMATION) 15-MAY-72

BLOCK LENGTH PLOTTED:	9999
BLOCK LENGTH FOR PARAMETER ESTIMATION:	9999
NUMBER OF POLES:	3
EXPONENTIAL ERROR WEIGHTING:	1.000000
TOTAL NORMALIZED WEIGHTED MEAN SQUARE ERROR:	0.272925E-04

Figure 20b Error of third order approximation.

Model Order	C_k/C_∞	R_kC_k	Normalized RMS Error	Normalized Peak Error
1	3.97×10^{-4}	1.05×10^{-2}	8.25×10^{-2}	2.26×10^{-1}
2	2.14×10^{-4} 2.33×10^{-4}	1.43×10^{-3} 3.67×10^{-2}	1.37×10^{-2}	7.38×10^{-2}
3	1.64×10^{-4} 1.23×10^{-4} 2.06×10^{-4}	7.43×10^{-4} 9.33×10^{-3} 7.36×10^{-2}	5.99×10^{-3}	4.77×10^{-2}
4	1.08×10^{-4} 1.37×10^{-4} 9.85×10^{-6} 2.20×10^{-4}	2.27×10^{-4} 3.29×10^{-3} 7.55×10^{-3} 4.56×10^{-2}	5.96×10^{-3}	1.55×10^{-2}
5	9.44×10^{-5} 7.58×10^{-5} 4.88×10^{-5} 2.50×10^{-5} 2.12×10^{-4}	4.17×10^{-4} 1.50×10^{-3} 4.10×10^{-3} 1.37×10^{-2} 4.02×10^{-2}	8.70×10^{-3}	3.52×10^{-2}
6	8.84×10^{-5} 6.43×10^{-5} 4.14×10^{-5} 2.70×10^{-5} 5.44×10^{-5} 1.82×10^{-4}	3.68×10^{-4} 9.79×10^{-4} 2.62×10^{-3} 7.06×10^{-3} 1.85×10^{-2} 4.33×10^{-2}	9.88×10^{-3}	2.57×10^{-2}
7	7.64×10^{-5} 5.93×10^{-5} 4.30×10^{-5} 2.85×10^{-5} 2.59×10^{-5} 6.59×10^{-5} 1.61×10^{-4}	3.46×10^{-4} 7.99×10^{-4} 1.86×10^{-3} 4.34×10^{-3} 1.02×10^{-2} 2.28×10^{-2} 4.79×10^{-2}	9.28×10^{-3}	2.62×10^{-2}
8	6.77×10^{-5} 5.41×10^{-5} 4.25×10^{-5} 3.15×10^{-5} 2.35×10^{-5} 2.76×10^{-5} 6.92×10^{-5} 1.47×10^{-4}	3.24×10^{-4} 6.93×10^{-4} 1.46×10^{-3} 3.05×10^{-3} 6.36×10^{-3} 1.33×10^{-2} 2.68×10^{-2} 5.20×10^{-2}	8.52×10^{-3}	2.59×10^{-2}

TABLE 1

Model parameters for .01 μF teflon capacitor, sample 1

Model Order	C_k/C_∞	R_kC_k	Normalized RMS Error	Normalized Peak Error
1	1.77×10^{-4}	1.17×10^{-2}	8.35×10^{-2}	2.24×10^{-1}
2	9.17×10^{-5} 1.10×10^{-4}	1.55×10^{-3} 3.93×10^{-2}	1.58×10^{-2}	7.17×10^{-2}
3	8.67×10^{-5} 6.23×10^{-6} 1.10×10^{-4}	1.47×10^{-3} 3.24×10^{-3} 4.06×10^{-2}	1.55×10^{-2}	6.83×10^{-2}
4	7.16×10^{-5} 1.30×10^{-5} 5.89×10^{-6} 1.15×10^{-4}	3.34×10^{-4} 1.18×10^{-3} 4.31×10^{-3} 3.37×10^{-2}	2.14×10^{-2}	8.24×10^{-2}
5	4.40×10^{-5} 2.90×10^{-5} 1.44×10^{-5} 1.41×10^{-5} 9.87×10^{-5}	4.97×10^{-4} 1.48×10^{-3} 4.40×10^{-3} 1.33×10^{-2} 3.73×10^{-2}	1.47×10^{-2}	3.41×10^{-2}
6	3.84×10^{-5} 2.78×10^{-5} 1.72×10^{-5} 9.21×10^{-6} 1.91×10^{-5} 9.22×10^{-5}	4.31×10^{-4} 1.09×10^{-3} 2.76×10^{-3} 7.03×10^{-3} 1.79×10^{-2} 4.28×10^{-2}	1.32×10^{-2}	3.90×10^{-2}
7	3.24×10^{-5} 2.55×10^{-5} 1.83×10^{-5} 1.13×10^{-5} 9.06×10^{-6} 2.82×10^{-5} 8.04×10^{-5}	4.01×10^{-4} 8.93×10^{-4} 1.99×10^{-3} 4.44×10^{-3} 1.00×10^{-2} 2.22×10^{-2} 4.74×10^{-2}	1.29×10^{-2}	3.60×10^{-2}
8	2.90×10^{-5} 2.37×10^{-5} 1.83×10^{-5} 1.26×10^{-5} 7.92×10^{-6} 9.64×10^{-6} 3.27×10^{-5} 7.29×10^{-5}	3.72×10^{-4} 7.56×10^{-4} 1.54×10^{-3} 3.12×10^{-3} 6.37×10^{-3} 1.31×10^{-2} 2.62×10^{-2} 5.15×10^{-2}	1.25×10^{-2}	3.87×10^{-2}

TABLE 2

Model parameters for .01 μF teflon capacitor, sample 2

Model Order	C_k/C_∞	R_kC_k	Normalized RMS Error	Normalized Peak Error
1	3.09×10^{-4}	8.67×10^{-3}	8.42×10^{-2}	2.41×10^{-1}
2	1.81×10^{-4} 1.68×10^{-4}	1.23×10^{-3} 3.58×10^{-2}	1.48×10^{-2}	8.87×10^{-2}
3	1.47×10^{-4} 3.66×10^{-5} 1.65×10^{-4}	8.89×10^{-4} 3.42×10^{-3} 3.57×10^{-2}	1.26×10^{-2}	7.01×10^{-2}
4	1.14×10^{-4} 5.25×10^{-5} 2.46×10^{-5} 1.60×10^{-4}	4.17×10^{-4} 1.96×10^{-3} 8.68×10^{-3} 3.17×10^{-2}	1.41×10^{-2}	3.21×10^{-2}
5	9.24×10^{-5} 5.67×10^{-5} 2.89×10^{-5} 3.24×10^{-5} 1.42×10^{-4}	3.90×10^{-4} 1.30×10^{-3} 4.28×10^{-3} 1.35×10^{-2} 3.76×10^{-2}	1.17×10^{-2}	3.27×10^{-2}
6	7.79×10^{-5} 5.46×10^{-5} 3.37×10^{-5} 2.19×10^{-5} 4.15×10^{-5} 1.26×10^{-4}	3.63×10^{-4} 9.81×10^{-4} 2.65×10^{-3} 7.06×10^{-3} 1.81×10^{-2} 4.29×10^{-2}	1.06×10^{-2}	3.44×10^{-2}
7	6.79×10^{-5} 5.11×10^{-5} 3.54×10^{-5} 2.27×10^{-5} 2.03×10^{-5} 4.83×10^{-5} 1.12×10^{-4}	3.41×10^{-4} 7.97×10^{-4} 1.87×10^{-3} 4.37×10^{-3} 1.01×10^{-2} 2.24×10^{-2} 4.76×10^{-2}	9.97×10^{-3}	3.41×10^{-2}
8	6.02×10^{-5} 4.74×10^{-5} 3.55×10^{-5} 2.46×10^{-5} 1.76×10^{-5} 2.17×10^{-5} 5.28×10^{-5} 1.00×10^{-4}	3.23×10^{-4} 6.80×10^{-4} 1.44×10^{-3} 3.03×10^{-3} 6.35×10^{-3} 1.32×10^{-2} 2.64×10^{-2} 5.16×10^{-2}	9.94×10^{-3}	3.35×10^{-2}

TABLE 3

Model parameters for .01 μF polystyrene capacitor, sample 1

Model Order	C_k/C_∞	R_kC_k	Normalized RMS Error	Normalized Peak Error
1	3.78×10^{-4}	7.20×10^{-3}	8.17×10^{-2}	2.37×10^{-1}
2	2.38×10^{-4} 1.87×10^{-4}	1.28×10^{-3} 3.53×10^{-2}	1.38×10^{-2}	8.43×10^{-2}
3	1.67×10^{-4} 9.66×10^{-5} 1.74×10^{-4}	6.02×10^{-4} 4.10×10^{-3} 4.33×10^{-2}	6.97×10^{-3}	4.88×10^{-2}
4	1.46×10^{-4} 7.30×10^{-5} 3.69×10^{-5} 1.72×10^{-4}	3.87×10^{-4} 1.86×10^{-3} 8.66×10^{-3} 3.17×10^{-2}	1.34×10^{-2}	3.16×10^{-2}
5	1.21×10^{-4} 7.69×10^{-5} 3.94×10^{-5} 3.96×10^{-5} 1.56×10^{-4}	3.62×10^{-4} 1.23×10^{-3} 4.17×10^{-3} 1.36×10^{-2} 3.77×10^{-2}	1.10×10^{-2}	2.83×10^{-2}
6	1.03×10^{-4} 7.38×10^{-5} 4.59×10^{-5} 2.71×10^{-5} 4.61×10^{-5} 1.41×10^{-4}	3.39×10^{-4} 9.31×10^{-4} 2.54×10^{-3} 6.98×10^{-3} 1.82×10^{-2} 4.30×10^{-2}	9.78×10^{-3}	2.70×10^{-2}
7	1.01×10^{-4} 5.14×10^{-5} 6.14×10^{-5} 6.08×10^{-5} 1.63×10^{-5} 1.03×10^{-5} 1.62×10^{-4}	1.47×10^{-4} 9.41×10^{-4} 2.26×10^{-3} 4.25×10^{-3} 9.52×10^{-3} 2.33×10^{-2} 5.05×10^{-2}	4.82×10^{-3}	1.43×10^{-2}
8	9.13×10^{-5} 4.91×10^{-5} 4.41×10^{-5} 5.84×10^{-5} 4.78×10^{-5} 6.75×10^{-6} 9.31×10^{-6} 1.61×10^{-4}	1.39×10^{-4} 6.40×10^{-4} 1.74×10^{-3} 3.41×10^{-3} 6.00×10^{-3} 1.27×10^{-2} 2.78×10^{-2} 5.53×10^{-2}	4.24×10^{-3}	1.26×10^{-2}

TABLE 4

Model parameters for .01 μF polystyrene capacitor, sample 2

VI. DEMONSTRATION OF THE NEW COMPENSATION TECHNIQUE

As a validation of the new compensation technique described in Chapter III, a compensator was built on the same breadboard as the test circuit described in Chapter IV, in order to compensate the capacitor under test. In this way, measurements were made using the same data acquisition procedure described earlier. All measurements were made using the same teflon capacitor whose characteristics were presented graphically in Figs. 10-17. A capacitor charge time of four minutes was used, and measured data were averaged over twenty runs.

According to Eq. 18, the coefficients returned by the data reduction program are

$$b_k^2 = V_B \frac{C_k}{C_\infty}$$

where V_B is the capacitor charging voltage (10 volts for all cases). There is a correction factor that should be applied, that has some impact on the compensation capacitors in the sections with shorter time constants, that modifies this to

$$b_k^2 = V_B \frac{C_k}{C_\infty} e^{-T_D/R_k C_k}$$

where T_D is the discharge time of the capacitor under test (50 μs for all cases). This factor accounts for the fact that, in terms of the model, the initial voltage across some of the capacitors at the beginning of the measurement interval was less than V_B due to the length of the discharge interval. Note that the inclusion of this factor in the gradient search program would not have altered the points of convergence,

and the factor is easily incorporated in the solution for C_k/C_∞. The parameters in Tables 1-4 include this correction.

The results of using a second order model for compensation are shown graphically in Fig. 21. From Table 1 the appropriate parameters are

$$C_1 = 2.14 \text{ pF}$$
$$C_2 = 2.33 \text{ pF}$$
$$R_1 = 668 \text{ M}\Omega$$
$$R_2 = 15.8 \text{ G}\Omega \quad .$$

The parameters of the compensation network, using 10% capacitors and 5% resistors, were

$$\alpha = 10^4$$
$$\alpha C_1 = .022 \text{ } \mu\text{F}$$
$$\alpha C_2 = .022 \text{ } \mu\text{F}$$
$$R_1/\alpha = 68 \text{ k}\Omega$$
$$R_2/\alpha = 1.6 \text{ M}\Omega$$
$$R_F = 10 \text{ k}\Omega$$
$$\alpha R_F = 100 \text{ M}\Omega \quad .$$

Figure 21 should be compared with Fig. 11b, which shows the ideal response of the compensated capacitor.

Fig. 22 presents the results of compensation with a third order model. Again, from Table 1, the model is specified by

$$C_1 = 1.64 \text{ pF}$$
$$C_2 = 1.23 \text{ pF}$$

$C_3 = 2.06$ pF

$R_1 = 453$ MΩ

$R_2 = 7.59$ GΩ

$R_3 = 35.7$ GΩ

and the compensation network by

$\alpha = 10^4$

$\alpha C_1 = .015$ μF

$\alpha C_2 = .015$ μF

$\alpha C_3 = .022$ μF

$R_1/\alpha = 47$ kΩ

$R_2/\alpha = 620$ kΩ

$R_3/\alpha = 3.3$ MΩ

$R_F = 10$ kΩ

$\alpha R_F = 100$ MΩ .

In this case, Fig. 12b shows the ideal error response.

Note that, in all cases, the compensation capacitors were chosen as standard values and the resistors chosen to match the appropriate time constants. In the first case, mylar compensation capacitors were used and in the second, ceramic.

Several other experimental runs were made covering many higher order models for some of the test capacitors, but these two examples accurately reflect the operation of the new compensation scheme as implemented here.

The success of the technique can readily be seen. In the first case, the peak error across the interval was reduced by a factor of 10.8; in

the second case by a factor of 15.7. There are, of course, some departures from the ideal responses.

The similarity of Figs. 21 and 11b are obvious. The recovery voltage of the compensated capacitor, however, shows an offset; this can, I believe, be attributed to component tolerances. It appears that C_1 is somewhat too small, thus not supplying enough charge to completely compensate over the first few milliseconds of the interval. Similar effect in other experimental runs could sometimes be reduced by altering component values, though this was not always successful due to the limited number of readily available capacitor values. Figure 22 shows greater departure from its ideal shape, which can also be attributed to the limited number of standard capacitor values. In this case, the nominal value of C_2 differs from the ideal value by some 20%. (Reduction of C_2 to .01 μF results in an error curve whose character is more like Fig. 12b, although it is offset to the other side of the axis by a greater amount due to the reduction in charge available to the compensation network.)

While the selection of more accurate compensation components would almost certainly have resulted in more nearly ideal recovery characteristics, the approach taken here is more representative of real-world engineering. The fact that we can reduce the peak error across the interval by more than a factor of ten, using only inexpensive garden-variety components, is a testament to the robustness of Dow's model.

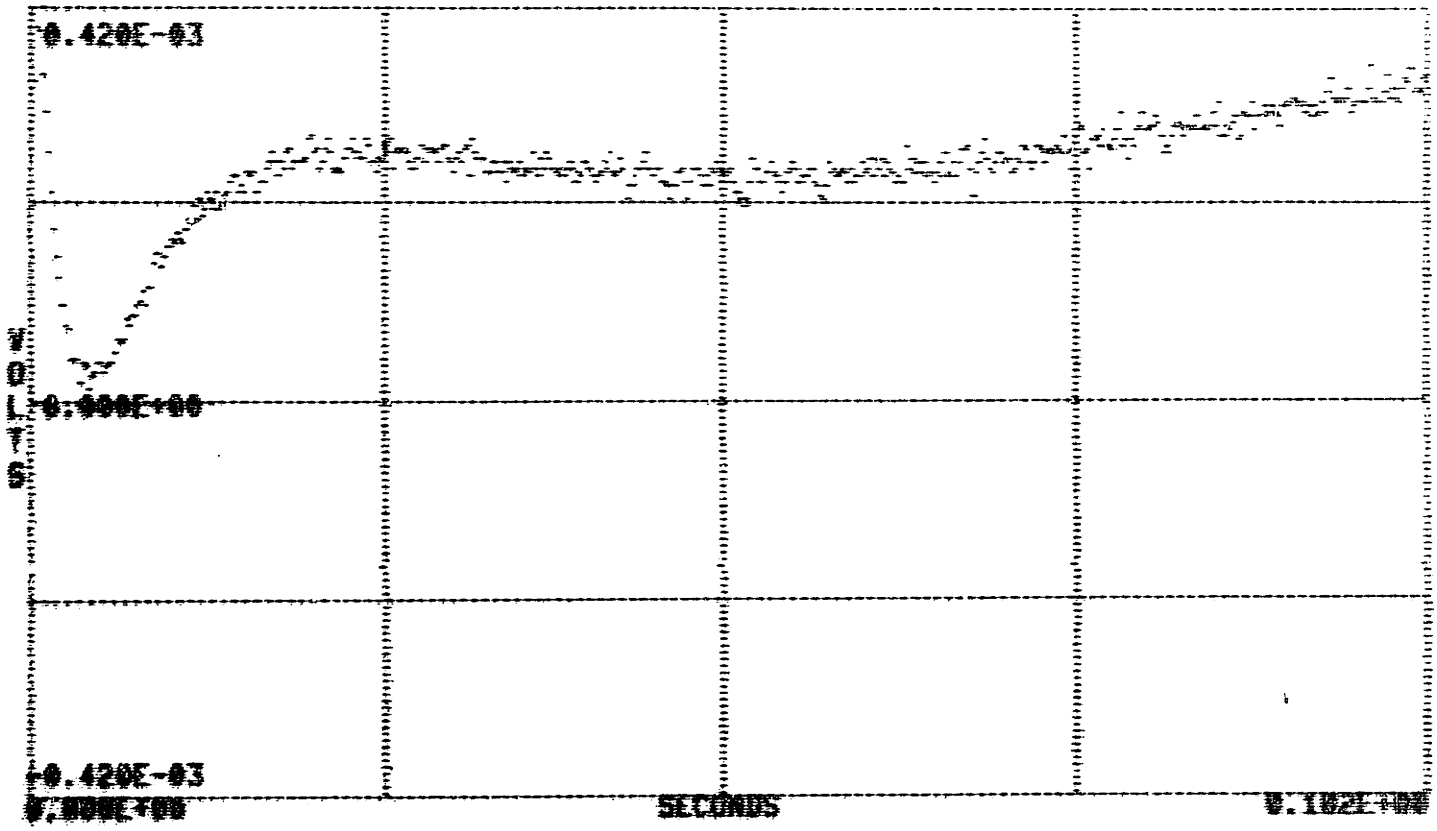

Figure 21 Recovery voltage of compensated .01 μF teflon capacitor, sample 1.

Second order compensation

102 ms interval

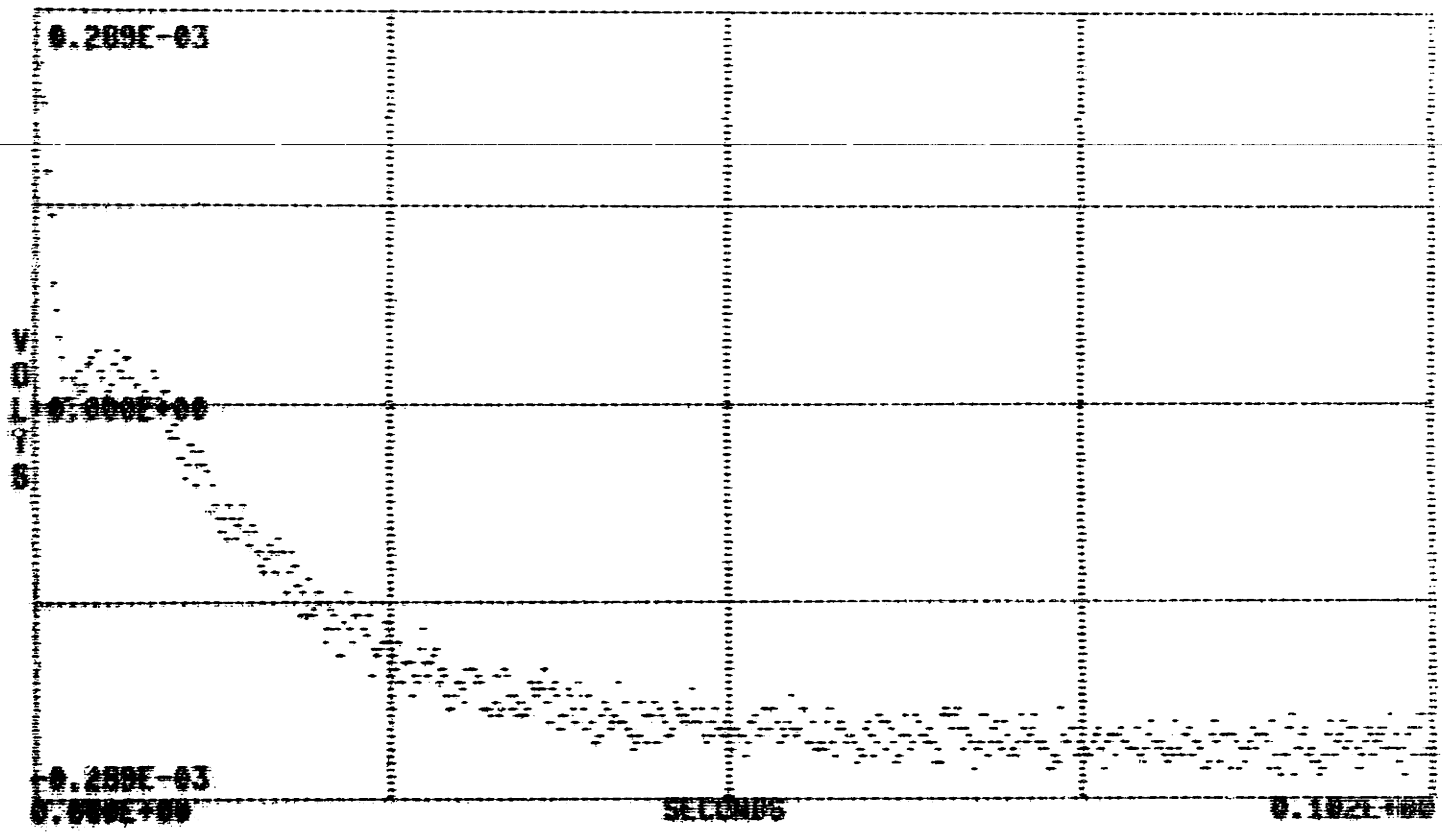

Figure 22 Recovery voltage of compensated .01 μF teflon capacitor, sample 1.

Third order compensation

102 ms interval

VII. CONCLUSIONS

A novel means of compensating for the effects of capacitor dielectric absorption in many circuits has been presented. The idea central to the technique is a positive feedback loop that supplies current, as a function of voltage across a capacitor, to cancel the charge released by the absorptive component of the dielectric. It was demonstrated that an order of magnitude reduction in recovery voltage could be achieved with this technique. Although it was applied over a single interval of 102 ms, there is no reason to believe that it would not be equally effective over much longer or shorter intervals; likewise, although the technique was presented using operational amplifiers as the active components for conceptual simplicity, the basic idea can easily be extended to other topologies.

A fundamental issue in building a compensator is determining accurate parameters for a linear model of the dielectric absorption characteristics. A procedure was described to do this, using Dow's model, and models of orders one through eight were presented for four .01 μF capacitors, two each of teflon and polystyrene. The parameters were determined to match the recovery voltage over an interval of 102 ms.

The procedure of obtaining an accurate model for a capacitor is time consuming and computationally burdensome. The results presented here indicate that an accurate model for any one dielectric is not feasible, at least at the present state of the capacitor manufacturing art. There is evidence, however, that a general model for a dielectric, fairly accurate to within a scale factor, may be feasible. The use of

such a model with the new compensation technique would allow accurately trimming the compensation by altering the value of a single resistor; this would be particularly advantageous in a production environment. This last speculation merits further investigation.

FOOTNOTES

[1] J. C. Maxwell, "Electricity and Magnetism," Oxford University Press, London, England, Vol. 1; 1892.

[2] K. W. Wagner, Ann. der Physik, Vol. 40; 1913.

[3] P. Debye, "Polar Molecules," Chemical Catalog Company, New York; 1929.

[4] K. S. Cole and R. H. Cole, "Dispersion and Absorption in Dielectrics — I. Alternating Current Characteristics," Journal of Chemical Physics, Vol. 9; April, 1941.

[5] K. S. Cole and R. H. Cole, "Dispersion and Absorption in Dielectrics — II. Direct Current Characteristics," Journal of Chemical Physics, Vol. 10; February, 1964.

[6] P. C. Dow, Jr., "An Analysis of Certain Errors in Electronic Differential Analyzers — II. Capacitor Dielectric Absorption," IRE Transactions on Electronic Computers; March, 1958.

[7] C. J. Sheehan, "An Analog Computer Simulation of the Restricted Three-Body Problem by Automatic Scale-Changing Techniques," IEEE Transactions on Electronic Computers; February, 1964.

[8] G. A. Korn, "Progress of Analog/Hybrid Computation," Proceedings of the IEEE; December, 1966.

[9] R. D. Guyton and J. M. McKay, "A Passive Network Method of Compensating an Analog Integrator for Dielectric Absorption," Simulation; February, 1968.

[10] J. W. Gray, "Integrator With Means for Compensating for Capacity Absorption Effects," U.S. Patent No. 3,047,808; July 31, 1962.

[11] C. H. Single and J. A. Brussolo, "Capacitor Low Frequency Characteristics," ISA Transactions, Vol. 2; July, 1963.

[12] R. W. Hamming, "Numerical Methods for Scientists and Engineers," McGraw-Hill, New York; 1962.

[13] L. G. Kelly, "Handbook of Numerical Methods and Applications," Addison-Wesley Publishing, Reading, Massachusetts; 1967.

[14] K. Steiglitz, "On the Simultaneous Estimation of Poles and Zeros in Speech Analysis," IEEE Transactions on Acoustics, Speech, and Signal Processing, Vol. 25; June, 1977.

[15] J. Makhoul, "Linear Prediction: A Tutorial Review," Proceedings of the IEEE, Vol. 63; April, 1975.

[16] F. Fletcher and M. J. D. Powell, "A Rapidly Convergent Descent Method for Minimization," Computer Journal, Vol. 6; 1963.

APPENDIX

Computer programs that were written for this thesis are included here. They are organized as follows:

Data Acquisition

Main program	DATA
Subroutine	IBGTF

Data Reduction

Main program	DATR
Subroutine	ESTIM
Subroutine	FLPOW
Subroutine	GRDNT
Subroutine	DERIV
Subroutine	WMSER

All programs are written in FORTRAN with the exception of IBGTF, which is in assembly language for speed of execution, and they are designed to run under RT-11 (the standard operating system for the PDP-11/03 computer). Subroutines not otherwise identified are supplied by Digital Equipment Corporation as part of the system.

```
      PROGRAM DATA
      DIMENSION VR(10000), LBUF(20000), NLBUF(80), NTBUF(80)
      LOGICAL*1 NLBUF, NTBUF
      EQUIVALENCE (VR(1),LBUF(1))
      EQUIVALENCE (LBUF(1),NLBUF(1)), (LBUF(40),NTBUF(1))
C
C     THIS IS A DATA ACQISITION PROGRAM TO ALLOW A
C     PDP-11/03 DECLAB SYSTEM TO MEASURE CAPACITOR
C     VOLTAGE RECOVERY, FOLLOWING DISCHARGE, DUE TO
C     DIELECTRIC ABSORPTION. THE BREADBOARD IS PROGRAMMED
C     VIA A PARALLEL DIGITAL OUTPUT CARD. THE SAMPLING
C     VOLTMETER IS A H-P MODEL 3437A, AND IS
C     PROGRAMMED VIA THE IEEE BUS.
C     THE CAPACITOR IS CHARGED FOR CTIM MINUTES, DISCHARGED
C     FOR ITIM MICROSECONDS, AND ALLOWED TO RECOVER AS
C     MEASUREMENTS ARE TAKEN. THERE ARE 9999 SAMPLES
C     TAKEN, AT INTERVALS OF 200 MICROSECONDS. SAMPLES ARE
C     SCALED AND STORED ON THE DISK IN FILE 'CAP.DAT'.
C     THERE ARE NRUN RUNS TAKEN, AND THE RESULTING DATA IS
C     AVERAGED AND STORED. BECAUSE THE POLARITY OF THE
C     CHARGING VOLTAGE IS REVERSED FOR SUCCESSIVE RUNS
C     (TO COMPENSATE FOR BIAS CURRENTS) NRUN SHOULD BE EVEN.
C
      TYPE 500
      ACCEPT 510, CTIM
      CTIM=CTIM*60.0
      TYPE 520
      ACCEPT 530, NRUN
      ITIM=50
      ITIM=-ITIM
      SCAL=10000
      SCAL=1/(SCAL*NRUN)
      POLA=1.0
      CALL ASSIGN(2,'DK:CAP.DAT')
      DEFINE FILE 2 (10000,2,U,IV)
C
C     PROGRAM THE BREADBOARD AND THE VOLTMETER
C
      CALL IPOKE('167762,'177777)
      START=SECNDS(0.0)+CTIM
      CALL IBINIT('160150,'420,NLBUF,80,NTBUF,80,0)
      CALL IBSLA(24)
      CALL IBSTA(-1,27,'EOS,N9999S,D.0002S,R3,T2,F2')
      CALL IBUNL
      CALL IBCMD('130)
C
C     START TAKING MEASUREMENTS
```

```
C
      DO 140, I=1,NRUN
100   IF (SECNDS(START) .LT. 0.0) GO TO 100
      CALL IBGTF(LBUF,ITIM)
      START=SECNDS(0.0)+CTIM
      DO 120, N=1,9999
      VR(N)=POLA*SCAL*FLOAT(LBUF(2*(N-1)+1))
      TEMP=0.0
      IF (I .NE. 1) READ (2'N) TEMP
      VR(N)=VR(N)+TEMP
      WRITE (2'N) VR(N)
120   CONTINUE
      POLA=-POLA
      TYPE 540, I
      TYPE 550
      TYPE 570, (N, VR(N), N=1,8)
      TYPE 560
      TYPE 570, (N, VR(N), N=9992,9999)
140   CONTINUE
      CALL IPOKE("167762,"000000)
      CALL IBUNT
      CALL CLOSE(2)
      CALL EXIT
C
C     FORMAT STATEMENTS
C
500   FORMAT (' CAPACITOR CHARGE TIME, IN MINUTES: '$)
510   FORMAT (F5.2)
520   FORMAT ('+NUMBER OF RUNS: '$)
530   FORMAT (I6)
540   FORMAT (///' RESULTS AFTER',I3,' RUNS')
550   FORMAT (/'   FIRST EIGHT POINTS')
560   FORMAT (/'   LAST EIGHT POINTS')
570   FORMAT (3X,I6,6X,E15.8)
      END
```

```
        R0=%0
        R1=%1
        R2=%2
        R3=%3
        R4=%4
        R5=%5
        SP=%6
        PC=%7
        IBS=160150      ;ADDRESS OF IBV11A STATUS REGISTER
        IBD=IBS+2       ;ADDRESS OF IBV11A DATA REGISTER
        KWS=170420      ;ADDRESS OF KWV11A STATUS REGISTER
        DRO=167762      ;ADDRESS OF DRV11 OUTPUT REGISTER
        DSABL=000200    ;PSW TO DISABLE INTERUPTS
        IBLST=000024    ;STATUS WORD TO PUT IBV11A IN LISTEN MODE
        LNR=000400      ;MASK FOR LISTENER READY BIT
        TRIG=000411     ;STATUS WORD TO TRIGGER KWV11A
        LSBCD=177760    ;MASK FOR LOWER BCD DIGIT IN DATA
        TEN=12          ;TEN, OCTAL
        HUN=144         ;ONE HUNDRED, OCTAL
        THO=1750        ;ONE THOUSAND, OCTAL
;
;THIS PROGRAM IS A FORTRAN CALLABLE SUBROUTINE
;THAT DECREMENTS A DIGITAL OUTPUT WORD,
;TRIGGERS A TIMING INTERVAL, ACCEPTS DATA
;AT HIGH RATE FROM THE IEEE BUS, REDECREMENTS
;THE DIGITAL OUTPUT WORD, AND REFORMATS THE
;ACQUIRED DATA IN INTEGER FORMAT
;
        .GLOBL IBGTF
;
IBGTF:  MOV 2(R5),R0    ;POINT TO DATA BUFFER
        MOV #IBS,R1     ;POINT TO IBV11A STATUS REGISTER
        MOV #IBD,R2     ;POINT TO IBV11A DATA REGISTER
        MOV #LNR,R3     ;SAVE MASK FOR IBV11A LNR BIT
        MOV #KWS,R4     ;POINT TO KWV11A STATUS REGISTER
        MFPS -(SP)      ;SAVE PSW
        MTPS #DSABL     ;LOAD NEW PSW TO DISABLE INTERUPTS
        MOV (R1),-(SP)  ;SAVE IBV11A STATUS
        MOV #IBLST,(R1) ;LOAD NEW IBV11A STATUS
        DEC @#DRO       ;DECREMENT DIGITAL OUTPUT WORD
        MOV @4(R5),2(R4);LOAD KWV11A DATA REGISTER
        MOV #TRIG,(R4)  ;TRIGGER TIMING INTERVAL
;
NEXT:   BIT R3,(R1)     ;SEE IF NEW BYTE IS AVAILABLE
        BEQ NEXT        ;IF NOT, LOOP BACK
        MOV (R2),(R0)+  ;STORE DATA FROM IBV11A
        BPL NEXT        ;BRANCH BACK IF NOT LAST DATA BYTE
```

```
;
        DEC @#DRO          ;REDECREMENT DIGITAL OUTPUT WORD
        MOV (SP)+,(R1)     ;RESTORE STATUS OF IBV11A
        MTPS (SP)+         ;REENABLE INTERUPTS
        MOV 2(R5),R5       ;POINT TO DATA BUFFER
;
FORM:   MOV 2(R5),R2       ;GET LOWER DATA BYTE
        BIC #LSBCD,R2      ;MASK OFF LSD
        MOV 2(R5),R1       ;GET LOWER DATA BYTE
        ASR R1
        ASR R1
        ASR R1
        ASR R1             ;SHIFT RIGHT TO GET SECOND DIGIT
        BIC #LSBCD,R1      ;MASK OFF SECOND DIGIT
        MUL #TEN,R1        ;MULTIPLY BY TEN
        ADD R1,R2          ;ADD TO ACCUMULATOR
        MOV (R5),R1        ;GET UPPER DATA BYTE
        BIC #LSBCD,R1      ;MASK OFF THIRD DIGIT
        MUL #HUN,R1        ;MULTIPLY BY ONE HUNDRED
        ADD R1,R2          ;ADD TO ACCUMULATOR
        MOV (R5),R1        ;GET UPPER DATA BYTE
        ASR R1
        ASR R1
        ASR R1
        ASR R1
        ASR R1             ;SHIFT RIGHT TO GET MSD
        BCC ZMSD           ;BRANCH IF MSD IS ZERO
        ADD #THO,R2        ;ADD ONE THOUSAND TO ACCUMULATOR
ZMSD:   ASR R1             ;SHIFT RIGHT TO GET SIGN BIT
        BCS POSI           ;BRANCH IF POSITIVE SIGN BIT IS SET
        NEG R2             ;NEGATE ACCUMULATED VALUE
POSI:   MOVB (R5),3(R5)    ;STORE BINARY DATA
        MOV R2,(R5)+       ;STORE ACCUMULATED VALUE
        ADD #2,R5          ;INCREMENT POINTER
        CMP R5,R0          ;COMPARE WITH TERMINAL COUNT
        BLO FORM           ;BRANCH IF COUNT IS NOT TERMINAL
        RTS PC             ;RETURN
        .END
```

```
      PROGRAM DATR
      COMMON PARAM(40)
      COMMON U, P, IV1, KS, W, W2, T
      COMMON EDATA, EMSER, ALPHA
      DIMENSION A(10), B(10)
      DIMENSION GRADA(10), GRADB(10)
      EQUIVALENCE (A(1),PARAM(1)), (B(1),PARAM(11))
      EQUIVALENCE (GRADA(1),PARAM(21)), (GRADB(1),PARAM(31))
      INTEGER U, P
      COMMON /DIRECT/ H(20,20)
C
C     THIS IS A DATA REDUCTION PROGRAM TO DO PARAMETER
C     ESTIMATION ON DATA ACQUIRED BY SAMPLING AND MEASURING
C     CAPACITOR VOLTAGE RECOVERY, FOLLOWING DISCHARGE, DUE
C     TO DIELECTRIC ABSORPTION. THE SAMPLING PERIOD IS T.
C     THE COEFFICIENTS AND TIME CONSTANTS OF THE 'BEST'
C     MODEL OF THE VOLTAGE RECOVERY ARE ESTIMATED BY FITTING
C     THE DATA OVER AN INTERVAL N=1,2,...,U WITH A SUM OF
C     P TERMS OF THE FORM B(K)*(1.0-EXP(-T*N/A(K))), K=1,2,...,
C     THE ERROR IN THE FIT OVER THE INTERVAL MAY BE WEIGHTED, I
C     DESIRED, BY THE FUNCTION W**N. THE MEASURE OF THE TOTAL
C     ERROR TO BE MINIMIZED IS THE SUM OF THE SQUARES
C     OF THE WEIGHTED ERROR AT EACH POINT IN THE INTERVAL.
C     MINIMIZATION IS DONE USING THE FLETCHER-POWELL
C     GRADIENT SEARCH TECHNIQUE.
C     THERE MUST BE AT LEAST U+1=M DATA POINTS IN DISK FILE
C     'CAP.DAT'. THE GRADIENT SEARCH ALGORITHM WILL ITERATE
C     A MAXIMUM OF NITER TIMES.
C
      TYPE 500
      ACCEPT 510, P
      TYPE 520
      ACCEPT 530, M
      TYPE 540
      ACCEPT 550, W
      TYPE 700
      ACCEPT 710, NITER
      U=M-1
      W2=W**2
      T=200E-6
      CALL ASSIGN(2,'DK:CAP.DAT')
      DEFINE FILE 2 (10000,2,U,IV1)
      CALL ASSIGN(3,'DK:CAP.PAR')
      DEFINE FILE 3 (50,2,U,IV2)
C
C     FIND SIGNAL ENERGY, ESTIMATE PARAMETERS, AND ITERATE
C
```

```
        CALL ESTIM
        NSTRT=1
150     DO 170, J=1,2*P
        DO 160, K=1,2*P
        H(J,K)=0.0
160     CONTINUE
        H(J,J)=1.0
170     CONTINUE
        IFLG=0
        DO 180, I=NSTRT,NITER
        TYPE 720, I-1
        TYPE 730
        TYPE 740, (B(J)**2, A(J)**2,
       1GRADB(J)/(2.0*B(J)), GRADA(J)/(2.0*A(J)), J=1,P)
        TYPE 750, EMSER/EDATA
        CALL FLPOW
        IF (KS .EQ. 0) GO TO 200
        IFLG=1
180     CONTINUE
        TYPE 810
        GO TO 220
200     IF (IFLG .EQ. 0) GO TO 210
        NSTRT=I+1
        GO TO 150
C
C       DISPLAY FINAL PARAMETERS
C
210     NITER=I
        TYPE 800
220     TYPE 820, NITER
        DO 230, J=1,P
        GRADA(J)=GRADA(J)/(2.0*A(J))
        GRADB(J)=GRADB(J)/(2.0*B(J))
        A(J)=A(J)**2
        B(J)=B(J)**2
230     CONTINUE
        TYPE 760
        TYPE 730
        TYPE 740, (B(J), A(J), GRADB(J), GRADA(J), J=1,P)
        TYPE 750, EMSER/EDATA
        TYPE 840
C
C       OUTPUT THE RESULTS
C
        WRITE(3'1) P
        WRITE(3'2) M
        WRITE(3'3) W
```

```
      WRITE(3'4) NITER
      WRITE(3'5) T
      WRITE(3'6) KS
      DO 250, J=11,50
      WRITE(3'J) PARAM(J-10)
250   CONTINUE
      CALL CLOSE(2)
      CALL CLOSE(3)
      CALL EXIT
C
C     FORMAT STATEMENTS
C
500   FORMAT (/' NUMBER OF POLES: '$)
510   FORMAT (I2)
520   FORMAT ('+NUMBER OF DATA POINTS: '$)
530   FORMAT (I5)
540   FORMAT ('+WEIGHTING: '$)
550   FORMAT (F8.5)
700   FORMAT ('+NUMBER OF ITERATIONS: '$)
710   FORMAT (I3)
720   FORMAT (//' RESULTS OF ITERATION ',I2)
730   FORMAT (/7X,'COEFFICIENTS',5X,'TIME CONSTANTS',4X,
     1'COEFF GRADIENT',4X,'TM CN GRADIENT'/)
740   FORMAT (4(7X,E11.4))
750   FORMAT (/' TOTAL NORMALIZED WEIGHTED MEAN SQUARE ERROR:',
760   FORMAT (//1X,25('*'),1X,'FINAL ESTIMATED PARAMETERS',1X,2
800   FORMAT (/' THE GRADIENT ALGORITHM IS CONVERGENT.')
810   FORMAT (/' THE GRADIENT ALGORITHM IS NON-CONVERGENT.')
820   FORMAT (' NUMBER OF ITERATIONS:',I4)
840   FORMAT (1X,78('*'))
      END
```

```
      SUBROUTINE ESTIM
      COMMON PARAM(40)
      COMMON U, P, IV1, KS, W, W2, T
      COMMON EDATA, EMSER, ALPHA
      DIMENSION A(10), B(10)
      EQUIVALENCE (A(1),PARAM(1)), (B(1),PARAM(11))
      INTEGER U, P
C
C     GUESS TIME CONSTANTS
C
      TEMP=ALOG10(FLOAT(U+1))
      DO 100, J=1,P
      TEMPA=-J*TEMP/(FLOAT(P+1))
      A(J)=EXP(-(10.0**TEMPA))
100   CONTINUE
C
C     FIND SIGNAL ENERGY AND ESTIMATE COEFFICIENTS
C
      TEMPN=0.0
      TEMPD=0.0
      EDATA=0.0
      DO 150, N=0,U
      READ(2'N+1) DATA
      ASUM=0.0
      DO 130, J=1,P
      ASUM=ASUM+(1.0-A(J)**N)
130   CONTINUE
      TEMP=DATA*ASUM
      ASUM=ASUM**2
      DATA=DATA**2
      IF (W .EQ. 1.0) GO TO 140
      WGT=W2**N
      TEMP=WGT*TEMP
      ASUM=WGT*ASUM
      DATA=WGT*DATA
140   TEMPN=TEMPN+TEMP
      TEMPD=TEMPD+ASUM
      EDATA=EDATA+DATA
150   CONTINUE
      TEMP=TEMPN/TEMPD
      DO 160, J=1,P
      A(J)=(-T/ALOG(A(J)))**0.5
      B(J)=TEMP**0.5
160   CONTINUE
      CALL DERIV
      RETURN
      END
```

```
      SUBROUTINE FLPOW
      COMMON PARAM(40)
      COMMON U, P, IV1, KS, W, W2, T
      COMMON EDATA, EMSER, ALPHA
      DIMENSION A(10), B(10)
      DIMENSION GRADA(10), GRADB(10)
      EQUIVALENCE (A(1),PARAM(1)), (B(1),PARAM(11))
      EQUIVALENCE (GRADA(1),PARAM(21)), (GRADB(1),PARAM(31))
      INTEGER U, P
      COMMON /DIRECT/ H(20,20)
      DIMENSION Y(20), SIGMA(20), BETA(20)
C
C     MODIFY THE DIRECTION OF SEARCH AND FIND MINIMUM
C
      DO 100, J=1,P
      Y(J)=GRADA(J)
      Y(J+P)=GRADB(J)
100   CONTINUE
      DO 120, J=1,2*P
      SIGMA(J)=0.0
      DO 110, K=1,2*P
      SIGMA(J)=SIGMA(J)+H(J,K)*Y(K)
110   CONTINUE
      IF (J .LE. P) GRADA(J)=SIGMA(J)
      IF (J .GT. P) GRADB(J-P)=SIGMA(J)
120   CONTINUE
      CALL GRDNT
      IF (KS .EQ. 0) RETURN
C
C     UPDATE THE FLETCHER-POWELL PARAMETERS
C
      DO 130, J=1,P
      Y(J)=GRADA(J)-Y(J)
      Y(J+P)=GRADB(J)-Y(J+P)
130   CONTINUE
      DO 150, J=1,2*P
      BETA(J)=0.0
      SIGMA(J)=-ALPHA*SIGMA(J)
      DO 140, K=1,2*P
      BETA(J)=BETA(J)+H(J,K)*Y(K)
140   CONTINUE
150   CONTINUE
      TEMPA=0.0
      TEMPB=0.0
      DO 160, J=1,2*P
      TEMPA=TEMPA+SIGMA(J)*Y(J)
      TEMPB=TEMPB+BETA(J)*Y(J)
```

```
160     CONTINUE
        DO 180, J=1,2*P
        DO 170, K=1,J
        H(J,K)=H(J,K)+(SIGMA(J)*SIGMA(K)/TEMPA)-(BETA(J)*BETA(K)/
        H(K,J)=H(J,K)
170     CONTINUE
180     CONTINUE
        RETURN
        END
```

```
      SUBROUTINE GRDNT
      COMMON PARAM(40)
      COMMON U, P, IV1, KS, W, W2, T
      COMMON EDATA, EMSER, ALPHA
      DIMENSION A(10), B(10)
      DIMENSION GRADA(10), GRADB(10)
      EQUIVALENCE (A(1),PARAM(1)), (B(1),PARAM(11))
      EQUIVALENCE (GRADA(1),PARAM(21)), (GRADB(1),PARAM(31))
      INTEGER U, P
C
C     FIND A REASONABLE STEP SIZE
C
      STPMIN=1.0E+12
      DO 220, J=1,P
      IF (A(J) .EQ. 0.0 .OR. GRADA(J) .EQ. 0.0) GO TO 200
      IF (ABS(A(J)/GRADA(J)) .LT. STPMIN) STPMIN=ABS(A(J)/GRADA
200   IF (B(J) .EQ. 0.0 .OR. GRADB(J) .EQ. 0.0) GO TO 220
      IF (ABS(B(J)/GRADB(J)) .LT. STPMIN) STPMIN=ABS(B(J)/GRADB
220   CONTINUE
      STPMIN=.01*STPMIN
      STPSIZ=16.0*STPMIN
      ALPHA=0.0
      ERR0=EMSER
      ERR1=ERR0
      KS=0
      NS=1
      NT=0
      TYPE 720, ALPHA, 0.0, 0, ERR0
C
C     STEP DOWN THE ERROR GRADIENT
C
      CALL WMSER(ALPHA+STPSIZ)
      ERR2=EMSER
250   TYPE 720, ALPHA, STPSIZ, NS, ERR2
      IF (ERR2 .GT. ERR1) GO TO 400
      IF (NS .EQ. 2) GO TO 300
C
C     HERE AFTER ONE STEP, ERROR DECREASING
C
      STPSIZ=2.0*STPSIZ
      NS=2
      ERR1=ERR2
      CALL WMSER(ALPHA+STPSIZ)
      ERR2=EMSER
      GO TO 250
C
C     HERE AFTER TWO STEPS, ERROR DECREASING
```

```
C
300       ERR0=ERR1
          TEMP=ERR2
          KS=1
          NS=1
          NT=1
          ALPHA=ALPHA+0.5*STPSIZ
          CALL WMSER(ALPHA+STPSIZ)
          ERR2=EMSER
          GO TO 250
400       IF (NS .EQ. 1) GO TO 500
C
C         HERE AFTER TWO STEPS, ERROR INCREASING
C
          IF (STPSIZ .LE. STPMIN) GO TO 600
          STPSIZ=0.5*STPSIZ
          ERR2=ERR1
C
C         HERE AFTER ONE STEP, ERROR INCREASING
C
500       IF (NT .EQ. 1) GO TO 550
          CALL WMSER(ALPHA+0.5*STPSIZ)
          TEMP=EMSER
550       ERR1=TEMP
          NT=0
          IF (STPSIZ .LE. STPMIN .AND. NS .EQ. 1) GO TO 600
          IF (ERR1 .GT. ERR0) GO TO 560
          NS=2
          GO TO 250
560       STPSIZ=0.5*STPSIZ
          ERR2=ERR1
          ERR1=ERR0
          NS=1
          GO TO 250
C
C         DETERMINE FINAL STEP SIZE
C
600       IF ((ERR0-2*ERR1+ERR2) .EQ. 0.0) GO TO 650
          TEMP=0.25*STPSIZ*(3*ERR0-4*ERR1+ERR2)/(ERR0-2*ERR1+ERR2)
          CALL WMSER(ALPHA+TEMP)
          ERR2=EMSER
          IF (ERR2 .GT. ERR0) GO TO 650
          IF (ERR2 .GT. ERR1) GO TO 650
          STPSIZ=TEMP
          GO TO 670
650       IF (ERR1 .GT. ERR0) GO TO 660
          STPSIZ=0.5*STPSIZ
```

```
        GO TO 670
660     STPSIZ=0.0
670     ALPHA=ALPHA+STPSIZ
        DO 680, J=1,P
        A(J)=A(J)-ALPHA*GRADA(J)
        B(J)=B(J)-ALPHA*GRADB(J)
680     CONTINUE
        CALL DERIV
        TYPE 720, ALPHA, STPSIZ, 0, EMSER
        RETURN
C
C       FORMAT STATEMENTS
C
720     FORMAT (' ALPHA=',E10.3,3X,'STPSIZ=',E10.3,
        13X,'NSTEPS=',I2,3X,'ERROR=',E10.3)
        END
```

```
      SUBROUTINE DERIV
      COMMON PARAM(40)
      COMMON U, P, IV1, KS, W, W2, T
      COMMON EDATA, EMSER, ALPHA
      DIMENSION A(10), B(10)
      DIMENSION GRADA(10), GRADB(10)
      DIMENSION AA(10), BB(10), AB(10), AEXP(10)
      EQUIVALENCE (A(1),PARAM(1)), (B(1),PARAM(11))
      EQUIVALENCE (GRADA(1),PARAM(21)), (GRADB(1),PARAM(31))
      INTEGER U, P
C
C     DETERMINE THE GRADIENT AND THE ERROR
C
      EMSER=0.0
      DO 100, J=1,P
      GRADA(J)=0.0
      GRADB(J)=0.0
      TEMP=T/(A(J)**2)
      AA(J)=EXP(-TEMP)
      BB(J)=B(J)**2
      AB(J)=TEMP*BB(J)/A(J)
100   CONTINUE
      DO 150, N=0,U
      READ(2'N+1) DATA
      APPRX=0.0
      DO 110, J=1,P
      AEXP(J)=AA(J)**N
      APPRX=APPRX+BB(J)*(1.0-AEXP(J))
110   CONTINUE
      ERROR=DATA-APPRX
      TEMPE=ERROR**2
      IF (W .EQ. 1.0) GO TO 120
      WGT=W2**N
      ERROR=WGT*ERROR
      TEMPE=WGT*TEMPE
120   EMSER=EMSER+TEMPE
      DO 140, J=1,P
      GRADA(J)=GRADA(J)+ERROR*N*AEXP(J)
      GRADB(J)=GRADB(J)-ERROR*(1.0-AEXP(J))
140   CONTINUE
150   CONTINUE
      DO 160, J=1,P
      GRADA(J)=4.0*AB(J)*GRADA(J)
      GRADB(J)=4.0*B(J)*GRADB(J)
160   CONTINUE
      RETURN
      END
```

```
      SUBROUTINE WMSER(STEP)
      COMMON PARAM(40)
      COMMON U, P, IV1, KS, W, W2, T
      COMMON EDATA, EMSER, ALPHA
      DIMENSION A(10), B(10), AA(10), BB(10)
      DIMENSION GRADA(10), GRADB(10)
      EQUIVALENCE (A(1),PARAM(1)), (B(1),PARAM(11))
      EQUIVALENCE (GRADA(1),PARAM(21)), (GRADB(1),PARAM(31))
      INTEGER U, P
C
C     DETERMINE THE ERROR
C
      EMSER=0.0
      DO 100, J=1,P
      AA(J)=EXP(-T/((A(J)-STEP*GRADA(J))**2))
      BB(J)=(B(J)-STEP*GRADB(J))**2
100   CONTINUE
      DO 150, N=0,U
      APPRX=0.0
      DO 110, J=1,P
      APPRX=APPRX+BB(J)*(1.0-AA(J)**N)
110   CONTINUE
      READ(2'N+1) DATA
      ERROR=(DATA-APPRX)**2
      IF (W .NE. 1.0) ERROR=ERROR*(W2**N)
      EMSER=EMSER+ERROR
150   CONTINUE
      RETURN
      END
```